Revisiting Erk signaling following B cell antigen receptor activation by different stimulatory agents

Doctoral thesis

In partial fulfillment of the requirements for the degree

“Doctor rerum naturalium (Dr. rer. nat.)”

in the Molecular Medicine Study Program

at the Georg-August-University Göttingen

Submitted by

Caren Bartsch

Born in Holzminden

Göttingen, June 2016

Members of the Thesis Committee:

Supervisor

Prof. Jürgen Wienands, Institute for Cellular and Molecular Immunology

Second member of the thesis committee

Prof. Uwe Groß, Institute of Medical Microbiology

Third member of the thesis committee

Prof. Michael Thumm, Department of Cellular Biochemistry

Date of Disputation: 15.09.16

Affidavit

Here I declare that my doctoral thesis entitled “Revisiting Erk signaling following B cell antigen receptor activation by different stimulatory agents” has been written independently with no other sources and aids than quoted.

Göttingen, June 2016

Table of Contents

Acknowledgements

First and foremost, I would like to express my gratitude to Professor Jürgen Wienands for giving me the opportunity to join his group to work in the inspiring field of B cell immunology; for his support and guidance throughout the past four years and also for the opportunity to develop my own ideas. In the same line, I would like to thank Niklas who always provided me with scientific advice and discussions, helping me bringing my research forward. Furthermore, I want to acknowledge the members of my thesis committee, Professor Michael Thumm and Professor Uwe Groß for their feedback and advice during the committee meetings.

Special thanks goes to our collaborators Peter Sondermann and Nicole Rieth from SuppreMol (Baxalta/Shire) in Munich who gave me the chance to work on an interesting issue as part of my thesis. Thanks for lively discussions, scientific advices and the chance to get a glimpse into a part of biopharmaceutical industry.

I am happy to have been a member of the Molecular Medicine study program of the Georg August University as well as of the Integrated research training group "B cells and beyond" of the SFB Transregio 130. Especially the Transregio provided a great opportunity to meet with people from the B cell family. Thanks Agnes for coordination, I will miss the annual visit to Lohr am Main.

I also want to say thank you to the present and former members of the institute, especially to Gabi and Ines for technical support and for managing the daily routine in the lab as well as to Rosemarie Döhne, Ingrid Teuteberg and Anika Schindler for management of the administrative part of our work. Thanks to Matthias, Michael, Julius, Niklas, Arshyia, Kanika, Vanessa, Sona, Kai, Kathrin, Christoffer, Henrike and Wiebke. I enjoyed all the chats and coffee breaks in the lab as well as activities outside the lab as barbeques, winetastings, concerts, regular meetings with the breakfast club, GNTM, Tabata and several running events. I'm looking forward to our annual half marathon meetings. Which city is next?

Thanks to my volleyball team, you definitely made the time run faster in Göttingen. Where did the past four years go? I enjoy being part of the team, celebrating all smaller and bigger occasions together; the biggest for sure our championship in the Regionalliga Nord-West this

year. Special thanks to Lexi, Micki, Lisa, Katrin and Krusi for awesome activities, travels and evenings full of chatter, wine and food.

Thanks to Kristin, Wiebke, Kathrin, Niklas, Christoffer, Nicole and Peter for critically proofreading my thesis.

“Side by side or miles apart, good friends are always close to the heart”. My, Marina, Sonja, Lea, Tine and Flizzi, I am so glad to have you and to count you to my closest friends. Even if we don’t talk every day, each time we meet it feels like nothing has changed.

Last but not least, I would like to thank my family for unconditional trust and support, especially my parents and my sisters; all this would not have been possible without you. I am grateful to have Josse at my side who is around through every mood, always finding the right encouraging words. You are my constant and distraction at the same time.

Abstract

B cell antigen receptor (BCR) ligation leads to activation of a number of intracellular signaling events that decide the fate of the B cell and thus is a key event in humoral immunity. BCR activation is tightly controlled by different inhibiting and activating coreceptors and Fc receptors. Dysregulation or imbalance between inhibiting and activating receptors can result in autoimmunity. The recombinant soluble (s)FcγRIIB has been tested in clinical trials as a promising treatment option for autoimmune diseases. Besides competing with membrane-bound Fcγ receptors for pathogenic immune-complexes, sFcγRIIB is also suggested to interfere with BCR signaling by binding to membrane IgG on memory B cells. Here, I showed that multimeric variants of recombinant sFcγRIIB induce BCR signaling events in human IgG-B cells, most probably by direct interaction with the IgG-BCR. BCR signaling induced by multimeric sFcγRIIB indicated an alternative pathway for activation of extracellular signal regulated kinase (Erk). Based on these findings, I revisited the Erk pathway in human B cells. According to current knowledge based on chicken and mouse B cells, BCR-mediated Erk activation is mainly mediated via diacylglycerol (DAG) and Ras guanyl nucleotide-releasing proteins (RasGRPs) and thus requires activation of phosphoinositide phospholipase C (PLC) γ2. In contrast, my data from human B cells showed no correlation between PLCγ activity and Erk activation, revealing species specific differences between chicken, mice and human. Instead, I showed that Erk activation depends on the growth factor receptor bound protein 2 (Grb2). This led to the suggestion that Erk activation in human B cells relies on the Grb2-Son of sevenless (Sos) signaling axis as described for many other receptor systems. The involvement of Grb2 in BCR-induced Erk activation raised the question for a Grb2-membrane anchor, linking the activated BCR to Erk activation. Indirect recruitment of Grb2 to the BCR complex via the adapter protein SHC1 turned out to be not important for Erk activation. Thus, I investigated another potential Grb2 membrane anchor, namely the recently-discovered Fc receptor for IgM (FcμR). In experiments with chimeric IgG2a-FcμR receptors, I showed that the cytoplasmic domain of the FcμR indeed harbors a Grb2 binding site, which confers costimulatory functions, at least to the chimeric protein. Rigorous elucidation of BCR signaling provides important knowledge to understand the molecular biology of lymphomagenesis and autoimmune disorders for the development of potential therapeutics.

List of Figures

List of Tables

Abbreviations

α		anti
aa		Amino acid
ADCC		Antibody-dependent cell-mediated cytotoxicity
AP		Affinity purification
APC		Antigen presenting cell
BCAP		B cell adapter for PI3K
BCR		B cell antigen receptor
bp		Base pair
BSA		Bovine serum albumine
Btk		Brutons tyrosine kinase
CaM		Calmodulin
CCL		Cleared cellular lysates
CD		Cluster of differentiation
CIN85		Cbl interacting protein of 85 kDa
CRISPR		Clustered regularly interspaced short palindromic repeats
DAG		Diacylglycerol
DC		Dendritic cell
DMEM		Dulbeccos modified eagle medium
DNA		Deoxyribonucleic acid
	G	deoxyguanosine monophosphate
	A	deoxyadenosine monophosphate
	T	deoxythymidine monophosphate
	C	deoxycytidine monophosphate
dNTP		Deoxynucleotide
DSB		Double strand break
EB		EcoBlast (Ecotropic receptor; Balsticydine resistence)
EBV		Epstein-Barr virus
ECL		Enhanced chemiluminescence
EGFR		Epidermal growth factor receptors
ER		Endoplasmic recticulum
Erk		Extracellular signal regulated kinase
Fab		Fragment of antigen binding
FACS		Fluorescence activated cell sorting
Fc		Fragment crystallizable
FCS		Fetal calf serum

Gab1	Grb2-asscociated binding protein 1
GEF	Guanine nucleotide exchange factor
GFP	Green fluorescent protein
GRAP	Grb2 related adapter protein
Grb2	Growth factor receptor protein 2
gRNA	Guide Ribonucleic acid
GST	Gluthatione S transferase
GTP	Guanosine triphosphate
ICS	Intracellular staining
Ig	Immunoglobulin
IgH	Immunoglobulin heavy chain
IgL	Immunoglobulin light chain
IP	Immunoprecipitation
IP3	Inositol-1,4,5-trisphosphate
IP3R	IP3 receptors
IRES	Internal ribosomal entry site
ITAM	Immunoreceptor tyrosine-based activation motif
ITIM	Immunoreceptor tyrosine-based inhibition motif
ITP	Immune thrombocytopenia
ITT	Immunoglobulin tail tyrosine
MAPK	Mitogen-activated protein kinase
MFI	Median fluorescence intensity
mRNA	Messenger Ribonucleic acid
NFAT	Nuclear factor of activated T cells
NFκB	Nuclear factor of kappa light polypeptide gene enhancer in Bcells
NK	Natural killer
NTAL	Non-T-cell activation linker
PAGE	Polyacrylamide gel electrophoresis
PAM	Protospacer adjacent motif
PBS	Phosphate buffered saline
PC	Plasma cell
PCR	Polymerase chain reaction
PH	Pleckstrin homology
PI3K	Phosphoinositide-3 kinase
PIP2	Phosphatidylinositol 4,5 bisphosphate
PIP3	Phosphatidylinositol 3,4,5-bisphosphate
PLC	Phospholipase C
RasGRP	Ras guanyl-releasing protein

rcf	Relative centrifugal force
RFP	Red fluorescent protein
RNA	Ribonucleic acid
RPMI	Roswell park memorial institute
RT	Room temperature
SA	streptavidin
SDM	Site directed mutagenesis
SDS	Sodium dodecyl sulfate
SFK	Src family kinase
SH2	Src homology domain 2
SH3	Src homology domain 3
SHC1	SH2 containing transforming protein 1
SHIP1	SH2-containing inositol polyphosphate 5'-phosphatase 1
SHIP2	SH2-containing inositol polyphosphate 5-phosphatase 2
SHP1	SH2 domain-containing protein phosphatase 1
SHP2	SH2 domain-containing protein phosphatase 2
SILAC	Stable isotope labeling with amino acids in cell culture
SLE	Systemic lupus erythematosus
SLP65	SH2 domain-containing leukocyte protein of 65 kDa
Sos	Son of sevenless
STIM	Stromal interaction molecules
Syk	Spleen tyrosine kinase
TALEN	Transcription activator-like effector nuclease
wt	Wild type

Units and Prefixes are in conformity with the International system of Units (Système international d'unitès, SI)

Amino acid letter code

Amino acid	3 letter code	1 letter code
Alanine	Ala	A
Arginine	Arg	R
Asparagine	Asn	N
Aspartic Acid	Asp	D
Cysteine	Cys	C
Glutamic Acid	Glu	E
Glutamine	Gln	Q
Glycine	Gly	G
Histidine	His	H
Isoleucine	Leu	L
Lysine	Lys	K
Methionine	Met	M
Phenylalanine	Phe	F
Proline	Pro	P
Serine	Ser	S
Threonine	Thr	T
Tryptophan	Trp	T
Tyrosine	Tyr	Y
Valine	Val	V

1 Introduction

1.1 The immune system – an overview

The human body is exposed to a wide variety of potential pathogens every day, including bacteria, viruses, fungi or parasites. To prevent diseases, vertebrates developed a complex, multicellular immune system during hundreds of millions of years of evolution. While simple defense mechanisms can even be observed in single-cell organisms, the immune system of higher vertebrates divides into two branches: the innate and the adaptive immune system that cooperate in recognition and elimination of potential pathogenic invaders (Beck & Habicht, 1996). The innate immune system as the first line of defense provides an immediate response to pathogens that breached the anatomical barriers. Elimination of intruders is facilitated by antimicrobial molecules such as defensines, lysozyme and the complement system as well as by the cells of the innate immune system, namely dendritic cells, macrophages, granulocytes and natural killer cells. However, this immediate early response is not pathogen specific, but rather relies on the differentiation between "self" and "non-self" by so called pattern recognition receptors (PRRs) expressed by the innate immune cells. PRRs recognize molecular microbial patterns, commonly shared by many types of microorganisms but not by the host (Medzhitov & Janeway, 2002; Kumar et al, 2009). The adaptive immune system complements the immune response by providing high specificity against a wide variety of potential pathogens as well as the ability to form a long term memory against pathogens to prevent recurrent infections. The cells of the adaptive immune system are T and B lymphocytes. In contrast to innate immune cells, each and every single B and T cell expresses an antigen receptor with individual specificity, ensuring the recognition of virtually all possible pathogens. These receptors are not germ-line encoded, but acquire their antigen specificity by somatic recombination during T and B cell development (Nemazee, 2000). T lymphocytes exert the cellular part of the adaptive immune response by killing of virus infected cells and by providing costimulatory signals for the differentiation of other lymphocyte types. B lymphocytes contribute to humoral immunity with the production of antibodies (Dempsey et al, 2003; Ahmed & Gray, 1996).

1.2 B cell biology

B cells were recognized as a functionally and developmentally separate lineage of lymphocytes in 1965 by Max Cooper, although the existence of antibody producing cells has been proposed already in 1897 by Paul Ehrlich. B cells were named after the bursa of Fabricius, a hind gut lymphoid organ in birds that was identified by Bruce Glick in 1956 to be the site for antibody production in chicken (reviewed in Cooper, 2015). In human as in all mammals, development of B cells takes place in the bone marrow, where they undergo random rearrangement of the immunoglobulin gene segments (V(D)J recombination). This leads to the formation of a B cell repertoire, expressing antigen receptors specific for a vast variety of antigens (reviewed in Pieper et al, 2013). However, due to the unpredictability of specificities resulting from this random rearrangement, this process also bears the risk of producing autoreactive B cells that could induce auto immune reactions. In order to prevent autoreactivity B cells undergo a number of self-tolerance mechanisms during the stages of development leading to elimination or inactivation of autoreactive T and B cells (Shlomchik, 2008; Ubelhart & Jumaa, 2015). For final development into mature naïve B cells, newly formed B cells migrate to the spleen (Osmond, 1986). Naïve B cells keep circulating through the bloodstream, thereby homing to secondary lymphoid organs (lymph nodes, spleen and other lymphoid tissues) regularly in order to raise the chance to come in contact with the corresponding antigen (Andrian & Mempel, 2003). B cells either recognize antigen in soluble form or presented on antigen presenting cells (APC) as dendritic cells or macrophages within the secondary lymphoid organs (Yuseff et al, 2013). Upon encounter with its antigen the B cell gets initially activated. Dependent on the B cell subtype the activated B cell requires costimulatory signals from helper T cells. Activation leads to proliferation and differentiation into memory B cells or antibody-secreting plasma cells. During the so called germinal center reaction some of the B cells additionally undergo somatic hypermutation of antigen receptor genes as well as affinity maturation to increase affinity of antigen receptors. Furthermore, some B cells also undergo class-switch recombination, in order to increase functional diversity of immunoglobulins by the generation of different antigen receptors subtypes depending on the type of antigen (Heesters et al, 2014; Silva & Klein, 2015). Compared to the innate immune response which takes a few hours to respond to an antigen, the adaptive immune response takes about a week to set in upon primary encounter of a pathogen. However,

memory B cell activation and differentiation into plasma cells upon secondary encounter with an antigen is much faster and hence requires less costimulatory signals by T cells (Engels et al, 2009; Kurosaki et al, 2015). This enables the organism to react faster and more effective against recurrent pathogens to prevent or ameliorate a second infection. This effect also underlies the principle of vaccination, where adaptive immunity is induced by administration of inactivated or attenuated antigenic material that mimics a natural infection.

1.2.1 Immunoglobulins: structure and function

Antibodies or immunoglobulins (Igs) are Y-shaped proteins and occur in two forms: membrane bound as part of the B cell antigen receptor (BCR) and as soluble form, secreted in large numbers by plasma cells (PCs), which represent finally differentiated B cells. The secreted form has the same antigen specificity and isotype as the BCR on naïve or memory B cell the plasma cell has differentiated from in response to the corresponding antigen. The main functions of secreted antibodies are neutralization of antigens, labelling of antigens for elimination by phagocytes (opsonization), activation of the complement system and antibody-dependent cell-mediated cytotoxicity (ADCC) by NK cells (Ravetch & Kinet, 1991).

Structurally, immunoglobulins (Ig) are composed of two Ig heavy chains and two Ig light chains. Both heavy chains are linked to each other and each light chain is linked to one of the heavy chains by disulfide bonds (figure 1). Each light chain is composed of a constant and a variable domain (C_L and V_L), while each heavy chain contains one variable domain (V_H) and, depending on the Ig subtype, three to four constant domains (C_H) (Woof & Burton, 2004). The immunoglobulin molecule can be dissected in two parts, defined as the fragment of antigen binding (Fab) consisting of the V region and the Fc fragment (fragment crystallizable) linked by a hinge region. This definition is based on experiments by Rodney R. Porter who observed that papain cleaves rabbit IgG-antibodies into three fragments; two of them retained antibody function, whereas the third one crystallized (Porter, 1959). Porter was, together with Gerald M. Edelmann, awarded the Nobel prize for medicine in 1972 for determining the chemical structure of antibodies. As its name implies, the Fab fragments mediates antigen recognition, while the Fc portion binds to certain receptors termed as Fc receptors mediating the antibodies effector function according to the Ig subtype. Fc receptors are membrane bound receptors specific for the Fc portion of the

respective Ig isotype, connecting the humoral to the cellular immune response, thereby mediating the major part of antibody effector functions as describe above (Woof & Burton, 2004). The role of Fc receptors in B cells will be reviewed later in this introduction.

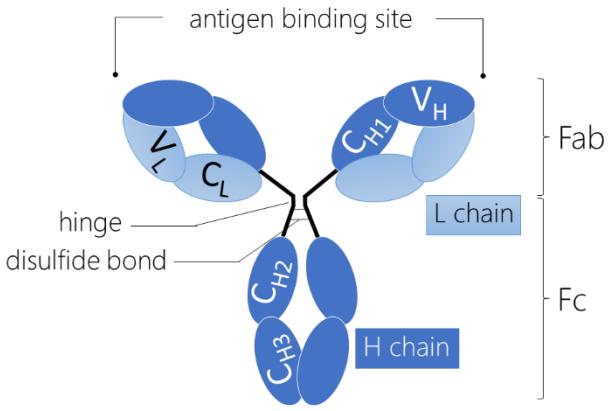

Figure 1. Representative depiction of an immunoglobulin. Immunoglobulin (here using the example of IgG) are composed of two heavy (H) chains (dark blue) and two light (L) chains linked by disulfide bonds. Each light and heavy chain contains variable (V) and constant (C) domains. The paired variable domains (V_H and V_L) constitute the antigen binding sites. Functionally, immunoglobulins are dissected into the Fragment of antigen binding (Fab) and the Fragment crystallizable (Fc), which by binding to Fc receptors expressed on different immune cells and by activation of the complement systems mediates the major part of antibody effector functions.

In order to achieve the extraordinary diversity of the immunoglobulin repertoire, rearrangement of immunoglobulin genes by V(D)J recombination, a unique mechanism of somatic recombination, is required. Ig H and L chain are encoded by genes on three independent loci, one for the H chain (IgH) and two for the L chain (Igκ and Igλ). Each contains multiple copies of variable (V), joining (J) and diversity (D; only IgH chain) gene segments as well as exons encoding the constant (C) regions. Random rearrangement of V and J gene segments on the Ig L chain loci and V, D and J gene segments on the Ig H locus leads to assembly of a complete V_L-region exon or V_H-region exon, respectively. The C region exons are joined to the V_H- or V_L-region exon by mRNA splicing for expression of a complete H or L chain (Tonegawa, 1983; Matsuda et al, 1998; Schatz & Ji, 2011; Jung et al, 2006). Following B cell activation, Igs are further modified by somatic hypermutation during the germinal center reaction. This process involves the introduction of point mutations into the V regions of heavy and light chain at a high rate, leading to alterations in antigen binding affinity. B cells with improved antigen binding affinity are selected for proliferation and further maturation, while B cells with decreased affinity die. This process is termed affinity maturation (Li et al, 2004; Odegard & Schatz, 2006).

Igs come in different isotypes: IgM, IgD, IgG, IgE and IgA. The class or isotype of Igs is defined according to the H chain constant region (C_H) that accordingly is termed μ, δ, γ, ε or α C_H region. The C_H region determines the effector function of an antibody by binding to specific Fc receptors expressed on almost all types of immune cells, mediating the major antibody functions as ADCC, elimination of pathogens by activation of phagocytes or release of inflammatory mediators (Raghavan & Bjorkman, 1996; Woof & Burton, 2004)

IgM is expressed on naïve B cells and hence is the first isotype secreted during an immune response. Since it is expressed before B cell activation, it has not undergone somatic hypermutation and affinity maturation and thus has a relatively low binding affinity (Boes, 2000; Schroeder, JR & Cavacini, 2010). Along with IgM also IgD is expressed on the cell surface of naïve B cells and to some extent is secreted. However, its role has not been fully elucidated (Chen & Cerutti, 2010). The other isotypes emerge after primary response to an antigen during the germinal center reaction in a process termed class-switch recombination or Ig isotype switching. This process involves the replacement of the μ and δ C_H regions with γ, ε or α C_H regions by DNA recombination of the C region exons on the H chain locus, leading to a switch from IgM and IgD surface expression to IgG, IgE or IgA expression (Stavnezer et al, 2008; Stavnezer & Schrader, 2014).

The most abundant Ig isotype is IgG which is found in blood and extracellular fluids. IgA is less abundant than IgG in serum but concentrates at mucosal surfaces and secretions, including saliva and breast milk. IgE is the least abundant immunoglobulin in serum, but constantly binds with high affinity to Fc receptors for IgE (Fcε receptors) on mast cells, eosinophils or basophils, thus being involved in hypersensitivity, allergy as well as in the response to worm infections (Schroeder, JR & Cavacini, 2010).

1.2.2 The B cell antigen receptor

Membrane and secreted forms of immunoglobulins originate from the same genetic loci and are processed by alternative mRNA splicing. The C-terminal part of the membrane Igs contains a transmembrane region as well as a cytoplasmic segment that are not found in the secreted form. However, the cytoplasmic domains differ between the different Ig isotypes: the cytoplasmic segment of IgD and IgM encompasses only three amino acids, while the cytoplasmic domain of

IgG and IgE comprises 28 amino acids. To form a functional BCR complex, the membrane immunoglobulin is noncovalently associated with two invariant protein chains, namely Igα (CD79a) and Igβ (CD79b), forming a heterodimer linked by disulfide bonds (Reth et al, 1991). This heterodimer is not only important for the transport of the BCR to the cell surface, but also mediates the signaling function of the BCR complex via so called immunoreceptor tyrosine-based activation motifs (ITAMs) with the consensus sequence D/E-x_7-D/E-x_2-**Y**-x_2-I/L-x_7-**Y**-x_2-I/L (x can be any amino acid). ITAMs are also present within the signaling chains of the T cell antigen receptor and certain Fc receptors (Reth, 1992; Reth & Wienands, 1997). Upon BCR stimulation and activation of protein tyrosine kinases the tyrosine (Y) residues within the ITAMs of Igα and Igβ get phosphorylated, leading to the initiation of several signaling pathways from the BCR (Gold et al, 1991; Clark et al, 1994).

1.2.3 B cell antigen receptor signaling

The mode of BCR activation on the cell surface has been discussed at least in two partially controversial models. Originally, antigen-specific activation of the BCR was explained by the cross-linking model, assuming that the BCR exists as a monomer and requires oligomerization by a polyvalent antigen in order to get activated and induce further downstream signaling (discussed in Yang & Reth, 2010b and Pierce & Liu, 2010). This model was supported by observations made in other receptors as well as by the finding that only bivalent F(ab')2 fragments derived from BCR specific antibodies were able to induce BCR signaling, while monovalent Fab fragments were not (Metzger, 1992; Lemmon & Schlessinger, 2010; Woodruff et al, 1967). However, Yang and Reth proposed an alternative model which they termed dissociation activation model: This model suggests the organization of the resting BCR in preformed clusters, forming stable auto-inhibiting oligomers that dissociate upon antigen binding and thereby form signaling active monomers (Yang & Reth, 2010b; Yang & Reth, 2010a; Klasener et al, 2014). Nevertheless, while the conformation and activation of the resting BCR is still controversially discussed, the knowledge about the downstream signaling events emerging from the BCR is more profound.

BCR ligation leads to phosphorylation of the ITAMs within the Igα/β hetero dimer by Src family kinases (SFKs) such as Lyn and Fyn and spleen tyrosine kinase (Syk). The doubly phosphorylated

ITAMs serve as docking sites for the tandemly arranged Src homology 2 (SH2) domains of Syk resulting in further activation of Syk. This leads to amplification of BCR signal transduction by Syk mediated ITAM phosphorylation of neighboring BCRs (Clark et al, 1994; Rowley et al, 1995; Futterer et al, 1998; Rolli et al, 2002). Furthermore, activated Lyn and Syk contribute to the activation of several downstream effectors resulting in various signaling pathways determining the B cells' fate in immune response and differentiation. Two early events, namely the activation of phosphoinositide-3 kinase (PI3K) and the activation of phosphoinositide phospholipase C (PLC) γ2, were shown to be important for propagation of downstream signals by the production of second messengers (figure 2) (Marshall et al, 2000).

1.2.3.1 PI3 kinase/Akt pathway

Following BCR activation the BCR co-receptor CD19 and the adapter protein B cell adapter for PI3K (BCAP) get phosphorylated by Lyn and brutons tyrosine kinase (Btk) which leads to the recruitment of PI3K to the plasma membrane (figure 2 ①) (Tuveson et al, 1993). Once activated, PI3K phosphorylates the membrane inositol phospholipid PIP2 (phosphatidylinositol 4,5-bisphosphate) leading to generation of PIP3 (phosphatidylinositol 3,4,5-bisphosphate) (reviewed in (Tuosto et al, 2015). PIP3 mediates translocation of Akt kinase to the plasma membrane where it gets activated by phosphoinositide dependent kinase (PDK) 1 and PDK2 (Osaki et al, 2004). Akt in turn leads to inactivation of several factors including GSK3β and FOXO1 that are involved in negative regulation of cell cycle progression (reviewed in Rickert, 2013).

1.2.3.2 Formation of the Ca^{2+} initiation complex and activation of PLCγ2

PIP2 also serves as substrate for PLCγ2 whose enzymatic products facilitate regulation of the most crucial signaling events following B cell activation. Activation of PLCγ2 requires formation of the so called Ca^{2+} initiation complex consisting of Btk, PLCγ2 itself and the adapter protein Src homology [SH2] domain–containing leukocyte protein of 65 kD (SLP65) also termed BLNK or BASH (Wienands et al, 1998; Fu et al, 1998; Goitsuka et al, 1998). SLP65 has been shown to be indispensable for B cell development and is a critical component in signal integration following BCR activation (Ishiai et al, 1999; Hayashi et al, 2000; Pappu et al, 1999). Following BCR activation SLP65 gets recruited to the plasma membrane which requires constitutive interaction with Cbl-interacting protein of 85 kDa (CIN85) (Kometani et al, 2011; Oellerich et al, 2011).

Additionally, SLP65 gets recruited to Igα by binding to a non-ITAM tyrosine and to auto-phosphorylated Syk via its SH2 domain (Engels et al, 2001; Kulathu et al, 2008). This in turn leads to tyrosine phosphorylation of SLP65 by Syk (Chiu, 2002). Once phosphorylated, it provides docking sites for Btk and PLCγ2, bringing them into close vicinity within the Ca^{2+} initiation complex. Syk phosphorylates and thereby activates Btk which in turn phosphorylates PLCγ2. Activated PLCγ2 mediates hydrolysis of PIP2 which results in the generation of the second messengers IP3 (inositol-1,4,5-trisphosphate) and membrane bound DAG diacylglycerol (DAG) (figure 2 ②) (Kurosaki et al, 2000).

1.2.3.3 Downstream of the Ca^{2+} initiation complex

IP3 mediates the mobilization of the second messenger Ca^{2+} from intracellular stores and from the extracellular space. In detail, IP3 binds to a set of IP3 receptors (IP3R1-3) that are located in the membrane of the endoplasmic reticulum (ER) and serve as ligand operated Ca^{2+} channels, leading to the release of Ca^{2+} from the ER into the cytosol. The rapid decrease of Ca^{2+} in the ER lumen is sensed by so called stromal interaction molecules (STIMs), transmembrane proteins in the ER membrane. Upon Ca^{2+} binding STIMs interact with and activate Calcium release activated channels (CRACs) in the plasma membrane that operate the influx of extracellular Ca^{2+} into the cytoplasm (figure 2 ③) (reviewed in Engelke et al, 2007; Scharenberg et al, 2007). The sustained increase in Ca^{2+} is required for the activation of the transcription factor nuclear factor of activated T cells (NFAT) via the phosphatase Calcineurin which is activated by the Ca^{2+}sensor Calmodulin (CaM) (figure 2 ④) (Macian, 2005). NFAT modulates proliferation and survival of peripheral B cells and differentiation into plasma cells (Engelke et al, 2007; Hock et al, 2013).

DAG, on the other hand, was shown to be involved in activation of the transcription factor NFκB (nuclear factor of kappa light polypeptide gene enhancer in B cells) (figure 2 ⑤) and extracellular signal regulated kinase (Erk) (figure 2 ⑥) (Spitaler & Cantrell, 2004). The activation of Erk following BCR activation is discussed in more detail in the following section. Activation of NFκB requires the recruitment of the serine/threonine protein kinase C (PKC)β to the membrane bound DAG. PKCβ gets fully activated upon Ca^{2+} binding and mediates activation of the IκBα kinase complex (IKK) which in turn phosphorylates the NFκB inhibitor IκB and marks it for proteasomal degradation. Consequently, NFκB is released from cytosolic retardation and

translocates to the nucleus where it is involved in regulation of various genes that regulate the immune response (figure 2 ⑤) (Li & Verma, 2002).

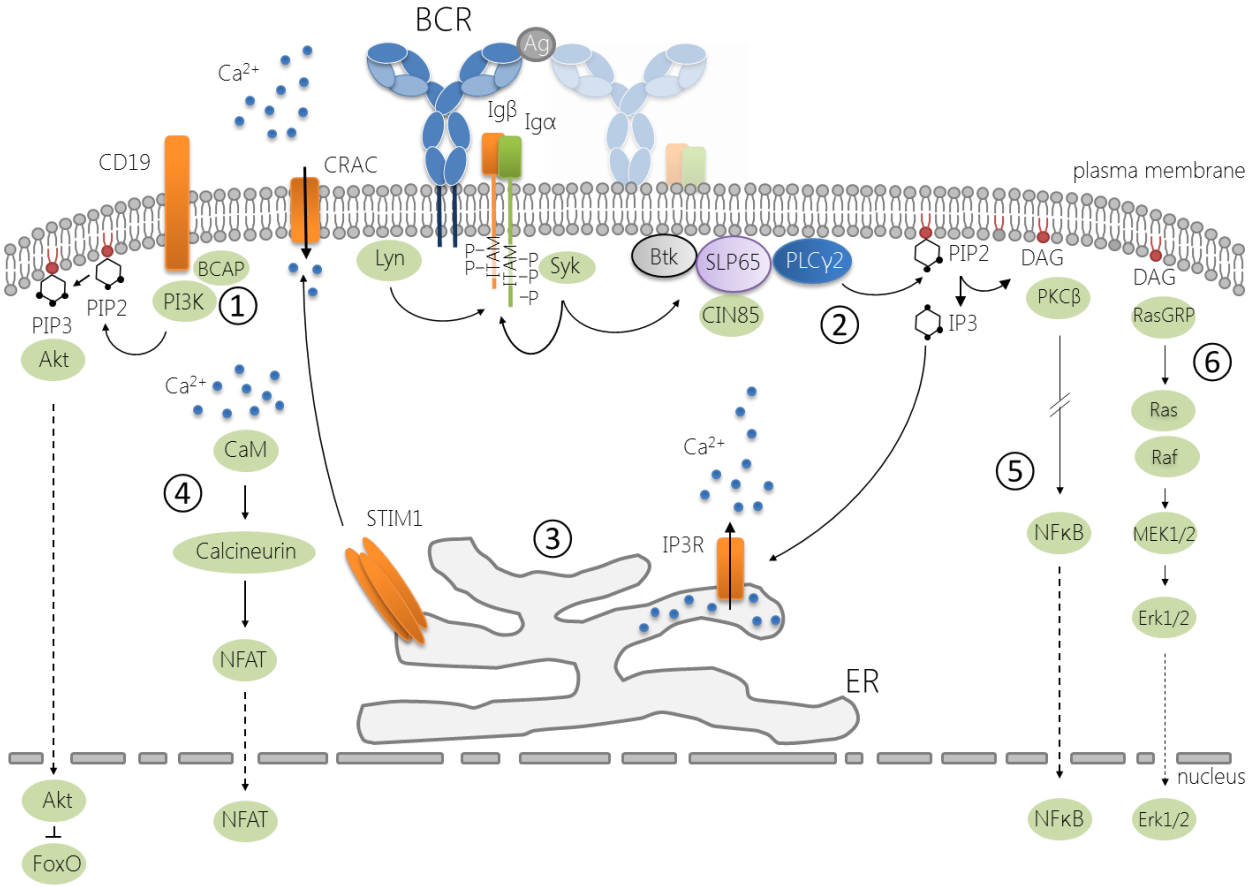

Figure 2. Schematic depiction of B cell antigen receptor (BCR) signaling. Following BCR ligation, activation of CD19 and BCAP leads to the recruitment of PI3K ①. PI3K mediates hydrolysis of PIP2 to PIP3, which recruits Akt kinase to the plasma membrane. Activated Akt inactivates nuclear transcription factors involved in negative regulation of cell cycle progression. Furthermore, Lyn and Syk activity leads to phosphorylation of the ITAMs within the Igα/β heterodimer and to phosphorylation of the Igα non-ITAM tyrosine. This in turn leads to phosphorylation of SLP65, which recruits Btk and PLCγ2 and mediates the formation of the Ca^{2+}initiation complex ②. Syk activates Btk, which in turn activates PLCγ2. PLCγ2 mediates hydrolysis of PIP2 to IP3 and DAG. IP3 induces mobilization of Ca^{2+} from intra- and extracellular sources via IP3R, STIM1 and CRACs ③. Increased Ca^{2+} entry is sensed by CaM, which via calcineurin mediates the activation of NFAT ④. DAG mediates the recruitment of PKCβ or RasGRPs to the plasma membrane which leads to activation of NFκB ⑤ and Erk via the Ras/Raf/MEK1/2 pathway ⑥. Solid arrows indicate direct effector functions, discontinuous arrow indicates indirect effector functions, blunt arrow indicates inhibition and dashed arrows indicate translocation.

1.2.4 Activation of Erk following BCR activation

Another crucial effector that was shown to get activated upon BCR activation is Erk. Erk plays an important role in cell cycle progression as well as survival and was shown to be essential for the differentiation of naïve and memory B cells into plasma cells (Yasuda et al, 2011). Activation is

mediated via the GTPase Ras which by virtue of farnesyl residues is associated with cellular membranes. Ras activates the protein kinase Raf that in turn activates MAPK/Erk kinase (MEK) which results in the activation of Erk (McCubrey et al, 2007; Yasuda & Kurosaki, 2008). Ras activity is regulated by guanine nucleotide exchange factors (GEFs). Initially, the RasGEFs Son of seven less 1 and 2 (Sos1/2) were assumed to mediate Ras activation following BCR ligation as it was described for growth factor receptors (Campbell et al, 1998; Egan et al, 1993; Buday & Downward, 1993). Sos is delivered to the activated receptor by the adapter protein growth factor receptor-bound protein 2 (Grb2), which constitutively interacts with Sos (Bar-Sagi, 1994). Supporting evidence came from *in vitro* kinase assays showing that Grb2 is partially required for activation of Erk (Hashimoto et al, 1998). However, studies in Sos1/2 deficient cells derived from the chicken B cell line DT40 revealed that Sos is dispensable for the BCR induced activation of Ras and Erk in this cell line. Moreover, further genetic analysis from the same study implied that rather the RasGEF Ras guanyl releasing protein 3 (RasGRP3) and PLCγ2 are important for Erk activation (Oh-hora et al, 2003). This was supported by data from RasGRP and PLCγ2 deficient mice (Coughlin et al, 2005; Bell et al, 2004). The necessity for PLCγ2 in Erk activation can be explained by the requirement for the recruitment of RasGRP to DAG, which is a product of PIP2 hydrolysis by PLCγ2 (figure 2 ⑥). However, a more recent study implied that both families of RasGEFs cooperate in the activation of Ras by revealing that Sos facilitates Erk activation upon suboptimal BCR stimulation via a RasGTP dependent positive-feedback loop (Roose et al, 2007; Das et al, 2009).

It is necessary to point out that all of the studies regarding Grb2/Sos involvement in BCR mediated Erk activation were conducted in the chicken cell line DT40 or in mouse models. How Erk activation following BCR ligation is mediated in human B cells is not known. Investigation of the role of Grb2 in Erk activation in human B cells is part of this thesis.

1.2.6 The adapter protein Grb2

Adapter proteins in general are important players in the initiation of signaling pathways from the activated antigen receptor. By providing distinct protein domains and phosphorylation sites they are important for mediating protein-protein interactions and the formation of larger complexes, thereby generating platforms for signal propagation. The adapter protein Grb2 is a simple

adapter protein that is abundantly expressed and involved in numerous signaling processes mediating activating as well as inhibiting functions. As mentioned before, Grb2 was first discovered as being recruited to growth factor receptors via its SH2 domain, thereby linking the activated receptor to Ras activation via the interaction with Sos (Lowenstein et al, 1992; Buday & Downward, 1993; Bar-Sagi, 1994). Null mutation of the Grb2 gene results in embryonic lethality supporting a crucial role for Grb2 in developmental processes (Cheng et al, 1998).

Grb2 has a molecular weight of 25 kDa and belongs to the Grb2 family of adapter proteins which also includes Grb2-related adapter protein (GRAP) and GRB2-related adapter downstream of Shc (Gads). While Grb2 is ubiquitously expressed in all cell types, GRAP and Gads expression is restricted to hematopoietic cells including T and B cells. Grb2 and GRAP share 60 % sequence homology (Trüb et al, 1997; Liu et al, 2001). Grb2 is composed of a central SH2 domain flanked by two SH3 domains (Lowenstein et al, 1992). The constitutive association with Sos is mediated by both SH3 domains (Rozakis-Adcock et al, 1993; Neumann et al, 2009), while the SH2 domain directly recognizes phospho-tyrosine containing sites with the consensus sequence pYXN (Kessels, Helmut W H G et al, 2002).

1.2.6.1 The differential role of Grb2 in BCR signaling

Despite its simple structural organization, Grb2 plays a versatile role in the regulation of BCR signaling. Many Grb2 interaction partners have been identified that play a crucial role in regulation of BCR signaling (figure 3) (Neumann et al, 2009). Hence, Grb2 is implied to act either as a negative or positive regulatory element by binding to different coreceptors or membrane adapter proteins that provide docking sites for Grb2. Whether Grb2 acts as a negative or positive regulatory element strongly depends on the developmental and differentiation stage of the B cell (Jang et al, 2009).

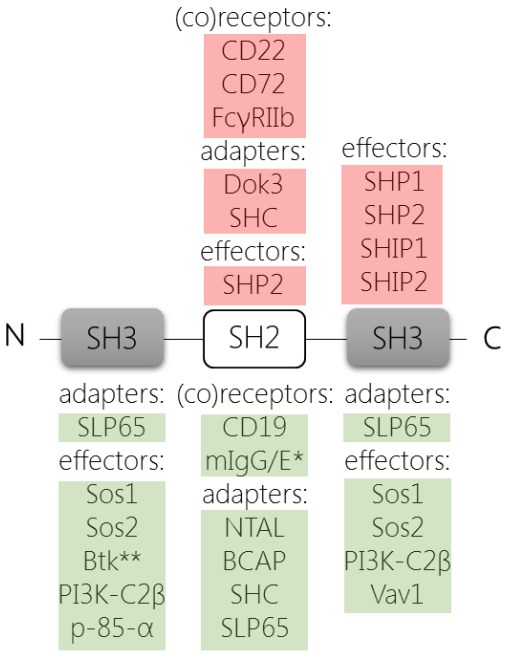

Figure 3. Selection of Grb2 interaction partners involved in BCR signaling. Grb2 interacts with both SH3 domains and the central SH2 domain with negative (red) and positive (green) regulators of BCR signaling. Interaction with some of the proteins requires involvement of more than one Grb2 domain. Based on Neumann *et al*, 2009, Engels *et al,* 2009 (*) and Engels *et al*, 2014 (**).

Grb2 was shown to be involved in amplification of signals initiated from the IgG/IgE-BCR of memory B cells. In contrast to the IgM-BCR, the IgG-and the IgE-BCR have an extended cytoplasmic domain that comprises a conserved tyrosine motif termed as immunoglobulin tail tyrosine (ITT) matching the consensus sequence pYXN. ITT phosphorylation following BCR activation leads to recruitment of Grb2 that confers signal amplification to the mIgG-BCR via recruitment of Btk (Engels et al, 2009; Engels et al, 2014). The ITT facilitates fast reactivation of memory B cells during a secondary immune response (Lutz et al, 2016).

A positive regulatory role for Grb2 was also proposed for CD19 signaling, thereby playing an important role in amplification of the signals emerging from the BCR and initiation of the PI3K/Akt pathway, probably by increasing the avidity of effector proteins that bind to CD19 (Rickert, 2005).

On the other hand, studies in chicken DT40 cells as well as in mice revealed a negative regulatory role of Grb2 in Ca^{2+} mobilization following BCR activation (Stork et al, 2004; Ackermann et al, 2011). Following BCR activation Grb2 gets recruited to the phosphorylated adapter protein

Downstream of kinase-3 (Dok3), which is located at the inner leaflet of the plasma membrane. Plasma membrane recruitment via Dok3 brings Grb2 into close proximity with Btk, inhibiting Btk-mediated PLCγ2 activation either by allosteric inhibition of Btk or by preventing the entry of Btk into the Ca^{2+} initiation complex. This process is antagonized by the transmembrane adapter non-T-cell activation linker (NTAL) that upon activation sequesters Grb2 via a phospho-YXN site (Stork et al, 2007; Stork et al, 2004).

Moreover, Grb2 is suggested to be involved in the negative regulation of B cell receptor signaling by inhibitory coreceptors such as CD22, CD27 and the low affinity Fc receptor for IgG (FcγRIIB). These receptors exert their function via so called immunoreceptor tyrosine-based inhibition motifs (ITIMs) that upon ligation get phosphorylated leading to the recruitment of protein-tyrosine phosphatases including SH2 domain-containing protein phosphatase 1 (SHP1) and 2 (SHP2) as well as the lipid phosphatase SH2-containing inositol polyphosphate 5-phosphatase (SHIP). This leads to dephosphorylation of important effectors as for example Igα and Igβ or hydrolysis of the second messenger PIP3 in order to downmodulate BCR signaling (Nitschke & Tsubata, 2004; Ono et al, 1996). While the involvement of Grb2 in negative signaling of CD27 is not elucidated, the formation of a quaternary complex between CD22 with Grb2, SHIP and the adapter protein SHC seems to be important for the CD22 mediated negative regulation of BCR signaling (Poe et al, 2000). In FcγRIIB dependent inhibition of BCR signaling, Grb2 seems to act as a stabilizer for SHIP and hence for SHIP-mediated signal inhibition (Neumann et al, 2011).

1.2.7 The role of Fc receptors on B cells

Fc receptors are expressed on almost all types of immune cells beside T cells, thereby transducing the main functions of antibodies as phagocytosis of opsonized pathogens, ADCC (antibody-dependent cell mediated cytotoxicity), degranulation and release of immunoregulatory molecules (Woof & Burton, 2004; Nimmerjahn & Ravetch, 2007). Several Fc receptors specific for the respective Ig isotypes are well described in structure and function. According to the Ig isotypes IgA, IgE and IgG they are termed Fcα, Fcε and Fcγ receptors (figure 4). An Fc receptor for IgM (FcμR) has only been identified recently. Cellular distribution and function of the FcμR is conversely discussed and still under investigation. However, in human

it is primarily if not exclusively expressed on cells of the adaptive immune system, namely T and B cells (Kubagawa et al, 2009). The most important and so far best described Fc receptor on B cells is the before mentioned FcγRIIB. As outlined in the previous section, the FcγRIIB plays an important regulatory role by downmodulating BCR mediated signaling.

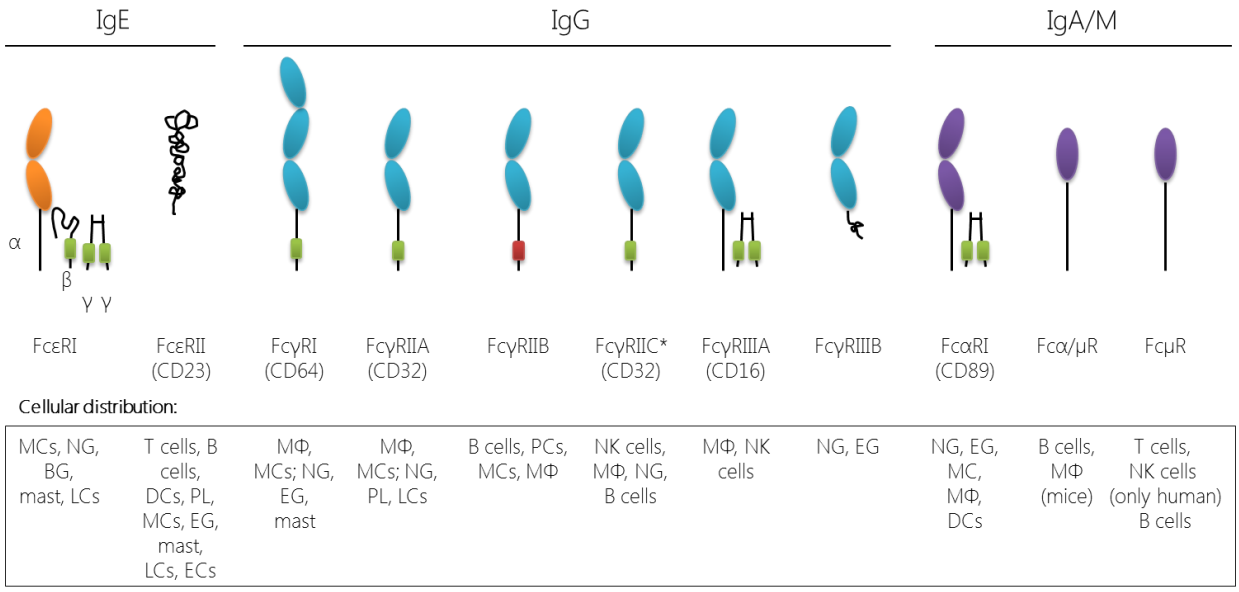

Figure 4. Human Fc receptors and their cellular distribution. ITAMs are indicated in green, ITIMs are indicated in red. are BG=basophil granulocytes, EG=eosinophil granulocytes, NG=neutrophils granulocytes, DC=dendritic cell, LC=langerhans cell, MC=Monocyte, MΦ=Macrophage, mast=mast cell, PL=platelets, EC=epithelial cell; (*pseudogene). Adapted from (Pleass & Woof, 2001).

1.2.7.1 The regulatory function of FcγRIIB

The FcγRIIB belongs to the Fcγ receptor family, the largest Fc receptor family specific for IgG. In human it contains six members, including five activating, namely FcγRI, FcγRIIA, FcγRIIC, FcγRIIIA, FcγRIIIB and the inhibitory FcγRIIB. Correspondingly, the different Fcγ receptor subtypes bind the different IgG subtypes IgG1-4 with varying affinities. Members of the Fcγ receptor family are expressed on virtually all immune cells including dendritic cells, macrophages, neutrophils, NK cells, B cells but not T cells. Activating Fcγ receptors mediate their function through ITAMs, while the inhibitory FcγRIIB encompasses an ITIM and thereby modulates ITAM mediated signaling and prevents overwhelming reactions (figure 4). Hence, simultaneous expression of both, activating and inhibitory Fc receptors on immune cells facilitates tight regulation of the immune response (Nimmerjahn & Ravetch, 2007; Nimmerjahn & Ravetch, 2008; Nimmerjahn & Ravetch, 2010).

While monocytes, macrophages, dendritic cells, basophils and mast cells express both types of Fcγ receptors, B cells only express the inhibitory FcγRIIB. It thereby is involved in modulation of signals emerging from the BCR and regulation of antibody homoeostasis by controlling plasma cell survival on several levels of B cell differentiation (Bolland & Ravetch, 1999; Baerenwaldt & Nimmerjahn, 2008). Lack or polymorphisms of *FCγRIIB* gene in human as well as in mice lead to the development of autoimmunity, underlining the important immunoregulatory role of this inhibitory receptor (Nimmerjahn & Ravetch, 2008; Baerenwaldt & Nimmerjahn, 2008). For example, a polymorphism in the human *FCγRIIB* gene resulting in the exclusion of FcγRIIB from lipid rafts is associated with the development of systemic lupus erythematosus (SLE) (Floto et al, 2005). SLE is a systemic autoimmune disease that can affect destruction of healthy tissue in multiple organs by the production of autoantibodies and is hence characterized by various symptoms (Bengtsson & Ronnblom, 2016).

1.2.7.2 A recombinant soluble FcγRIIB as treatment option in autoimmune diseases

In autoimmune diseases that are characterized by the production of autoantibodies, as for example SLE or immune thrombocytopenia (ITP), tissue destruction is driven by constant ligation of activating Fc receptors by immune complexes. This in turn leads to proinflammatory responses and chronic inflammation through the activation of macrophages and other Fc receptor expressing cells. Cell debris further activate the immune response, perpetuating the cycle of autoantigen presentation and generation of autoantibodies. In ITP for example, the body develops autoantibodies against several platelet surface antigens, resulting in the destruction of platelets by splenic macrophages and hence in a low platelet count (Cines & Blanchette, 2002; Coopamah et al, 2003; Rodeghiero et al, 2009). Treatment of ITP and other Ig driven autoimmune disease involves immune suppressive drugs as corticosteroids and immunoglobulin therapy. In persistent or chronic ITP depletion of the B cell compartment by rituximab, a monoclonal antibody against the pan B cell marker CD20 or splenectomy are applied (Cines & Bussel, 2005). However, a new promising treatment option for Ig mediated autoimmune diseases is provided by a recombinant soluble FcγRIIB as antagonist for the membrane bound Fc receptors in immune-complex binding (Sondermann, 2016). Early studies already revealed the therapeutic potential of recombinantly expressed soluble Fcγ receptors in immune complex

mediated tissue damage. Several *in vitro* and *in vivo* studies revealed that soluble Fcγ receptors interfere with the formation of immune complexes and their binding to membrane bound Fcγ receptors, thereby inhibit immune cell activation (Gavin et al, 1995; Wines et al, 2003; Astier et al, 1994). Ierino *et al* showed that recombinant human FγRII competes with membrane bound FcγR *in vitro* and that it inhibited immune-complex mediated inflammatory response (Arthus reaction) in a rat model (Ierino et al, 1993). Another study revealed an ameliorative effect of recombinant soluble FcγIIIa in the disease course of SLE in lupus prone NZB/NZW mice, characterized by lowered levels of autoantibodies and an improved disease course (Watanabe et al, 1998). A new generation of recombinant human soluble FcγRIIB was expressed in *E. coli* to prevent contamination and crossreaction through co-purified TGF-β (Sondermann & Jacob, 1999; Sondermann et al, 1999; Galon et al, 1995). Successful preclinical studies revealed amelioration and suppression of the disease course in rheumatoid arthritis-, SLE- and epidermolysis bullosa acquisita-animal models also with the *E. coli*-derived soluble FcγRIIB (Magnusson et al, 2008; Werwitzke et al, 2008; Iwata et al, 2015; Sondermann, 2016). A Phase 0/Ia clinical trial revealed excellent safety and tolerability of the sFcγRIIB in healthy volunteers (Tillmanns et al 2011). Moreover, the sFcγRIIB has been tested in phase II clinical studies in patients with chronic ITP or SLE with promising results (Konstantinova 2012, Tillmanns 2014). After only a single cycle of treatment with four infusions of 12 mg/kg sFcγRIIB, patients with chronic ITP exhibited a sustained increase in platelet counts from 30 x 10^9/L to a median platelet count of 70 x 10^9/L for up to three months (Konstantinova, 2012). Although, the sFcγRIIB efficiently can compete for pathogenic immune complexes, this is, due to the short half-life time of sFcγRIIB, no sufficient explanation for the long term effect observed in ITP patients. Moreover, it is conceivable that the sFcγRIIB also interacts with the Fc portion of membrane IgG as part of the BCR and hence interferes with the activation of memory B cells and formation of plasma cells. Whether the sFcγRIIB is capable of binding to the IgG-BCR and whether it interferes with BCR mediated signaling has been investigated as part of this thesis.

1.2.7.3 The enigmatic FcμR

Another Fc receptor that has been recently discovered to be expressed on B cells is the long sought-after Fc receptor for IgM, the FcμR. It was originally designated as Toso/Faim3 with

inhibitory activity on Fas mediated apoptosis and was rediscovered as Fc receptor solely binding IgM seven years ago (Kubagawa et al, 2009). The cellular distribution of the FcμR is still controversially discussed. RNA expression analyses in human and mice revealed broad transcript expression in almost all lymphoid and myeloid cells, while the highest transcript levels were measured in B cells (Choi et al, 2013; Hitoshi et al, 1998; Shima et al, 2010). However, reports about FcμR protein expression are quite divergent. Kubagawa *et al.* initially reported that FcμR expression is restricted to T-, B- and NK cell in human and to B cells in mice which was confirmed for mice by Ohno *et al*. (Kubagawa et al, 2009; Shima et al, 2010). On the other hand, another group found the FcμR to be expressed also on myeloid cells, including monocytes, macrophages, granulocytes and DCs (Lang et al, 2013; Lang et al, 2015). As divergent as reports about FcμR expression are studies dealing with the phenotype of FcμR deficient mice. Two different mouse models have been investigated by three groups with conflicting results, especially with regard to B cell development and distribution of B cells (summarized in Wang et al, 2016). However, all of them commonly observed increased levels of autoreactive antibodies (Choi et al, 2013; Honjo et al, 2012; Ouchida et al, 2012).

Results from the same studies revealed a positive modulatory role of the FcμR in tonic BCR signaling as well as a reduction in proliferation and survival following BCR activation of splenic B cells isolated from $Fc\mu R^{-/-}$ mice *in vitro* (Ouchida et al, 2012; Choi et al, 2013). Hence, these results reveal a regulatory role of FcμR in BCR signaling mediating survival. Accordingly, ligation of FcμR led to serine and tyrosine phosphorylation of its cytoplasmic domain in B cells and to PLCγ and Erk activation in NK cells (Kubagawa et al, 2009; Murakami et al, 2012). However, different from other Fc receptors the FcμR lacks a conventional ITAM or ITIM, but the cytoplasmic tail contains three other conserved tyrosine residues. The most C terminal tyrosine constitutes a putative phosphorylation motif (DYIN) which matches the ITT motif (DYXN) present in membrane IgG/E and thereby is a potential docking site for Grb2 (Kubagawa et al, 2009). Thus, it is conceivable that the FcμR mediates signal integration via the ITT-like motif by the recruitment of Grb2 which due to several interaction partners provides multiple possibilities to interfere with signal transduction. Examination of the FcμR-ITT-like motif as a potential Grb2 membrane anchor has been part of this thesis.

1.3 Aims of this study

My PhD thesis is divided into three parts addressing the following issues:

1 Investigation of regulation of intracellular B cell antigen receptor signaling events by a recombinant soluble FcγIIB receptor

The recombinant soluble human FcγRIIB as a new treatment option for Ig mediated autoimmune diseases is proposed to have a dual mode of function: On the one hand it prevents binding of immune complexes to membrane bound FcγRs. On the other hand, it could also interact with membrane bound IgG as part of the BCR on memory B cells and thus interfere with the formation of antibody producing plasma cells. Here, I addressed whether the soluble FcγRIIB is able to bind to the IgG-BCR and affects BCR signaling events *in vitro*.

2 Investigation of the Erk signaling pathway following BCR activation in human B cells

The activation of Erk following BCR activation is a critical determinant in B cell development and differentiation. Studies addressing the mechanisms of Erk activation were mainly performed in chicken cells and mice suggesting a neglectable role of Grb2 in Erk activation. However, stimulation of B cells with FcγRIIB suggested an alternative route for BCR mediated Erk activation in humans independent of PLCγ2 activity and Ca^{2+} mobilization. I analyzed activation of Erk following BCR stimulation with regard to the role of Grb2 in human B cells.

3 Elucidation of the molecular characteristics and signaling properties of the FcμR

The adapter protein Grb2 was shown to be recruited to several (co)receptors upon ligation and phosphorylation of the latter. Thereby it contributes to negative and positive regulation of BCR signaling. The recently discovered FcμR carries a putative Grb2 docking site (ITT-like motif) in its cytoplasmic domain but lacks conventional signaling motifs. Here, I examined the putative ITT-like motif of the FcμR in terms of Grb2 recruitment and signaling properties.

2 Materials and Methods

2.1 Materials

2.1.1 Instruments

Table 1. Instruments used in this thesis.

Instrument/Application	Manufacturer
Agarose Gelelectrophoresis System	Peqlab
Balance BP61	Sartorius
Balance H95	Sartorius
BioPhotometer	Eppendorf
BD FACSCalibur™	Becton Dickinson
Cell culture incubator HeraCell 150 CO2	Heraeus
Centrifuge RC 3B Plus	Sorvall®
Chemi Lux Gel Imager	Intas Science Imaging
Electrophoresis power supply EPS 301	Amersham
Electrophoresis system Agarose gels	Peqlab
Electrophoresis system Hoefer SE600	Amersham
Flow cytometer LSR II	Becton Dickinson
Freezer HERAfreeze	Heraeus
Freezer Platilab 340	Angelantoni life science
Ice machine	Ziegra
Incubation shaker Unitron	Infors
Incubator Kelvitron t	Heraeus
Laminar flow cabinet HERA safe	Heraeus
Light microscope TELAVAL 31	Zeiss
Magnetic stirrer M21/1	Framo® Gerätetechnik
Mastercycler epgradient	Eppendorf
Microcentrifuge 5415D	Eppendorf
Microcentrifuge 5417R	Eppendorf
Mini PROTEAN Tetra Cell Electrophoresis system	Biorad
Multifuge 3SR	Heraeus
NanoDrop 2000	Thermo scientific
Neubauer improved cell counting chamber	Laboroptik
Nucleofector™ II Device	Amaxa/Lonza
pH-Meter inoLab ®	WTW
Rocking shaker	Neolab

Instrument/Application	Manufacturer
Semiphor Transphor Unit TE77	Amersham
Shaker 3006	GFL
Ultrasonic device Sonoplus	Bandelin
Thermomixer comfort	Eppendorf
UV illuminator	Intas systems
Vortex Genie 2	Scientific industries
Water purification system arium 611	Sartorius
Water bath	Schütt Labortechnik

2.1.2 Consumables

Table 2. Consumables used in this study.

Name	Manufacturer
1.5 ml, 2 ml reaction tubes	Greiner bio-one
10 ml Syringes	BD Bioscience
14 ml reaction tubes	Greiner bio-one
15 ml, 20 ml reaction tubes	Greiner bio-one
2 ml, 5 ml, 10 ml, 25 ml serological pipettes	Greiner bio-one
5 ml flow cytometry tubes	Sarstedt
60 mm, 100 mm, 145 mm dishes	Greiner bio-one
96 well suspension culture plates	Greiner bio-one
Cryo tubes	Greiner bio-one
Filter tips	Greiner bio-one
Nitrocellulose membrane Hybond ECL	Amersham biosciences
Parafilm	American national can
PCR tubes 0.2 ml	Sarstedt
Photometer cuvettes	Roth
Pipette tips	Greiner bio-one
Pipette tips	Greiner bio-one
Sterile filter Filtropur, S 0.2, S 0.45	Sarstedt
Whatman filter paper	GE Healthcare

2.1.3 Chemicals and reagents

Table 3. Chemicals and reagents used in this study

Name	Manufacturer
Acrylamide Rotiphorese Gel 30	Roth
Agar-Agar	Roth
Agarose	Peqlab
Ammonium persulfate (APS)	Roth
Ampicillin	Roth
L-Arginine:HCl ($^{13}C_6$)	Cambridge Isotope Lab
Bovine serum albumin	Serva
Brom-chlor:indoxyl-β-D-galactosid (X-gal)	Roth
Bromphenol blue	Merck
100x Bovine serum albumin (BSA)	NEB
Calcium chloride ($CaCl_2$)	Merck
Coomassie Brillant Blue R-250	Roth
Cytofix™ Fixation Buffer	Becton Dickinson
Dimethyl sulfoxide (DMSO)	Roth
DNA ladder GeneRuler 1 kb	Fermentas
Deoxynucleoside triphosphpate (dNTP) mix	NEB
Dithiothreitol (DTT)	Roth
Ethylendiaminetetraacetic acid (EDTA)	Roth
Ethanol	Roth
Ethidium bromide	Roth
Fetal calf serum (FCS), dialyzed	PAN biotech
Fetal calf serum (FCS)	Biochrom
D-Glucose	Roth
Glycerol	Roth
Glycine	Roth
Hydrogen peroxide (H_2O_2)	Roth
Hydrochloric acid (HCl)	Roth
4-(2-hydroxyethyl)-1-piperazineethansulfonic acid (HEPES)	Roth
Hexadimethrine bromide (polybrene)	Sigma Aldrich
Igepal CA-630 (NP40)	Sigma Aldrich
Indo-1 AM	Life technologies
Isopropyl-β-D-thiogalactopyranoside (IPTG)	Roth
Isopropanol	Roth
Kanamycin	Roth
Luminol	Sigma Aldrich

Name	Manufacturer
L-Lysine:2HCl (4,4,5,5-D_4)	Cambridge Isotope Lab
Magnesium chloride ($MgCl_2$)	Roth
Methanol (MeOH)	Roth
NEBuffer 1, 2, 3, 4, Cutsmart	NEB
NuPAGE LDS sample buffer	Invitrogen
NuPAGE sample reducing agent	Invitrogen
p-Coumaric acid	Sigma Aldrich
Penicillin	Sigma Aldrich
Phosflow™ Perm/Wash Buffer I, 10x	Becton Dickinson
Phusion HF reaction buffer	NEB
Phusion GC reaction buffer	NEB
Pluronic F-127	Life technologies
Potassium chloride (KCl)	Roth
Potassium dihydrogen phosphate (KH_2PO_4)	Merck
Prestained protein marker broad range	NEB
Protease Inhibitor Cocktail P2714	Sigma Aldrich
Puromycin	InvivoGEN
Sodium azide (NaN_3)	Roth
Sodium chloride (NaCl)	Roth
Sodium dodecyl sulfate (SDS)	Roth
di-Sodium hydrogen phosphate (Na_2HPO_4)	Roth
Sodium orthovanadate (Na_3VO_4)	Sigma Aldrich
Streptomycin	Sigmal Aldrich
T4 DNA Ligase buffer	NEB
Tetramethylethylenediamine (TEMED)	Roth
Trans-IT® 293 transfection reagent	Mirus
Tris (hydroxymethyl)-aminomethane (Tris)	Roth
Triton X-100	Roth
Trypsin	Gibco
Trypton/Pepton	Roth
Tween 20	Roth
Yeast extract	Roth

2.1.4 Buffers and solutions

Table 4. Buffers and solutions

Name	**Composition**
Antibody dilution solution	1 % BSA, 0.01 % NaN_3 in TBS-Tween
Blotting buffer	48 mM Tris, 39 mM glycine, 0.0375 % SDS, 0.001 % NaN_3, 20 % MeOH, ddH_2O
Coomassie staining solution	40 % MeOH, 10 % HOAc, 0.1 % Coomassie Brilliant Blue R250 in ddH_2O
Coomassie destaining solution	40 % MeOH. 10 % 10 % HOAc, in ddH_2O
6x DNA loading buffer	60 mM EDTA, 10 mM Tris/HCl, 60 % glycerol, 0.03 % bromophenol blue, pH7.6, in ddH_2O
ECL solution	4 ml ECL solution A, 400 µl ECL solution B, 1.2 µl H_2O_2 (30 %)
ECL Solution SA	100 mM Tris/HCl, 0.28 mM Luminol, pH 8.6, in ddH_2O
ECL solution SB	6.7 mM p-coumaric acid in 100 % DMSO
Krebs-Ringer solution	140 mM NaCl, 10 mM D-Glucose, 10 mM HEPES, 4 mM KCl, 1 mM $MgCl_2$ (1 mM $CaCl_2$), in ddH_2O
4x Laemmli loading buffer	250 mM Tris/HCl (pH 6.8), 8 % SDS, 35 % Glycerol, 0.04 % bromophenol blue, 0.3 M DTT in ddH_2O
NP-40 Lysis buffer	137 mM NaCl, 50 mM Tris/HCl (pH 7.8), 0.5 mM EDTA (pH 8), 10 % Glycerol, 1 % NP-40; added freshly: 1:50 protease inhibitor cocktail, 1 mM Sodium orthovanadate (Na_3VO_4), in ddH_2O
PBS	137 mM NaCl, 2.4 mM KCl, 4.3 mM Na_2HPO_4, 1.4 mM KH_2PO_4. pH 7.4, in ddH_2O
SDS-PAGE buffer	192 mM glycine, 25 mM Tris, 0.1 % SDS, in ddH20
Resolving gel buffer	1.5 M Tris, pH 8.8, in ddH_2O
Stacking gel buffer	0.5 M Tris (pH 6.8), in ddH_2O
TAG lysis buffer	10 mM Tris (pH 8), 50 mM KCl, 0.45 & NP40, 0.45 % Tween 20 in in ddH_2O
TAE buffer	40 mM Tris/HOAc, 10 mM NaOAc, 1 mM EDTA, pH 7.8, in ddH_2O
TBS-T	137 mM NaCl, 20 mM Tris, 0.1 % Tween20, pH 7.6, in ddH_2O
Western blot blocking solution	5 % BSA, 0.01 % NaN_3 in TBS-T

2.1.5 Oligonucleotides

Table 5. Oligonucleotides used in this study

Oligonucleotides	Sequence	Application
EcoRI GRAPEx2_fwd	ATAGAATCCGCACTGAGGAACGAGGGCTT	Cloning
EcoRI GRAPEx2_rev	GTACTTAAGTGGCTCACGTCCTCAGTGT	Cloning
EcoRI_PLCy1_fwd	ATAGAATTCTGGCGGGCGCCGCGTCCCCTTGC	Cloning
EcoRI_PLCy1_rev	ATAGAATTCCTAAAGGCGGTTGTCTCCATTGACCCG	Cloning
EcoRI-p46SHC1 fwd	ATAGAATTCTGGCTGCATCCCAACGACAAAGTC	Cloning
EcoRI-p52SHC1 fwd	ATAGAATTCCATGAGGCCCTGGACATGAACA	Cloning
EcoRI-PLCy1fwd	ATAGAATTCCTGGCGGGCGCCGCGTCCCCTTGC	Cloning
EcoRI-PLCy1fwd	ATAGAATTCCTGGCGGGCGCCGCGTCCCCTTGC	Cloning
EcoRI-PLCy1rev	ATAGAATTCGGAAGGCCGCCACAGGGGGCTGC	Cloning
EcoRI-PLCy1rev	ATAGAATTCGGAAGGCCGCCACAGGGGGCTGC	Cloning
EcoRI-SHC1rev	ATAGAATTCTCACAGTTTCCGCTCCACAGGTTG	Cloning
FcmR ITT_fwd	CAGCAGACGATCTCCGATGACTACATAAACGTGCCTGGGCAGGGAGCCTC	Mutagenesis
FcmR ITT_rev	GAGGCTCCCTGCCCAGGCACGTTTATGTAGTCATCGGAGATCGTCTGCTG	Mutagenesis
g2aFcmR ITT (YF)_fwd	CGATCTCCGATGACTTCATAAACGTGCCTGG	Mutagenesis
g2aFcmR ITT (YF)_rev	CCAGGCACGTTTATGAAGTCATCGGAGATCG	Mutagenesis
GRAPEx2_fwd	GCACTGAGGAACGAGGGCTT	Cloning
GRAPEx2_rev	GTGGCTCACGTCCTCAGTGT	Cloning
GRB2 R86K fwd	GATGGGGCCTTTCTTATCAAAGAGAGTGAGAGCGCTC	Mutagenesis
GRB2 R86K rev	GAGCGCTCTCACTCTCTTTGATAAGAAAGGCCCCATC	Mutagenesis
GRB2 SH2 R86L_fwd	GGCCTTTCTTATCCTAGAGAGTGAGAGCG	Mutagenesis
GRB2 SH2 R86L_rev	CGCTCTCACTCTCTAGGATAAGAAAGGCC	Mutagenesis
GRB2 W193K fwd	GATAACTCAGATCCCAATAAGTGGAAAGGGGCCTGCC	Mutagenesis
GRB2 W193K fwd	GGCAGGCCCCTTTCCACTTATTGGGATCTGAGTTATC	Mutagenesis
GRB2 W36K fwd	CGAAGAATGTGATCAGAACAAGTACAAGTACAAGGCAGAGCTTAATG	Mutagenesis
GRB2 W36K rev	CATTAAGCTCTGCCTTGTACTTGTTCTGATCACATTCTTCG	Mutagenesis
hFcmRcyt_fwd	ATAAGGGTACCGGCCGTTGAAAGGAGGAAA	Cloning
hFcmRcyt_rev	GTAGGATCCGAATTCTCAGGCAGGAACATTGATGTAG	Cloning
hFcmRYF_fwd	ATTCAGATGACTTCATCATGTTCCTG	Mutagenesis
hFcmRYF_rev	CAGGAACATTGATGAAGTCATCTGAAT	Mutagenesis
IGHG_fwd	ATGGACTGGACCTGGAGGATC	Cloning
IGHG1 TAG-TGG_fwd	CTTCTTCAAGGTGAAGTGGATCTTCTCCTCGGTGG	Mutagenesis
IGHG1 TAG-TGG_rev	CCACCGAGGAGAAGATCCACTTCACCTTGAAGAAG	Mutagenesis
IGHG1 Xho1_fwd	GCTGGAATTCGCCCTTACTCGAGTCCACCAAGGGCCCATC	Cloning
IGHG1 Xho1_rev	GATGGGCCCTTGGTGGACTCGAGTAAGGGCGAATTCCAGC	Cloning
IGHG1_rev	ATAGAATTCCTAGGCCCCCTGTCCGATCATGTT	Cloning

Oligonucleotides	Sequence	Application
IgMG Xho1_fwd	GTCTTCCCCCTCGAGTCCTGCGAGAGCC	Cloning
IgMG Xho1_rev	GGCTCTCGCAGGACTCGAGGGGGAAGAC	Cloning
PLCy2 Ex2 EcoRI fw	ATA GAA TCC CGA TTC CTT CCT TCT CC	Cloning
PLCy2 Ex2 EcoRI rev	GTA CTT AAG CTA TGA GTT TCT GCA GGC	Cloning
PLCy2 Ex2001 fwd	TCCCGATTCCTTCCTTCTCC	Cloning
PLCy2 Ex2001 rev	AGCTATGAGTTTCTGCAGGC	Cloning
SHC1Ex5TV2fwd	GGTGCTAAGGGGAGATCTAG	Cloning
SHC1Ex5TV2rev	TGATTCACAGGGTCTTTGGC	Cloning
SHC1Guide#5fwd	CACCGCAAATGAGATAGATTGCATG	CRISPR
SHC1Guide#5rev	AAACCATGCAATCTATCTCATTTGC	CRISPR

2.1.6 Enzymes

Table 6. Enzymes used in this study

Enzymes	Company
Calf intestine phosphatase (Cip)	NEB
Dpn1	NEB
Phusion® DNA polymerase	NEB
Plasmid-Safe™	Biozym
Restriction endonucleases	NEB
Taq DNA polymerase	NEB
T4 DNA Ligase	NEB

2.1.7 Reaction systems (Kits)

Table 7. Ready-to-use reaction systems.

Kit	Company
CD19 pluriBead® Cell separation kit	pluriselect
First strand cDNA synthesis Kit	Fermentas
Human B cell nucelofector® Kit	Lonza
Invisorb® spin plasmid mini two	Invitek
NucleoSpin® RNA	Macherey-Nagel
The original TA cloning® kit	Invitrogen
Wizard® SV Gel and PCR clean up kit	Promega

2.1.8 Plasmids

Table 8. Cloning vectors

Vector	cDNA	Source
pBluescript	IgG/M	N. Engels
pBluescript	IgG/M_Xho1	This thesis
pBluescript	VH-IGHG1	This thesis
pBluescript	VH-IGHG1 TAG-TGG	This thesis
pCR 2.1	hFcmR-Cyt	This thesis
pCR TOPO	IGHG1	This thesis
pCR TOPO	IGHG1_Xho1	This thesis
pCR2.1	CD8/hFcmR-Cyt	This thesis
pCR2.1	CD8/hFcmR-Cyt (Y385F)	This thesis
pCR2.1	CD8/αITT	N. Engels
pCR2.1	g2a wt	N. Engels
pCR2.1	g2a-(ITT-Fcmr)	This thesis
pCR2.1	g2a-(ITT-Fcmr) YF	This thesis
pCR2.1	g2a-DAP10	N. Engels
PCR2.1	g2aFcmR (Y385F)	This thesis
PCR2.1	g2aFcmR WT	This thesis
pCR2.1	GRAP	N. Engels
PCR2.1	hFcmRcyt (Nhe1)	This thesis
pCR2.1	mGrb2 R86K	L. König
pCR2.1	mGrb2 W193K	L. König
pCR2.1	mGrb2 W36K	L. König
pCR2.1	mGrb2 W36K R86L W193K	This thesis
pCR2.1	mGrb2 wt	L. König
pCR2.1	SHC1 p46	This thesis
pCR2.1	SHC1 p52	This thesis
pCR-Blunt II TOPO	hFcmR(Y385F)	This thesis
pCR-Blunt II TOPO	human FcμR	H. Kubagawa
pCR-XL-TOPO	PLCy1	Dharmacon
p-OTB7	SHC1 p52 complete cDNA	Dharmacon

Table 9. Retroviral expression vectors

Construct	Description	Source
pMSCV-puro	CD8/hFcmR-Cyt	This thesis
pMSCV-puro	CD8/hFcmR-Cyt (Y385F)	This thesis
pMSCV-puro	g2a wt	This thesis
pMSCV-puro	g2a YF	This thesis
pMSCV-puro	g2a-(ITT-Fcmr)	This thesis
pMSCV-puro	g2a-(ITT-Fcmr) YF	This thesis
pMSCV-puro	g2aFcmR (Y385F)	This thesis
pMSCV-puro	g2aFcmR wt	This thesis
pMSCV-puro	GFP	K. Schulz
pMSCV-puro	GRAP	This thesis
pMSCV-puro	hFcmR	This thesis
pMSCV-puro	hFcmR (Y385F)	This thesis
pMSCV-puro	mGrb2 R86K	This thesis
pMSCV-puro	mGrb2 W193K	This thesis
pMSCV-puro	mGrb2 W36K	This thesis
pMSCV-puro	mGrb2 W36K R86L W193K	This thesis
pMSCV-puro	mGrb2 wt	This thesis
pMSCV-puro	RasGRP3-HA	K. Gronke
pMSCV-puro	VH-IGHG1	This thesis
pMSCV-puro	VH-IGHG1 TAG-TGG	This thesis
pMSCV-puro/monomeric GFP/T7 tag	PLCy2	N. Engels
pMSCVpuro-IE	-	C. Hitzing
pMSCVpuro-pCitrine	PLCγ1	This thesis

Table 10. GST expression vectors

Vector	Insert	Source
pGEX-4T1	Grb2-SH2	N. Engels
pGEX-4T1	Grb2-SH2 R86L	N. Engels

Table 11. TALEN and CRISPR/Cas cloning vectors

Vector	Source
pTAL4Titanium	C. Hitzing
pFusA5A	C. Hitzing
pFusA5B	C. Hitzing
pFusA5C	C. Hitzing
pFusB1B	C. Hitzing
pFusB2B	C. Hitzing
pFusB3B	C. Hitzing
pFusB4B	C. Hitzing
pFusB4	C. Hitzing
pSpCas9(BB)-2A-GFP	Addgene

Table 12. Transient expression vectors for gene targeting

Vector	Insert	Source
pmaxKS IRES EGFP	GRAP Ex2 TAL1	This thesis
pmaxKS IRES EGFP	PLCG1 Ex2-3 TAL1	K. Vanshylla
pmaxKS IRES EGFP	PLCG2 Ex2 TAL1	This thesis
pmaxKS IRES tagRFP	GRAP Ex2 TAL2	This thesis
pmaxKS IRES tagRFP	PLCG1 Ex2-3 TAL2	K. Vanshylla
pmaxKS IRES tagRFP	PLCG2 Ex2 TAL2	This thesis
pSpCas9(BB)-2A-GFP	SHC1 Ex5	This thesis

2.1.9 Software and data bases

Table 13. Software

Application	Name	Manufacturer
Flow cytometer data acquisition	FACSDiva	BD Bioscience
Flow cytometer data analysis	Flowjo	Treestar
Image processing	ImageJ	W. Rasband
Sequence data analysis	Clone manager	Sci-Ed software
Sequence data analysis	Finch TV	Geospiza
Text processing	Microsoft office	Microsoft
Western blot documentation	Chemostar professional	Intas

Table 14. Data bases

Program	Application
http://crispr.mit.edu/	CRISPR design
http://web.expasy.org/translate/	DNA-Protein translation
http://www.ensembl.org/index.html	Genomic blast
http://www.ncbi.nlm.nih.gov/	Genomic blast
http://bioinfo.ut.ee/primer3-0.4.0/	Primer design
http://www.uniprot.org/	Protein information
http://multalin.toulouse.inra.fr/multalin/	Sequence alignment
https://tale-nt.cac.cornell.edu/node/add/talen	TALEN design

2.1.10 Antibodies and B cell stimulation reagents

Table 15. Antibodies and reagents used for cell stimulation.

Antibody/reagent	Company
dimeric soluble FcγRIIB	provided by SuppreMol, part of Baxalta (now part of Shire)
goat F(ab')2 α-human IgG	Jackson Immuno Research
goat F(ab')2 α-human IgM	Jackson Immuno Research
goat F(ab')2 α-mouse IgG	Jackson Immuno Research
goat-α-mouse IgG-BIOT	Southern biotech
monomeric soluble FcγRIIB	provided by SuppreMol, part of Baxalta (now part of Shire)
monomeric soluble FcγRIIB-bio	provided by SuppreMol, part of Baxalta (now part of Shire)
streptavidin	Jackson Immuno Research

Table 16. Primary antibodies for Western blot analysis. Primary antibodies were diluted according to the manufacturer's instructions in 1% BSA/TBS-T and 0.01 % NaN_3

Primary antibody	Isotype	Company
α-Actin	rabbit	Sigma Aldrich
α-Actin	mouse IgG2b	CST
α-BLNK	mouse IgG2a	Becton Dickinson
α-BTK	rabbit	CST
α-CD79a (EP3618)	rabbit	Abcam
α-Erk	mouse IgG2a	Becton Dickinson
α-FYB/SLAP130	mouse IgG1	Becton Dickinson
α-GRAP	rabbit	ATLAS antibodies
α-Grb2 (3F2)	mouse IgG1	Millipore
α-pAkt (Ser473) (D9E)	rabbit	CST
α-pBLNK (Tyr96)	rabbit	CST

Primary antibody	Isotype	Company
α-pErk (E10)	mouse IgG1	CST
α-PLCγ1	rabbit	Santa Cruz
α-PLCγ2	rabbit	Santa Cruz
α-RasGRP1	mouse IgG1	Santa Cruz
α-RasGRP2	rabbit	Abcam
α-RasGRP3	mouse IgG1	Santa Cruz
α-SHC (HPA046595)	rabbit	Abcam

Table 17. Secondary antibodies for Western blot analysis. Secondary antibodies were diluted 1:10000 in TBS-T

Secondary antibody	Isotype	Company
α- mouse IgG1-HRP	goat	Southern biotech
α-mouse IgG2a-HRP	goat	Southern biotech
α-mouse IgG2b-HRP	goat	Southern biotech
α-mouse IgG-HRP	goat	Southern biotech
α-rabbit IgG-HRP	goat	Southern biotech

Table 18. Antibodies for FACS analysis

Antibody	Fluorochrome	Isotype	Company
α-human IgM	FITC	goat F(ab')2	Southern biotech
α-CD19	PE-Cy7	mouse	Becton Dickinson
α-human IgG	FITC	goat	Southern biotech
α-mouse IgG2a	Cy5	goat	Southern biotech
α-pErk (Thr202/Tyr204)	ALEXA Fluor® 647	mouse IgG1	Becton Dickinson

2.1.11 Media

Table 19. Media for eukaryotic cell lines

Medium	Company	Cell type	Supplements
DMEM	Merck Millipore	Plat E	10 % FCS 1 % Penicillin/Streptomycin 1 mM L-Glutamine
RPMI 1640	Merck Millipore	DG75, DOHH2, HF1, Raji, Ramos, SUDHL, JURKAT	10 % FCS 1 % Penicillin/Streptomycin 1 mM L-Glutamine
SILAC RPMI 1640	Thermo scientific		10 % dialyzed FCS, 0.12mM L-arginine (13C6) (+6), 0.27mM L-lysine (4,4,5,5-D4) (+4), 1 % Penicillin/Streptomycin

Table 20. Media for bacteria. LB medium was used for E.coli Top10F' or gene hogs; YT medium was used for protein expression in E.coli BL21. Before use, media were autoclaved for 30 min at 121°C, 1.25 bar. For selection, media were supplemented with the respective antibiotics: 100 µg/ml Ampicillin, 50 µg/l Kanamycin, 50 µg/ml Spectinomycin, 10 µg/ml Tetracyclin.

Medium	Ingredients
LB medium	10 g/l tryptone 5 g/l yeast extract 5 g/l NaCl pH 7
YT medium	16 g/l tryptone 15 g/l yeast extract 5 g/l NaCl pH7

2.1.12 Bacteria

Table 21. Bacterial strains used in this study. TOP10F' were

Strain	Manufacturer
One Shot TOP10F' chemically competent *E.coli*	Invitrogen
One Shot BL21 (DE3) chemically competent *E.coli*	Invitrogen
Electrocomp™ GeneHogs® E	Invitrogen

2.1.13 Eukaryotic cell lines

DG75 (DSMZ-No: ACC 83)

Human burkitt lymphoma cell line derived from a pleural effusion of a 10-year old boy with Burkitt lymphoma (refractory, terminal) in 1975. Epstein-Barr virus (EBV)-negative suspension cell line that expresses IgM paired with a κ light chain (membrane bound and secreted) (Gabay et al, 1999). In this work DG75 EB (EcoBlast) cells (generated by L. König) transduced with an ecotropic receptor were used to enable efficient retroviral transduction with ecotropic viruses

Table 22. Knock-out cell lines derived from DG75.

Genetic background	**Source**
BTK-/-	W. Schulze (Engels et al, 2014)
GRAP-/-	This work
GRB2-/-	J. Lutz (Engels et al, 2014)
GRB2/GRAP-/-	This work
PLCG1-/-	K.Vanshylla, unpublished
PLCG1/2-/-	This work
PLCG2-/-	This work
SHC1-/-	This work
SLP65-/-	C. Hitzing (PhD thesis 2015)

DOHH-2

Non-Hodgkin's lymphoma derived, EBV-negative B cell line expressing surface IgG paired with a λ light chain (Kluin-Nelemans et al, 1991)

HF-1

Phenotypically mature EBV-negative B cell line derived from a patient with follicular lymphoma expressing surface IgG paired with a κ light chain (Eray et al, 1994).

SUDHL-4

SUDHL (Southwestern University Diffuse Histiocytic Lymphoma) 4 is a diffuse histiocytic lymphoma cell line expressing surface IgG paired with a κ light chain. (Epstein & Kaplan, 1979)

Raji

Burkitt's lymphoma derived EBV-positive B cell line expressing surface IgM with κ light chain (Epstein et al, 1966).

Ramos

Burkitt's lymphoma derived EBV-negative B cell line expressing surface IgM with λ light chain (Klein et al, 1975).

JURKAT

Immortalized T cell line isolated from peripheral blood of a boy with T-cell leukemia (Schneider et al, 1977).

Platinum-E (PlatE)

HEK 293T-derived retroviral packaging cell line stably transfected with the structural genes *gag, pol* and *env* of the moloney murine leukemia virus (MMLV) for generation of viral particles used for retroviral transduction (Morita et al, 2000).

2.2 Methods

2.2.3 Molecular Biology

2.2.3.1 Isolation of genomic DNA

To isolate genomic DNA from human B cell lines, cells were collected and washed in PBS. $1x10^6$ cells were resuspended in 200 µl Tag lysis buffer plus 1 µl proteinase K and incubated at 55°C for 3 h, following a 15 min incubation step at 95°C. Lysates were either directly used for polymerase chain reaction (PCR) or stored at -20°C until further use.

2.2.3.2 Generation of cDNA libraries

Isolation of mRNA

Isolation of mRNA was performed by using a NucleoSpin® RNA reaction kit (Macherey-Nagel) according to the manufacturer's recommendations. mRNA concentrations were measured by the NanoDrop 2000 (Thermo scientific). mRNA was directly used for transcription to cDNA or stored at -80°C until further use.

Reverse transcription of mRNA

For reverse transcription of mRNA into cDNA the First strand cDNA synthesis Kit (Fermentas) was used following the manufacturer's instructions regarding single strand cDNA synthesis. cDNA was directly used for PCR or stored at -20°C until further use.

2.2.3.3 Polymerase chain reaction (PCR)

Primer design

Primers were designed by using the web based program primer 3 (http://primer3.ut.ee/) considering the following guidelines (Primer guidelines, Howard Judelson, 10.06, p. 1):

1. Melting temperature (Tm) between 55 and 65°C (usually corresponds to 45-55% G+C for a 20-mer)
2. Absence of dimerization capability
3. Absence of significant hairpin formation (usually >3 bp)
4. Lack of secondary priming sites in the template
5. Low specific binding at the 3' end, to avoid mispriming

Primers were ordered and synthesized from eurofins MWG.

PCR sample preparation and amplification program

Amplification of DNA fragments from cDNA templates or genomic DNA was performed by using PCR. Therefore, in general Phusion® DNA polymerase was used. Samples were prepared according to the protocol supplied with the polymerase as depicted in the following table (table 23).

Table 23. Composition of the PCR reaction mix

Vol [µl]	Reagent	Final Concentration
10	5x Phusion® HF buffer or GC buffer(*)	1x
1	dNTPs (10 mM, New England Biolabs)	200 µM
2.5	Forward primer (10 µM)	0.5 µM
2.5	Reverse primer (10 µM)	0.5 µM
1.25	DMSO (optional)	2,5%
1	Template	50–250 ng/µl
0.5	Phusion® polymerase (2,000 units/ml); New England Biolabs)	1 Units/50 µl PCR
	ddH_2O (to 50 µl)	

(* GC buffer was used for DNA templates with high GC content)

The PCR was carried out following the protocol supplied with the Phusion® polymerase (New England Biolabs) as designated in the subsequent table (table 2). Annealing temperature was adjusted to ca. 3 -5°C below the melting temperature of the primers (Tm_{primer}). Elongation time was chosen according to the size of the template (30 sec/kb).

Table 24. Standard PCR program

	Step	Temperature	Time
	Initial denaturation	98°C	5 min
35 cycles	Denaturation	98°C	30 sec
	Annealing	x °C (*)	10 sec
	Elongation	72°C	30 sec/kb
	Final Elongation	72°C	10 Min
	Stop	11°C	∞

* Annealing temperature = Tm_{primer} – 3-5°C

PCR products were separated and analyzed by agarose gel electrophoresis. For further use the DNA was extracted from the gel by using the Promega Wizard® SV Gel and PCR Clean-Up System

2.2.3.4 Site directed mutagenesis

In order to change single bases within a cDNA-containing plasmid to achieve the exchange of single amino acids within the respective protein, PCR site-directed mutagenesis (SDM) was

performed. Thereby, the whole plasmid serves as a template and needs to be amplified. To this end, complementary primers with the desired mutation were designed and analyzed by using the web-based program primer x (http://www.bioinformatics.org/primerx/) considering the following guidelines.

1. Primer length: between 25 and 45 bases
2. Melting temperature ≥ 78°C (considering the percentage of mismatch)
3. The desired mutation should be in the middle of the primer with ~10-15 bases of correct sequence on both sides
4. GC content: at least 40 %
5. Primer should terminate in one or more C or G bases

PCR reaction mix and PCR program were chosen as described in the previous section (table 23 & 24). Following PCR, the PCR product was incubated with 1 µl of Dpn1 for 1 h at 37°C in order to enzymatically remove the original plasmid. Amplification of the plasmid and digest of the original plasmid by Dpn1 were analyzed by agarose gel electrophoresis. After Dpn1 treatment, 2 µl of the reaction mix were used for transformation of competent bacteria (Top10').

2.2.3.5 Restriction enzyme digest

Preparative digest

Preparative digest of DNA was performed in order to prepare for ligation of DNA fragments; usually for ligation of an insert into another vector backbone. Therefore, 2-3 µg of DNA were incubated with the respective restriction enzyme(s) (NEB) and the appropriate buffer composition according to the manufacturer's instructions for 2-3 h at 37°C. If only one enzyme was used for restriction digest, the vector backbone had to be additionally treated with Calf intestinal alkaline phosphatase (Cip; NEB) for at least 45 min to prevent re-ligation of the vector backbone due to self-compatible ends. DNA fragments were separated by agarose gel electrophoresis followed by gel extraction.

Analytical digest

For analytical digest the reaction mix was assembled as above-mentioned according to the manufacturer's instructions regarding the respective enzyme. Incubation was performed for 1 h at 37°C. The digest was analyzed by agarose gel electrophoresis.

2.2.3.6 Agarose gel electrophoresis

The agarose gel was prepared by dissolving the appropriate amount of 0.7-2% agarose (Peqlab) in TAE buffer and heating of the suspension to near-boiling point. After cooling of the melted agarose to ~50°C, 0.1 % (v/v) ethidium bromide were added and the agarose was poured into a horizontal casting tray with a comb to create the sample wells. Once the gel has set completely, the gel was transferred to the agarose gel electrophoresis chamber (Peqlab) and covered with TEA buffer. The comb was removed and the samples were loaded after addition of 6x DNA loading buffer. Agarose gel electrophoresis was performed at 220 mA and 100 V for 30-45 min.

2.2.3.7 Purification of DNA from agarose gel

DNA fragments were extracted from agarose gels by using the Promega Wizard®SV Gel and PCR Clean-Up System. Therefore, the bands corresponding to the size of the product were cut out and extracted following the manufacturer's instructions. DNA was eluted with 40 µl of nuclease free H_2O.

2.2.3.8 TA cloning

Cloning of PCR products into the pCR2.1 vector via TA cloning requires the addition of a 3'-adenine overhang at each end of the PCR product. Therefore, PCR products were run on agarose gel and purified as described in section 2.2.3.7. After purification, DNA was eluted in 20 µl nuclease free water instead of 40 µl. For the reaction 2 µl of Taq buffer, 1 mM of dATPs and 0.2 µl of Taq polymerase were added and the mix was incubated at 72°C for 20 min. Afterwards, the DNA fragment was ligated into pCR2.1 topo as described in the following section and used for bacterial transformation. Blue-white selection was used to check for success of ligation. Therefore, transformed bacteria were plated along with 40 µl Brom-chlor:indoxyl-β-D-galactosid (XGal; 50 mg/ml in DMF) and 40 µl 0.1 M Isopropyl-β-D-thiogalactopyranoside (IPTG). Bacteria

that incorporated a plasmid with inserted DNA fragment formed white colonies, while Bacteria carrying a plasmid without insert formed blue colonies.

2.2.3.9 Ligation of DNA fragments

Following purification from agarose gel (section 2.2.3.7), DNA fragments were ligated according to the protocol supplied by NEB. Therefore, 4 µl of DNA insert were mixed with 0.5-1 µl of the respective vector, 0.5 µl T4-DNA ligase, and 1 µl 10x ligase buffer. The total volume was adjusted to 10 µl with ddH_2O. The ligation mix was incubated either for 1 h at room temperature or overnight at 16°C. Afterwards, ligation mix was ready for transformation of bacteria.

2.2.3.10 Transformation of chemically competent bacteria

For transformation, 2-5 µl of plasmid DNA were added to an aliquot of chemically competent bacteria (TOP10F', GeneHog or BL21). After 30 min incubation on ice the bacteria were incubated at 42°C for 30 s, followed by a 2 min incubation step on ice. Bacteria transformed with plasmids carrying an ampicillin resistance were plated directly on selective LB agar plates. Bacteria transformed with kanamycin-resistance plasmids required a further incubation step in 1 ml of antibiotic-free LB medium at 37°C for at least 30 min. Plated bacteria were incubated at 37°C for 12-16 hours maximum.

2.2.3.11 Preparation of Plasmid DNA

In order to expand bacteria for isolation of Plasmid DNA, 4 ml of selective LB medium were inoculated with single clones from plated bacteria and incubated at 37°C for 12-16 hours. Preparation of plasmid DNA was performed using the Invisorb® Spin Plasmid Mini Two preparation kit (Invitek) according to the manufacturer's instructions. Different from the protocol, elution of DNA was done in 40 µl nuclease free water instead of 50 µl of the supplied elution solution.

2.2.3.12 Sequencing of DNA

Sequence validation of PCR products or plasmids was performed by the DNA sequencing service of the company Seqlab (Sequence Laboratories, Goettingen). In preparation for the sequencing 1.2 µg of the DNA sample were added to a total volume of 15 µl (filled up

with ddH_2O). Sequencing primers were either added directly to the mix in a total concentration of 30 pmol or chosen from the Seqlab standard primer list.

2.2.4 Genome editing techniques

In order to generate constitutive knock-out cell lines, two techniques, namely the Transcription Activator-like Effector Nuclease (TALEN) -based or the Clustered Regularly Interspaced Short Palindromic Repeats (CRISPR)/Cas-based genome editing technique were applied. Both techniques are useful tools to target distinct DNA sequences in order to modify genes of interest by introduction of double strand breaks. The cell's DNA repair mechanisms induce errors leading to an incomplete or unfunctional gene product (Pu et al, 2015).

Transcription activator-like effector nucleases (TALEN) are composed of a TAL effector DNA binding domain (TALE) that can be engineered to bind any DNA sequence and a nuclease (FokI) (figure 5 a). The tandemly arranged modules of the DNA binding domain consist of 34 amino acids, which are almost identical for each repeat; except for two amino acids at position 12 and 13 termed repeat variable diresidue (RVD). Four different variants of RVDs that either bind G, A, T or C, establish the DNA binding specificity of the DNA binding domain. Since the FokI activity requires dimerization, a TALEN pair needs to be generated recognizing DNA sequences to the left and to the right site of the intended cut site (Pu et al, 2015). Assembly of the tandem repeats of the DNA binding domain specific for a desired target requires several steps of cloning. The CRISPR/Cas genome editing technique uses a so called guide RNA (gRNA), which specifically binds to the target DNA, to direct the nuclease (Cas9) to the desired cut site (figure 5b). Furthermore, for efficient DNA binding, the Cas9 requires a protospacer adjacent motif (PAM) adjacent to the 5' end of the targeted DNA region. The Cas9 introduces double-strand breaks (DSBs) ~3 bp upstream of the PAM sequence (Ran et al, 2013, Pu et al, 2015). In contrast to the TALEN-technique the CRISPR/Cas system only requires a single step of cloning which makes the design of constructs much easier.

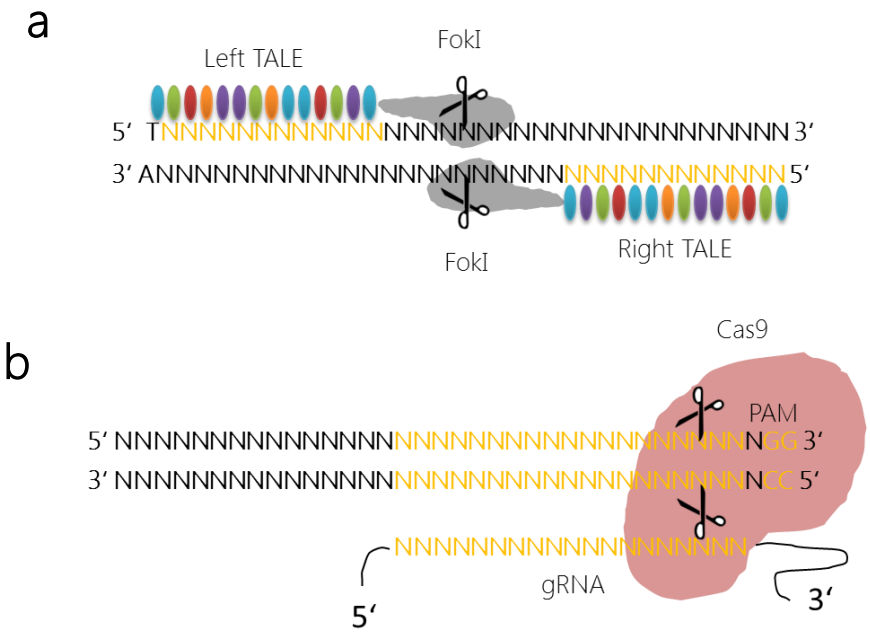

Figure 5. Genome editing by TALEN- and CRISPR/Cas sytems. (a) TALEN-based genome editing. Tandem repeats of the DNA-binding domains (TALE) depicted in blue, green, red and purple spheres bind to the target sequences (orange; N being any nucleotide) in order to induce dimerization of the nuclease FokI (grey) leading to induction of a double strand break (DSB). (b) CRISPR/Cas-based genome editing. Guide RNA (gRNA) pairs with the nuclease Cas9 (red) and together with the protospacer adjacent motif (PAM) guides it to the target sequence (orange; N being any nucleotide) in order to induce a DSB (modified from Pu et al, 2015)

2.2.4.1 TALEN-based genome editing

TALEN design and Golden Gate TALEN assembly

TALEN constructs were planned by using the web based program "TAL Effector Nucleotide Targeter 2.0" (https://tale-nt.cac.cornell.edu/). Thereby, the TALEN cut site was chosen to lie within a suitable restriction site for later activity tests. TALEN assembly was performed following the protocol supplied with the Golden Gate TALEN and TAL Effector Kit 2.0 (addgene; modified; see also PhD thesis, C. Hitzing). After TALEN assembly, the two constructs encoding the TALEN pair were subcloned into two different pMAX vectors carrying a red fluorescent protein (RFP) or green fluorescent protein (GFP) expression cassette, respectively. Both constructs were introduced simultaneously into DG75 B cells by nucleofection as described in section 2.2.6.4. RFP and GFP expressing, double positive cells were enriched by flow cytometry based cell sorting as

described in section 2.2.6.7 48 h after electroporation. Once the cells have recovered from the cell sorting procedure, they were subcultured by seeding one cell per well in 96 well plates.

Activity test

To test the activity of the TALEN constructs, genomic DNA was isolated from the population by cell sorting. Following, the exon targeted by the TALEN constructs was amplified by PCR. The PCR product was separated on agarose gel and extracted from the gel. Different from the gel extraction protocol, the DNA was eluted in 20 µl instead of 40 µl. The purified PCR product was incubated with the appropriate restriction enzyme according to the manufacturer's instructions. The digested PCR product was analyzed by agarose gel electrophoresis. TALEN constructs could be confirmed as active, once the restriction site was no longer intact, leading to an incomplete digest of the PCR product.

Screening of potential knock out clones

Single cell clones were expanded and analyzed for deficiency of the respective protein by Western blot analysis (2.2.5.7). Single cell clones that displayed low expression or a complete lack of expression were subjected to sequence analysis of the exon to verify the defect on DNA level. Therefore, the exon targeted by the TALEN constructs was amplified by PCR from genomic DNA of the single cell clone. The PCR product was subcloned into pCR2.1 in order to get a single sequence of each allele of the exon. To confirm the exon sequence, at least seven exons were sent for sequencing. Cells were considered as knock-out cell lines, when both alleles of an exon showed a deletion, leading to an early stop codon.

2.2.4.2 CRISPR/Cas–based genome editing

For cloning of CRISPR/Cas-based genome editing constructs I used a pSpCas9(BB)-2A-GFP vector (gift from the Zhang lab; addgene plasmid #48138), which encodes all necessary elements on one vector. Design of guide RNA was performed by using the CRISPR/Cas Design software (http://crispr.mit.edu/). Guide RNAs were selected that had a high score, which corresponds to low numbers of off-targets and that overlapped with a restriction site for later activity tests. Phosphorylated oligonucleotides encoding the guide RNA were ordered from eurofins MWG. Assembly of the CRISPR/Cas construct was performed according to the protocol of the Zhang

lab (Ran et al, 2013). Following steps including nucelofection, activity test and screening of potential knock-out clones were conducted as described for the TALEN-based genome editing method (2.2.4.1).

2.2.5 Biochemistry

2.2.5.1 Stimulation of the B cell receptor for signaling analysis

Cells were harvested by centrifugation (300 rcf, 4 min) and washed 1x with PBS. Subsequently, cells were starved in R0 medium (RPMI w/o FCS) at 37°C for 30 min in order to reduce stimulatory effects due to the FCS. For expression and phosphorylation studies 1-2x10^6 cells per sample were reconstituted in 100 µl R0, while for interaction studies (affinity purification or immunoprecipitation) 3-4x10^7 cells per sample were reconstituted in 1 ml of R0. Following starvation, the cells were stimulated via the BCR with 10 µg/ml anti (α)-IgM F(ab')2 or α-IgG F(ab')2, depending on the Ig isotype of the respective cell type. Stimulation was performed at 37°C and stimulation times were chosen according to the type of experiment. In order to stop the stimulation process, cells were pelleted quickly by a short run of centrifugation and washed once with ice cold PBS (300 rcf, 4°C). Subsequently, cells were lysed as described in the next section (2.2.5.2).

2.2.5.2 Preparation of cleared cellular lysates

For preparation of cleared cellular lysates (CCL), cells were resuspended in 20 µl of 0.1% NP40 lysis buffer per 1x10^6 cells and incubated on ice for at least 15 min. For lysis of higher cell numbers, incubation was performed at 4°C under mild rotation. Following lysis, the cytosolic fraction was cleared from nuclei and cell debris by centrifugation at 16000 rcf, 4°C for 15 min. The supernatant was transferred to a fresh 1.5 ml Eppendorf tube and supplemented with one-fourth volume of 4x Laemmli loading buffer in preparation for the SDS-PAGE. Samples were boiled at 95°C for 3 min and stored at -20°C until further use.

2.2.5.3 Immunoprecipitation

For immunoprecipitation (IP) 35x10^6 cells were stimulated and lysed as described before (2.2.5.2). For mIgG-IP cells were directly stimulated with 10 µg/ml of the precipitating antibody (biotinylated- goat-α-mouse IgG; Southern biotech) instead of α-IgG F(ab')2. In order to

precipitate the IgG-BCR, lysates were incubated with Streptavidin Sepharose® Bead Conjugate (CST) for 1 h at 4°C under mild rotation. Following, the beads were washed 3x with NP-40 lysis buffer, resuspended in 30 µl 4x Laemmli buffer and boiled at 95°C. Lysates were either stored at -20°C until further use or analyzed directly on SDS-PAGE/Western Blot.

2.2.5.4 Affinity purification

Expression and purification of GST fusion proteins

GST fusion proteins for affinity purification were produced in the *E.coli* strain BL21. Therefore, bacteria were transformed with the respective cDNA cloned into the bacterial expression vector pGEX as described before (2.2.3.10) Single colonies were transferred to 4 ml 2YT medium, grown over night at 37°C under mild agitation (300 rcf) and transferred to a 50 ml culture the next day. Cell expansion was controlled by measuring the optical density (OD) at 600 nm. Protein expression was induced at an OD_{600} = 0.6 with 100 µM IPTG at 37°C and mild agitation for 3-5 h. Expression of the construct coding for GST-Grb2-SH2 R86L required incubation at 25°C instead of 37°C in order to increase protein yield. Afterwards, cells were pelleted by centrifugation (3000 rcf, 30 min) and the supernatant discarded. At this point cells were either stored at -80°C until further use, or directly resuspended in 2 ml PBS plus proteinase inhibitor (50x). Cells were lysed by sonication (3x 30 sec, 1 cycle, 50 %) on ice. Subsequently, lysates were supplemented with 0.25 % of 10 % TritonX-100 and incubated on ice for 30 min. Afterwards, lysates were cleared by centrifugation at 6000 rcf and 4°C for 20 min. 100 µl Glutathione Sepharose 4B (GE healthcare) were washed once in PBS in order to remove containing ethanol and added to the cleared lysates. Samples were incubated for 2 h at 4°C under mild agitation. Following, beads were washed twice with PBS and reconstituted in 100 µl PBS for storage. Purification yield of the samples was determined by running 2 µl of the sample along with a BSA standard on SDS-PAGE following Coomassie staining.

GST-pulldown assay

For GST-pulldown assay, $35x10^6$ cells per sample were stimulated via the BCR and lysed as described before (2.2.5.2). After clearance of lysates by centrifugation, lysates were mixed with ~10 µg of GST-fusion protein (equal ca. 25-30 µl of bead slurry) and incubated for 1h at 4°C

under mild rotation. Subsequently, beads were washed 3x with NP-40 lysis buffer by centrifugation (500 rcf, 4°C) and proteins were eluted by adding 30 µl of 4x Laemmli buffer boiling at 95°C for 3 min. Afterwards, samples were directly analyzed by SDS-PAGE and Western Blot or stored at -20°C until further use.

2.2.5.5 SDS polyacrylamide gel electrophoresis

For separation of proteins from CCLs, affinity purification or IP samples, discontinuous SDS-PAGE (sodium dodecyl sulfate polyacrylamide gel electrophoresis) was used, as originally established by U. Laemmli. SDS-PAGE facilitates separation of proteins according to their electrophoretic mobility (size, conformation and charge) under denaturing conditions (Laemmli, 1970). Discontinuous polyacrylamide gels consist of a stacking gel for initial concentration of the proteins and a resolving gel for separation of proteins. Solution for each, stacking and resolving gel, were prepared as depicted in the following table (table 25)

Table 25. Composition of Resolving and Stacking gel for SDS polyacrylamide gel electrophoresis

Reagent	**Resolving gel**	**Stacking gel**
1.5 M Tris/HCL (pH 8.8)	375 mM	-
0.5 M Tris/HCL (pH 6.8)		125 mM
Acrylamid	10 %	4.8 %
TEMED*	0.1 %	0.1 %
10 % APS*	0.1 %	0.1 %
ddH2O	To final volume	To final volume

*TEMED and APS were added directly before polymerization

First, the resolving gel was polymerized between two glass plates before the stacking gel was casted on top with a comb to form sample wells. After polymerization, samples were loaded along with a Prestained protein marker broad range (NEB). Gel electrophoresis was performed by using either the Mini PROTEAN system (Biorad) at a current of 15-25 mA or the electrophoresis system Hoefer SE600 (Amersham) at a current of 7-10 mA (o/n) or 20-40 mA (by day). Following SDS-PAGE, the gel was either subjected to Coomassie staining or Immunoblot.

2.2.5.6 Coomassie staining

For unspecific visualization of proteins separated on SDS-PAGE the dye Coomassie Brilliant Blue R-250 was used. Therefore, the gel was stained in Coomassie Brilliant Blue for 10-20 min at RT. Following, the gel was incubated in Coomassie destaining solution for 20 min or in ddH_2O o/n at RT in order to destain the polyacrylamide gel and visualize the proteins.

2.2.5.7 Western blot

For specific analysis of proteins by immunoblot the cellular lysates separated on SDS PAGE were transferred from the gel to a nitrocellulose membrane by using the semi dry western blot technique (Towbin et al, 1992). Therefore, the nitrocellulose membrane, the gel and two pieces of Whattman paper were equilibrated in 1x blotting buffer. To facilitate transfer of negatively charged proteins to the nitrocellulose membrane, the components were assembled in the following order from the bottom to the top: [Cathode] – bottom Whattman paper – nitrocellulose membrane – SDS gel – upper Whattman paper - [Anode]. Transfer was performed with constant amperage of 1 mA/cm² for 70 min. Voltage was restricted to 16 V. Following transfer, the membrane was incubated in blocking solution (5% BSA in TBS-Tween + 0.1 % NaN_3).

Incubation with primary antibody was performed at 4°C o/n or at RT for 1h. Afterwards, the membrane was washed with TBS-Tween three times for 20 min before it was incubated with a HRP-labeled secondary antibody (1:10 000 in TBS-T) for 1 h at RT. Following, the membrane was washed again three times for 20 min with TBS-T. The immobilized proteins were visualized by adding ECL solution to the membrane. The emitted chemiluminescence resulting from the reaction of the HRP with the ECL solution was recorded by the Chemi Lux Gel Imager (Intas).

2.2.6 Cell Biology

2.2.6.2 Cell culture and maintenance

All human B cell lines were cultured in RPMI supplemented with 10% FCS, 1 % Penicillin/Streptomycin and 1 mM L-Glutamine (further referred to as R10 medium). For maintenance DG75 and SUDHL4, cells were splitted every second day in a 1:10 ratio, while HF1 cells were splitted every second day in a 1:5 ratio. The retroviral packaging cell line Platinum-E

(PlatE) was cultured in DMEM medium supplemented with 10%FCS, 1 % Penicillin/Streptomycin and 1 mM L-Glutamine (further referred to as D10 medium). For maintenance PlatE cells were splitted every 2-3 days in a 1:10 ratio.

2.2.6.3 SILAC labeling of human B cell lines

The cells were cultured in SILAC RPMI-1640 medium containing 0.12 mM L-arginine (13C6) (+6) and 0.27 mM L-lysine (4,4,5,5-D4) (+4), 10 % dialyzed FCS and Penicillin/Streptomycin. To achieve a complete labeling, the cells were cultured at least for five to six passages in this medium. The unlabeled control cells were cultured in RPMI-1640 medium supplemented with 10 % dialyzed FCS and Penicillin/Streptomycin.

2.2.6.4 Amaxa ® Nucelofection

Nucleofection of human B cell lines was performed by using the Amaxa® Human B Cell Nucleofector® Kit. To this end, cells were grown to a density of less than $1x10^6$ cells/ml. On day of nucleofection, $3x10^6$ cells per sample were harvested by centrifugation. The supernatant was removed completely. Subsequently, cells were resuspended in the nucleofection suspension, consisting of 82 µl Human B cell nucleofector solution, 18 µl of Supplement 1 and 2 µg of the respective DNA. The cell/DNA suspension was transferred to a cuvette supplied with the kit and inserted into the NucleofectorTM II device (Amaxa/Lonza). Transfection was accomplished by using program T-015. Afterwards, cells were seeded in a 5 cm culture dish in prewarmed R10.

2.2.6.5 Retroviral transduction of human B cell lines

Transfection of PlatE cells

In preparation of the retroviral transduction of human B cell lines, the virus-packaging cell line PlatE was transfected with the respective plasmid DNA in order to produce virus particles. Therefore, PlatE cells were plated ca. 24 h before transfection on a 5 cm Petri dish in DMEM with a ratio of 1:5 in order to achieve around 70% confluence the next day. Transfection of PlatE cells was performed by using the TransIT transfection reagent (Mirus). For each sample 8 µl TransIT were added to 250 µl R0 medium and incubated at RT for 15 min. Subsequently, 3-5 µg of the respective plasmid DNA (and if required 1 µg of the VSV-G pMSCV plasmid) were added, mixed and again incubated at RT for 15-30 min. Meanwhile, the D10 medium was removed from the

PlatE cells and replaced by 2.5 ml of fresh prewarmed R10 medium. After incubation, the DNA mix was added dropwise to the PlatE cells. After 24 h the medium of the transfected PlatE cells was filled up to a total volume of 5 ml with R10 medium.

Infection of B cell lines

48 h after transfection of PlatE cells the virus containing supernatant (virus-supe) was collected and used for infection of B cell lines. Therefore, 5 ml of the virus-supe were supplemented with 4 mg/ml Polybrene and centrifuged at 300 rcf for 4 min in order to remove detached PlatE cells. Meanwhile, $2x10^6$ B cells were collected, resuspended in 500µl R10 medium, combined with the virus-supe and transferred to a 5 cm Petri dish. After 24 h the Polybrene was removed by centrifugation and the cells were reconstituted in fresh R10 medium. Once the cells had recovered from the infection process, cells expressing the transduced construct were selected by addition of the respective antibiotic to the culture.

2.2.6.6 Isolation of human primary B cells from peripheral blood

Isolation of human primary B cells from peripheral blood was performed by using the CD19 pluriBead® Cell separation kit (pluriselect) following the manufacturers protocol. Blood from healthy donors was collected and supplemented with 30 µl heparin per 50 ml blood to prevent coagulation. Different from the protocol, 5 µl of CD19 pluriBeads® were added to 1 ml blood. Purity of isolated B cells was checked by surface staining of CD19 after 30 min incubation in R10 at 37°C and 5 % CO_2 or by surface staining of CD20.

2.2.6.7 Flow cytometry

Staining of cell surface proteins

For detection of cell surface proteins/receptors $1x10^6$ cells were harvested by centrifugation and washed 1x with PBS. Cells were reconstituted in 300 µl PBS and transferred to FACS tubes. The fluorescence-labeled antibodies used for surface staining were diluted according to the manufacturer's recommendations. After 20 min incubation on ice, cells were washed 1x with ice cold PBS and reconstituted in 300 µl PBS for flow cytometric measurement.

Detection of phosphorylated protein by intracellular flow cytometry

If required, cells were stimulated as described in section 2.2.5.1 Per sample, 0.5-1x10^6 subconfluently cultured cells were harvested and washed once in PBS. Subsequently, cells were reconstituted in 100 µl R0 and starved for 20-30 min at 37°C. Following, cells were stimulated via the BCR either with 10 µg/ml α-IgM F(ab')2 or α-IgG F(ab')2 depending on the Ig isotype of the respective cell type for different time points. Reaction was stopped by adding an equal volume of Cytofix™ Fixation Buffer (Becton Dickinson) and cells were incubated for 10 more minutes at 37°C for fixation. Afterwards, cells were centrifuged at 500 rcf for 8 min and the supernatant was discarded. For permeabilisation, cells were reconstituted in 400 µl 1x Phosflow™ Perm/Wash Buffer I, incubated for 20 min at room temperature and washed 1x with 400 µl 1x Perm/Wash Buffer I. Following, cells were reconstituted in 100 µl Perm/Wash buffer again and stained with the respective antibody for 30-60 min. Antibodies were applied as described by the manufacturer, expect for Alexa Flour® 647 Mouse A-Erk1/2 (pT202/pY204); here, 10 µl per 1x10^6 cells instead of 20 µl were used. Following staining, samples were filled up with 1 ml 1x Perm/Wash Buffer I, and again centrifuged for 8 min at 500 rcf. The supernatant was discarded and cells were reconstituted in 300 µl Perm/Wash buffer for flow cytometric measurement.

Ca^{2+} mobilization assay

Mobilization of Ca^{2+} is a key event in BCR signaling. Intracellular Ca^{2+} concentration can be measured by using Indo-1-AM, a Ca^{2+} sensitive, cell-permeable, ratiometric dye, which shifts its fluorescence emission wavelength upon Ca^{2+} binding from 475 nm (blue) to 400 nm (violet). For Ca^{2+} mobilization assays, cells were grown to a density less than 1x10^6 cells per ml in order to prevent preactivation caused by stress. 1x10^6 cells were harvested by centrifugation and transferred to light-opaque microcentrifuge tube. Cells were loaded with 1 µM Indo-1-AM in 700 µl R10 medium supplemented with 0.015 % pluronic acid. Following incubation at 30°C for 30 min, samples were filled-up with 750 µl of R10 medium and were incubated for another 10 min at 37°C. Afterwards, cells were washed 2x by centrifugation (1.5 min, 300 rcf) with Krebs-Ringer buffer supplemented with 1 mM $CaCl_2$. Finally, 1x10^6 cells were reconstituted in 300 µl Krebs-Ringer buffer and incubated at 30°C for 15 min prior measurement in order to rest and minimize preactivation of cells. Measurement of Ca^{2+} flux was performed at the flow cytometer

LSR II (Becton Dickinson). Ca^{2+} flux was measured 30 s before stimulation in order to record a base line of resting cells and 4.5 min after stimulation via the B cell receptor. B cell receptor stimulation was performed by using 10 µg/ml α-IgM F(ab')2 or α-IgG F(ab')2. Data were analyzed using the FlowJo software.

Cell sorting by Flow Cytometry

Separation of cell populations with distinct characteristics from a heterogeneous population was done by Flow cytometry based cell sorting. This was performed by the Central Service Unit Cell Sorting at the University Medical Center in Göttingen.

3 Results

3.1 Regulation of intracellular B cell antigen receptor signaling events by a recombinant soluble FcγIIB receptor

The human recombinant soluble FcγRIIB has currently been tested in clinical trials for the treatment of ITP and SLE. The study results revealed a long-lasting therapeutic effect of human recombinant soluble FcγRIIB in ITP with a sustained increase in platelet counts after only a single cycle of treatment. Consequently, it was assumed that the soluble FcγRIIB has a dual mode of action: First, it can compete with membrane-bound Fcγ receptors for immune complex binding and hence prevents destruction of platelets and activation of immune cells via membrane FcγRs. Second, it is also suggested to interfere with memory B cell and/or plasma cell formation and thus with production of new autoantibodies which would explain the observed sustained effects in ITP patients. We hypothesized that the human recombinant soluble FcγRIIB interacts with membrane IgG (mIgG) as part of the BCR, thereby interfering with memory or plasma cell formation. In order to test the hypothesis, I functionally examined human recombinant soluble FcγRIIB and related molecules for their direct effects on the B cell response *in vitro*.

3.1.1 Cellular system

Due to the weak binding affinity of sFcγRIIB to IgG, it is not possible to directly prove binding to membrane IgG by using fluorescence-labelled sFcγRIIB-antibodies for FACS or fluorescence-labelled sFcγRIIB itself. Furthermore, human B cells express endogenous membrane FcγRIIB that would additionally complicate the proof of sFcγRIIB on the cell surface. Hence, I aimed to investigate the interaction of sFcγRIIB with membrane IgG indirectly by using functional read-out methods as Ca^{2+} mobilization and Western blot analysis of signaling effectors downstream of the BCR. Therefore, I compared expression of membrane IgG and the ability of BCR induced Ca^{2+} mobilization in three different IgG-positive human B cell lines, namely the follicular lymphoma B cell line HF1, non-Hodgkin's lymphoma B cell line DOHH-2 and the diffuse histiocytic lymphoma cell line SUDHL4. Surface staining of mIgG with FITC-labeled α-human IgG on HF-1, DOHH-2 and SUDHL-4 cells (figure 6 a) revealed similar mIgG expression levels, whereas Ca^{2+} mobilization upon stimulation via mIgG was different (figure 6 b). While HF-1 cells

(figure 6 b; red line) exhibited the highest mobilization of Ca^{2+}, the Ca^{2+} profile in DOHH-2 cells initially had a similar strength but was not as sustained as compared to HF-1 cells. SUDHL4 cells had a low potential to mobilize Ca^{2+} compared to HF-1 and DOHH-2. Thus, I chose the HF-1 cell line as a representative model to investigate signaling induced by sFcγRIIB.

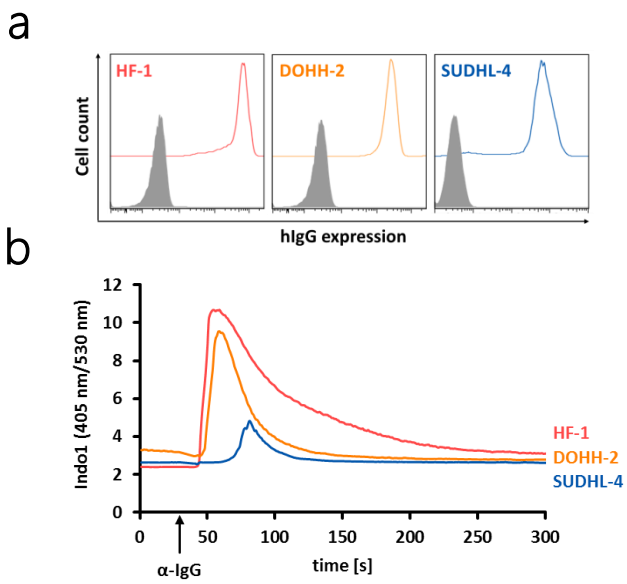

Figure 6. Analysis of potential model IgG-B cell lines. a) Surface expression of membrane IgG on the human IgG^+ B cell lines HF-1 DOHH-2 and SUDHL-4. Cells were incubated with a fluorescence-labelled antibody against hIgG and analyzed for IgG surface expression by flow cytometry. b) Different qualities of Ca^{2+} mobilization of IgG+ cell lines. Cells were stimulated with 10 µg/ml α-IgG F(ab')2 fragments. Ca2+ mobilization was monitored for 300 s by flow cytometry using the Ca^{2+} sensitive dye Indo-1.

3.1.2 Dimeric and tetrameric sFcγRIIB induce BCR signaling events on IgG expressing B cells

3.1.2.1 Dimeric sFcγRIIB dose-dependently induces Ca^{2+} mobilization in IgG^+ B cells

To assess whether the soluble FcγRIIB has an impact on BCR signaling of IgG-positive B cells, I stimulated HF-1 cells with different concentrations of monomeric or dimeric sFcγRIIB while Ca^{2+} mobilization was monitored by flow cytometry using the ratiometric Ca^{2+} sensitive dye Indo-1. The human Burkitt lymphoma B cell lines DG75 and Ramos expressing membrane IgM served as negative controls. Additionally, I treated the cells with the solvent only, serving as placebo. As an internal control, I additionally stimulated the cells via their endogenous IgG- or IgM-BCR by using F(ab')2 α-IgM or F(ab')2 α-IgG, respectively, in order to test Ca^{2+} mobilization capacity in general. Treatment of the IgG-negative cell lines Ramos and DG75 with either monomeric sFcγRIIB or dimeric sFcγRIIB did not induce any Ca^{2+} mobilization, although Ca^{2+} mobilization following stimulation via the BCR with F(ab')2 α-IgM was normal (figure 7 a & b). Whilst stimulation with monomeric sFcγRIIB did not lead to Ca^{2+} mobilization in the IgG expressing HF-1 cells (figure 7 c; blue lines), stimulation of these cells with dimeric sFcγRIIB induced Ca^{2+}

mobilization in a dose dependent manner (figure 7 d; red lines). However, the signal induced by dimeric sFcγRIIB was weaker but more sustained compared to IgG-stimulation with F(ab')2 α-IgG, thus is of different quality. Thus, I assumed that sFcγRIIB is capable of binding to membrane IgG. However, monomeric sFcγRIIB that comprises only one binding site for IgG was not sufficient to induce signaling events in IgG-positive B cells. Hence, I concluded that sFcγRIIB can induce BCR signaling only when it is multimeric, at least dimeric, by cross-linking two or more IgG molecules on the cell surface.

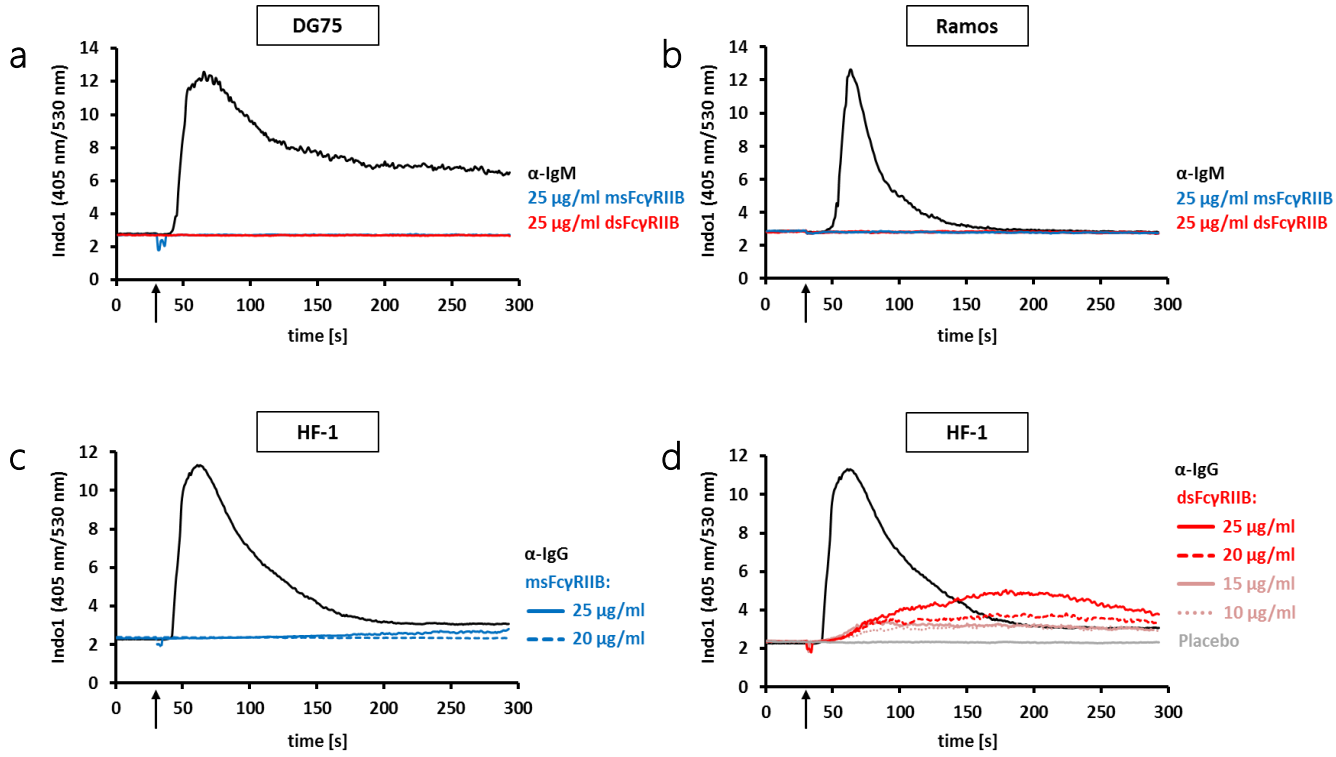

Figure 7. Dose dependent effects of msFcγRIIB and dsFcγRIIB on Ca^{2+} mobilization in IgG^+ B cells. IgM^+ IgG^- B cells (DG75 and Ramos; a & b) and IgM^- IgG^+ B cells (HF-1; c & d) were stimulated via their BCR with 10 µg/ml F(ab')2 α-IgM or α-IgG or different concentrations of msFcγRIIB and dsFcγRIIB. Mobilization of the second messenger Ca^{2+} was monitored by flow cytometry for 300 sec using the Ca^{2+} sensitive dye Indo-1. The arrow indicates time point of stimulation.

3.1.2.2 Multimeric sFcγRIIB induces BCR signaling events in B cells

To further test, whether only multimeric sFcγRIIB is able to induce BCR signaling in IgG-positive B cells, I used biotin-labeled monomeric sFcγRIIB (sFcγRIIB-bio) that upon interaction with streptavidin (SA) forms a stable tetramer. Stimulation with the preformed complex of 20 µg/ml msFcγRIIB-bio and 1 µg SA induced Ca^{2+} mobilization in IgG-positive HF-1 cells (figure 8 a) while stimulation with monomeric sFcγRIIB or SA alone was not sufficient to induce any Ca^{2+} signal. Dose reduction of msFcγRIIB and SA (2 µg/ml + 0.1 µg) correspondingly led to less mobilization of Ca^{2+} in HF-1 cells. Stimulation of IgG-negative DG75 control cells does not induce Ca^{2+} mobilization (figure 8 b).

To check whether effector proteins downstream of Ca^{2+} mobilization get activated upon stimulation with dimeric and tetrameric sFcγRIIB, I analyzed phosphorylation of Akt and Erk kinases (figure 8 c). Therefore, I stimulated HF-1 or DG75 cells with monomeric or tetrameric sFcγRIIB (20 µg/ml msFcγRIIB-bio + 1 µg SA). Besides, cells were stimulated via the BCR F(ab')2 α-IgM or F(ab')2 α-IgG as a positive control. Cells were lysed and analyzed by Western blot, probing for phosphorylated Akt, SLP65 or Erk.

The data acquired from the Western blot analysis corresponded to the Ca^{2+} mobilization data regarding Akt and Erk activation. Stimulation with dimeric and tetrameric sFcγRIIB led to phosphorylation of Akt and Erk in HF-1 cells, but not in the DG75 control B cells (figure 8 c). The activation levels were comparable with Akt- and Erk- phosphorylation following BCR activation with F(ab')2 α IgG. However, stimulation with either dimeric sFcγRIIB or tetrameric sFcγRIIB was not sufficient to induce SLP65 (figure 8 d) activation which occurs upstream of Ca^{2+} mobilization and Akt and Erk activation (reviewed in Kurosaki, 1999).

Taken together, these data reveal that multimeric variants of the sFcγRIIB but not the monomeric sFcγRIIB can induce BCR signaling in IgG-positive human B cells with different strength and quality compared to conventional BCR activation regarding Ca^{2+} mobilization and phosphorylation of downstream effectors.

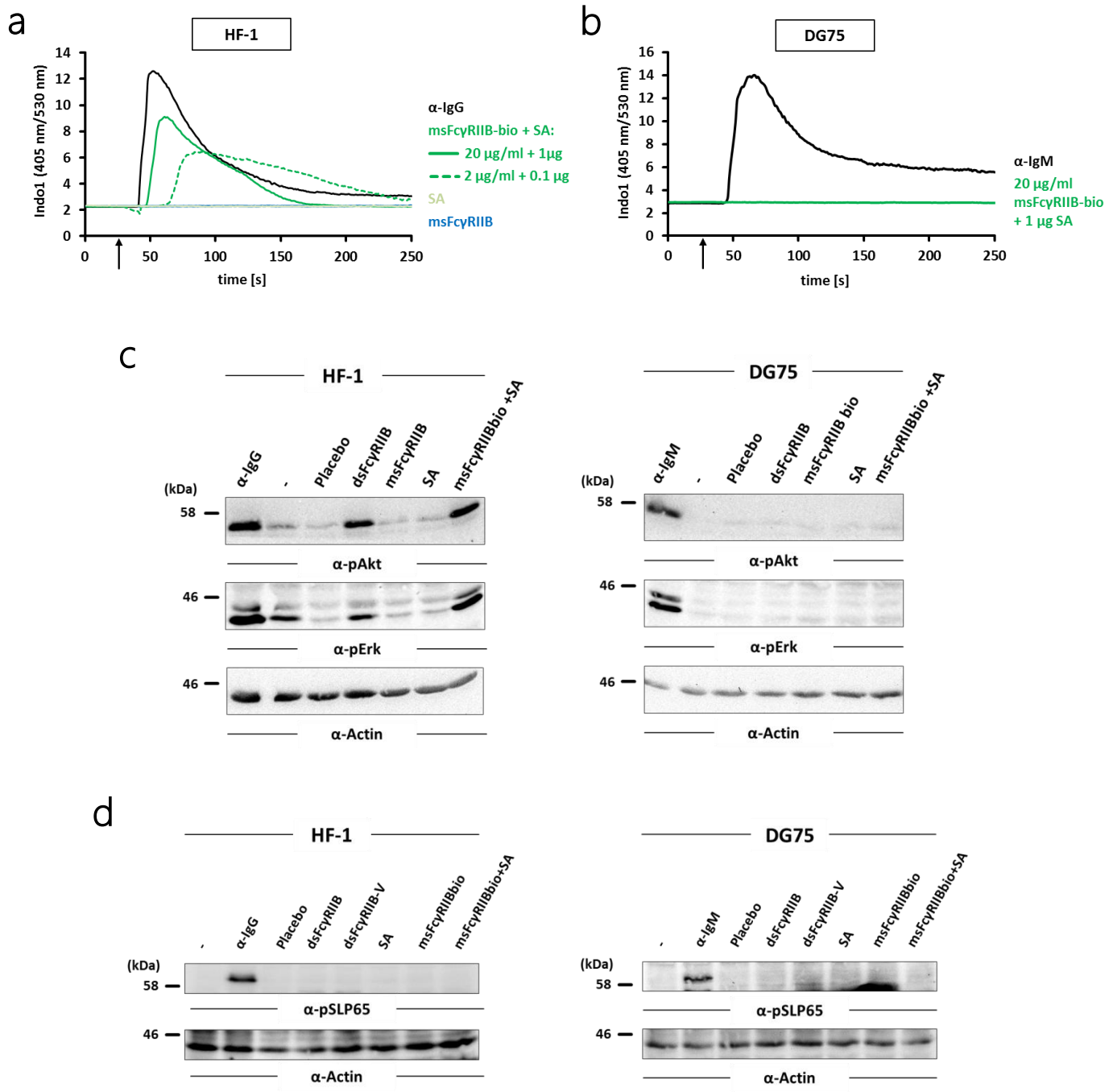

Figure 8. Dimeric and tetrameric sFcγRIIB induce signaling events in IgG-positive B cells. HF-1 cells (a) were stimulated with 10 µg/ml F(ab')2 α-IgG, 20 µg/ml msFcγRIIB-bio + 1 µg SA, 2 µg/ml msFcγRIIB-bio + 0.1 µg SA, SA only or msFcγRIIB-bio only. DG75 cells (b) were stimulated with 10 µg/ml F(ab')2 α-IgM or 20 µg/ml msFcγRIIB-bio + 1 µg SA (arrow indicates time point of stimulation). Ca^{2+} mobilization was monitored for 250 seconds by flow cytometry using the Ca^{2+} sensitive dye Indo-1. For Western blot analysis (c & d) cells were stimulated with the before mentioned reagents for 3 min. Activation of downstream effector proteins as Akt kinase, the adapter protein SLP65 or Erk kinase was analyzed by Western blot, probing with phospho-specific antibodies (α-pAkt, α-pErk and α-pSLP65) for the respective protein.

3.1.3 Activation of BCR signaling by multimeric sFcγRIIB is IgG-BCR specific

To test whether the BCR signaling in human IgG-positive B cells induced by treatment with multimeric variants of sFcγRIIB is due to specific binding to the IgG-BCR, I exogenously expressed the heavy chain of IgG1 in IgG negative DG75 B cells. Once expressed the IgG1 heavy chain pairs with the endogenous κ-light chain and forms a functional BCR complex together with the endogenous Igα/Igβ heterodimer. The IgG expressing DG75 B cells were termed DG75-hIgG. Stimulation of DG75-hIgG with F(ab')2 α-IgG induced Ca^{2+} mobilization with exactly the same strength as in DG75-hIgG B cells stimulated F(ab')2 α-IgM (figure 9 a), whereas the control cells (DG75 wild type; wt) as expected did not respond to stimulation with F(ab')2 α-IgG (figure 9 b). Correspondingly, Erk and Akt phosphorylation reached the same strength upon stimulation of DG75 hIgG cells with F(ab')2 as compared to stimulation via the endogenous IgM-BCR (figure 9 c). Upon stimulation with dimeric and tetrameric sFcγRIIB, DG75-hIgG cells exhibited a delayed mobilization of Ca^{2+} compared to stimulation with F(ab')2 α-IgG with around 40 % of the signaling strength (figure 9 a), while in DG75 wt cells stimulation with sFcγRIIB did not induce a Ca^{2+} signal (figure 9 b). However, Akt kinase exhibited only a weak activation after stimulation of DG75 hIgG cells with dimeric and tetrameric sFcγRIIB, whilst Erk kinase did not show any phosphorylation (figure 9 c). To sum up, the analysis of IgG-positive DG75 transfectants and DG75 parental cells treated with multimeric variants of sFcγRIIB confirmed IgG-specific BCR signal induction with sFcγRIIB, which is most probably mediated by the interaction of multimeric sFcγRIIB with the IgG BCR.

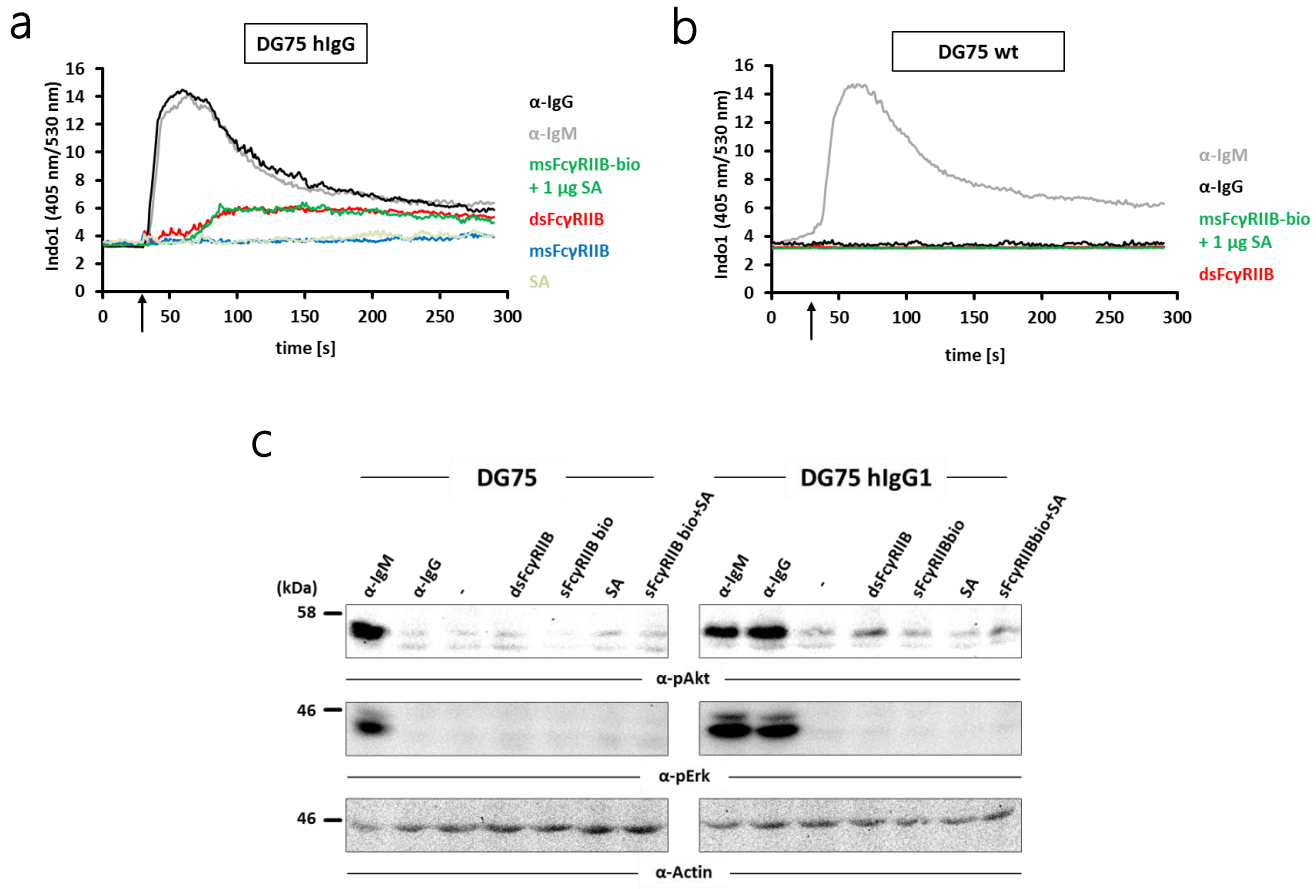

Figure 9. IgG-BCR-specific stimulation of DG75 B cells retrovirally transduced with hIgG. The IgM expressing human B cell line DG75 was retrovirally transduced with the heavy chain of human IgG in order to form an IgG-BCR complex on the cell surface. DG75 wt cells served as negative control. For Ca2+ mobilization IgM/IgG double positive DG75 hIgG (a) and DG75 wt cells (b) were stimulated with 10 µg/ml F(ab')2 α-IgM, 10 µg/ml F(ab')2 α-IgG, 40 µg/ml m sFcγRIIB, 20 µg/ml dimeric sFcγRIIB or tetrameric sFcγRIIB (25 µg/ml sFcγRIIB-bio + 2 µg SA). Stimulation with 2 µg SA only served as negative control. Arrows indicate time point of stimulation Ca^{2+} mobilization was monitored for 250 seconds by flow cytometry using the Ca^{2+} sensitive dye Indo-1. For Western Blot analysis (c) cells were stimulated with the same reagents as for the Ca^{2+} measurement for 3 min. Activation of downstream effector proteins as Akt kinase or Erk kinase was analyzed by Western blot, probing with phospho-specific antibodies for the respective protein (p-Erk and p-Akt). Probing for Actin served as loading control.

Here I could show by functional assays that multimeric but not monomeric sFcγRIIB binds to the IgG-BCR and induces BCR-specific signaling events. Signaling could only be induced when using multimeric variants of FcγRIIB. Although I did not observe signaling, I cannot exclude that the monomeric sFcγRIIB does not bind to mIgG. Once multimerized by streptavidin also the monomeric variant induces IgG-BCR specific signaling, though with different quality as compared to direct BCR stimulation by BCR specific F(ab')2 Ca^{2+} mobilization induced by multimeric sFcγRIIB was delayed and about 40-70 % weaker than the Ca^{2+}signal induced by BCR

specific F(ab')2. Although I could observe Ca^{2+} mobilization, SLP65 activation was not detectable. SLP65 is important for the formation of the trimolecular Ca^{2+} mobilization complex.

3.2 BCR mediated activation of extracellular signal regulated kinase Erk

Ligation of the BCR leads to the activation of a wide variety of pathways regulating gene expression and hence the fate of B cells. One pathway that gets activated upon BCR ligation is the mitogen-activated protein kinase (MAPK)/Erk-pathway resulting in activation of the extracellular signal regulated kinase Erk. Erk promotes cell cycle progression, cell survival and plays a role in B cell development and differentiation into plasma cells (Yasuda & Kurosaki, 2008; Yasuda et al, 2011). Data from DT40 chicken B cells and mouse models revealed that BCR-induced activation of Erk in these systems is mediated via RasGRP3 and DAG. RasGRP3 activity is dependent of the activity of PLCγ2 and thus is accompanied by the mobilization of the second messenger Ca^{2+} (Oh-hora et al, 2003; Coughlin et al, 2005). With the sFcγRIIB I found a new tool to stimulate BCR activation only by binding to the Fc portion of the mIgG. However, my results showed that stimulation with the sFcγRIIB induces strong activation of Erk independent of SLP65 activation, which is important for the formation of the Ca^{2+} initiation complex and thus for the mobilization of Ca^{2+}. From that I hypothesized, that activation of the MAPK/Erk pathway in human B cells, different from chicken B cells, occurs independently of Ca^{2+} mobilization, indicating species specific differences between chicken, mice and human B cells. Thus, I revisited the BCR signaling pathway with regard to the activation of Erk in the human B cell line DG75 and different DG75-derived sublines deficient for various candidates of the BCR pathway.

3.2.1 Erk activation is independent of mobilization of the second messenger Ca^{2+}

Activation of PLCγ2 requires the formation of the Ca^{2+} initiation complex consisting of SLP65, Btk and PLCγ2. To investigate the relevance of Ca^{2+} mobilization in Erk activation in human B-cells, I compared Ca^{2+} mobilization and Erk activation in DG75-sublines deficient for SLP65 (*SLP65*$^{-/-}$) or Btk (*BTK*$^{-/-}$; kindly provided by C. Hitzing and W. Schulze,). Furthermore, I included DG75 B cells deficient for the adapter protein Grb2 (GRB*2*$^{-/-}$, kindly provided by J. Lutz) in this analysis. Due to its permanent association with the guanine nucleotide exchange factor Sos Grb2 was suggested to be involved in activation of the MAPK/Erk pathway following BCR stimulation as it was described for the EGFR pathway (Lowenstein et al, 1992).

For analysis of Erk phosphorylation the different DG75 sub-cell lines were stimulated via the BCR and analyzed for Ca^{2+} mobilization by flow cytometry (figure 10 a) and for phosphorylation of Erk by Western blot (figure 10 b) or intracellular staining (ICS) for flow cytometry (figure 10 c & d) using phospho-specific antibodies. The relative median fluorescence intensity (MFI) of three independent experiments was plotted in a bar diagraph (figure 10 d).

In accordance to published data, Ca^{2+} mobilization (figure 10 a) in DG75 B cells deficient for SLP65 (*SLP65*$^{-/-}$) and Btk (*BTK*$^{-/-}$) was up to 50 % diminished compared to parental cells (wt) whereas the lack of Grb2 did not have any effect on Ca^{2+} mobilization. In contrast, both, Western blot analysis (figure 10 b) and ICS for phosphorylated Erk (figure 10 c & d) showed a remarkable decrease in Erk activation upon 3, 10 and 20 min BCR stimulation in Grb2-deficient DG75 (*GRB2*$^{-/-}$) compared to parental cells (wt), while Erk activation in SLP65- (*SLP65*$^{-/-}$) and Btk- (*BTK*$^{-/-}$) deficient DG75 was not affected. Quantification of ICS data revealed a 50 % decrease of Erk phosphorylation in Grb2 deficient DG75 (*GRB2*$^{-/-}$) compared to parental cells (wt) (figure 10 d). In summary, these results reveal that Erk activation in the human B cell line DG75 does not depend on SLP65 or Btk and hence is independent of Ca^{2+} mobilization. This is in contrast to the observations made in the chicken B cell line DT40, which requires Ca^{2+} mobilization for sufficient activation of Erk following BCR induction (Oh-hora et al, 2003). Instead, the adapter protein Grb2 plays an important role in BCR mediated Erk activation in human B cells.

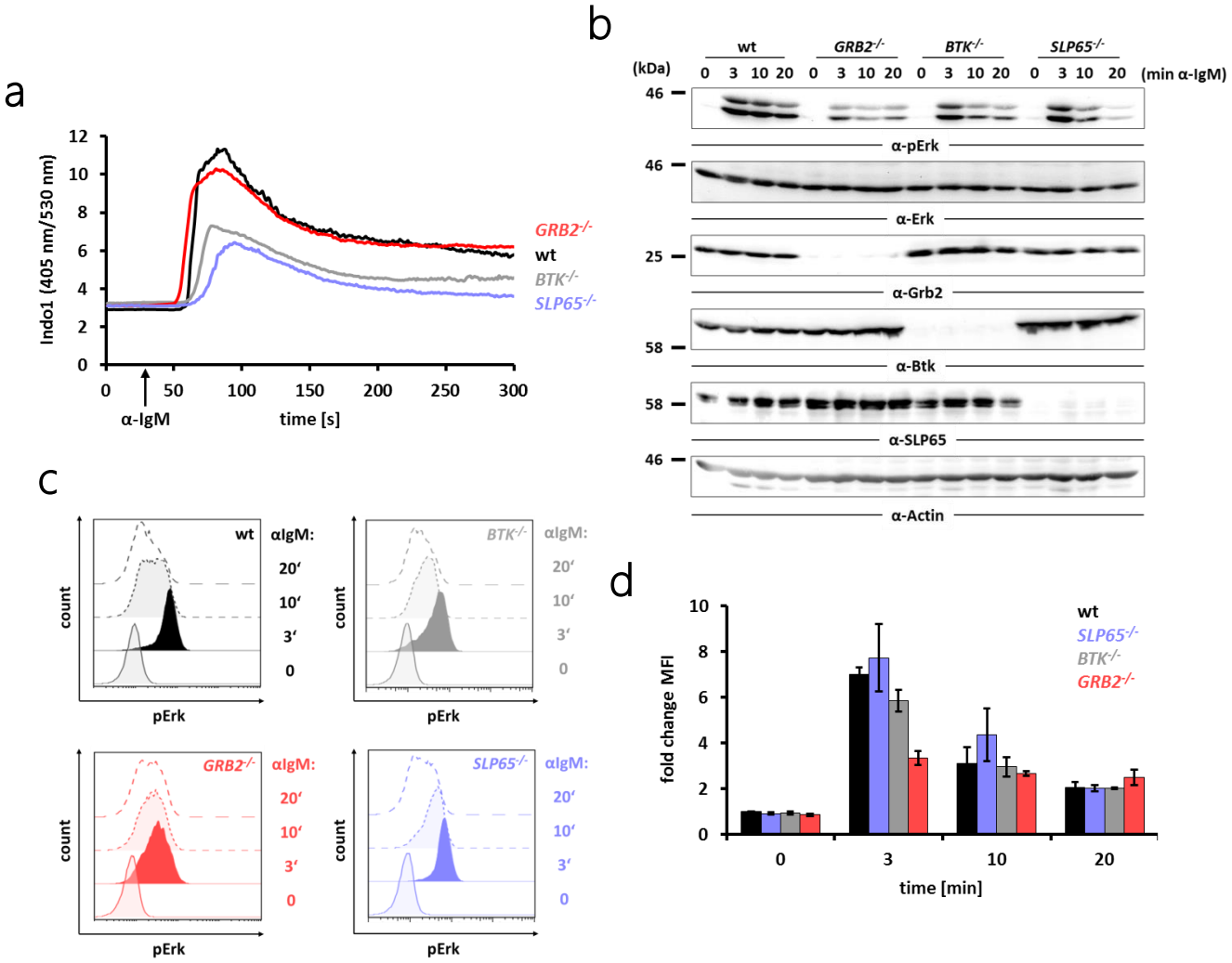

Figure 10. Ca^{2+} independent activation of Erk in human B cells. (a) Mobilization of Ca^{2+} in DG75 B cells deficient for Btk (*BTK*$^{-/-}$), SLP65 (*SLP65*$^{-/-}$), or Grb2 (*GRB2*$^{-/-}$) or DG75 parental cells (wt). Cells were loaded with the ratiometric dye Indo-1. Baseline was recorded for 30 s before cells were stimulated with 10 µg/ml F(ab')2 α-IgM. Ca^{2+} mobilization was monitored for 300 s by flow cytometry. (b) Western blot analysis of phosphorylated Erk. Cells were stimulated with 10 µg/ml F(ab')2 α-IgM for 0, 3, 10 or 20 min, lysed and analyzed by Western blot probing for phosphorylated Erk (α-pErk). Expression of total Erk, Grb2, Btk and SLP65 was verified with respective antibodies. Actin served as loading control. (c & d) Intracellular staining for phosphorylated Erk. Cells were stimulated with 10 µg/ml F(ab')2 α-IgM for 0, 3, 10 or 20 min, fixed and permeabilized, stained with α-pErk-Alexa 647 and analyzed by flow cytometry. (c) Representative histograms of Erk phosphorylation in different DG75 sub-cell lines. (d) fold change of median fluorescence intensity (MFI)/Erk phosphorylation in DG75 sub-cell lines. Mean values and standard deviation of three independent experiments.

3.2.2 PLCy is dispensable for the activation of Erk

Having shown that Erk activation following BCR activation occurs independently of the mobilization of Ca^{2+}, I aimed to analyze the role of PLCγ in Erk activation directly. To this end, I generated a DG75 sub-cell line deficient for PLCγ2 (*PLCG2*$^{-/-}$) and a sub-cell line deficient for both, PLCγ1 and 2 (*PLCG1/2*$^{-/-}$) using the TALEN-based genome editing technique. PLCγ2 is a key molecule in BCR signaling, since it generates the second messenger DAG. Thus, it is indispensable for the activation of RasGRP3 and Erk in chicken B cells and mice. PLCγ1 is the structural homologue to PLCγ2 and its functional analogue in T cells (Oh-hora et al, 2003; Bell et al, 2004; Kane et al, 2000).

3.2.2.1 Generation of a PLCγ2 deficient cell line

For targeting the *PLCG2* gene by TALEN, I chose exon 2 which according to the ensembl.org database is present in all transcript variants (figure 11 a). TALEN constructs were planned by using the web based program "TAL Effector Nucleotide Targeter 2.0". For later activity tests, I chose a TALEN pair that locates the nuclease (FokI) to a BsrBI restriction site. In case of a functional TALEN pair the restriction site is damaged and cannot be cut by the respective restriction enzyme anymore. The two TALEN constructs were cloned in a pMAX vector each, carrying either IRES-RFP- or IRES-GFP expression cassette and simultaneously introduced into the target cells by nucleofection as described in section 2.2.6.4. Afterwards, RFP^+ GFP^+ cells were enriched by cell sorting. In order to test the activity of the TALEN pair, I amplified exon 2 of *PLCG2* from DG75 parental cells (wt) or from cells transfected with the TALEN pair by PCR, treated the product with BsrBI and analyzed it by agarose gel electrophoresis (figure 11 b). Treatment of exon 2 derived from the parental cells (wt) led to cleavage of the exon to a fragment of ca. 500 bp and a fragment of around 100 bp (not detectable), while the PCR product of exon 2 derived from cells transfected with the TALEN pairs was intact following BsrBI treatment (figure 11 b). Thus, the PLCG2-TALEN pair was considered as active. For clonal expansion of single-cell clones from the sorted cell population, the cells were diluted and subcultured in 96 well plates. After expansion of single-cell clones, PLCγ2 expression was analyzed by Western blot. In total, six out of 59 analyzed clones exhibited a PLCγ2 deficiency on protein level (figure11 c). Figure 11 d exemplarily shows lack of PLCγ2 expression in clone #33 on

Western blot. Three (clone #16, #33 and #45) out of six clones were analyzed by Sanger sequencing in order to confirm mutation on genomic level. Therefore, genomic DNA from each clone was isolated; Exon 2 was amplified by PCR and cloned into pCR2.1 vector in order to sequence both alleles of the exon separately. Subclone #33 was confirmed to carry a 7 bp deletion on allele 1 and a 4 bp deletion on allele 2 resulting in a premature stop codon (*) (figure 11 e). For clone #16 only one allele with a 2bp deletion could be successfully sequenced, while clone #45 carries a 22 bp deletion on one allele and a 15 bp (multiple of three) deletion on the other allele (not shown). Therefore, clone #33 was used for further experiments, referred to as PLCγ2-deficient DG75 (*PLCG2*$^{-/-}$).

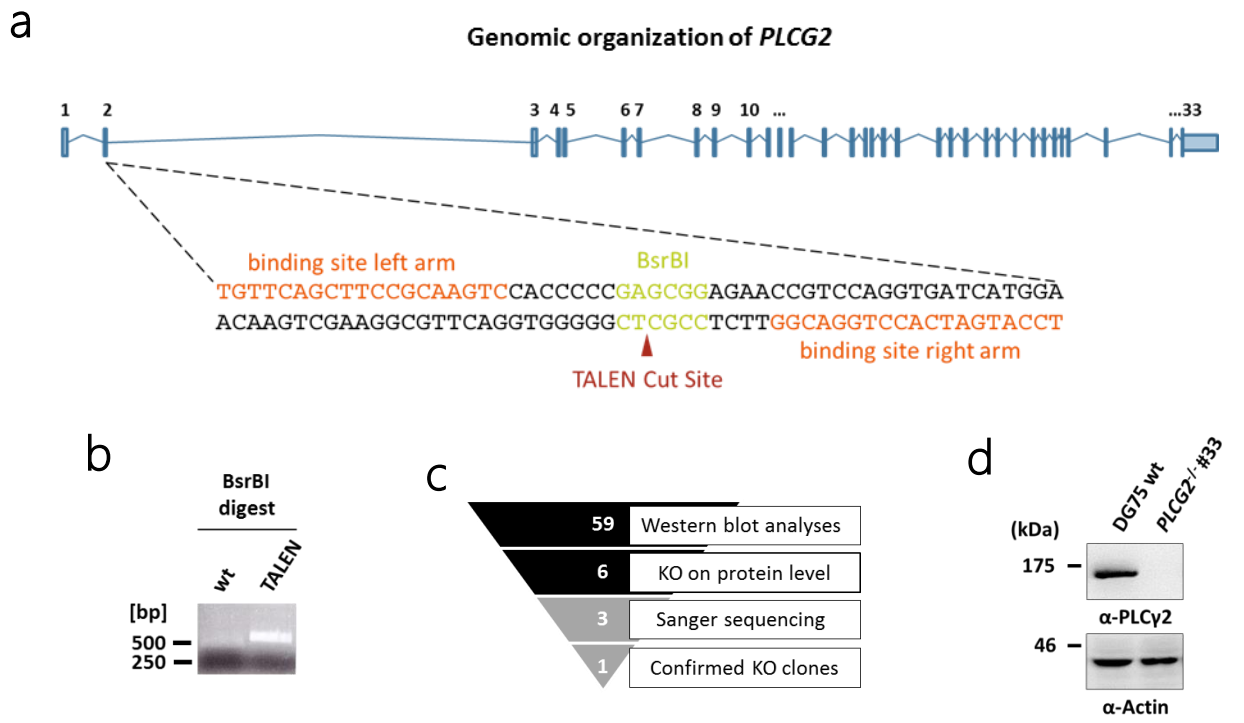

e

DNA sequence Exon 2 *PLCG2*

```
wt      ...TCAGCTTCCGCAAGTCCACCCCCGAGCGGAGAACCGTCCAGGTGATCATG...
#33 allele 1 ...TCAGCTTCCGCAAGTCCA-------GCGGAGAACCGTCCAGGTGATCATG...  Δ 7 bp
    allele 2 ...TCAGCTTCCGCAAGTCCACCCCCG----GAGAACCGTCCAGGTGATCATG...  Δ 4 bp
```

amino acid sequence

```
wt      ...sfrkstperrtvqvim...
#33 allele 1 ...sfrkssgepsr*
    allele 2 ...sfrkstpgepsr*
```

Figure 11. Generation of PLCγ2-deficient DG75 cells using TALEN. (a) Genomic organization of the PLCG2 gene. Exon 2 was chosen for targeting by TALEN constructs. Binding sites for left and right TALEN constructs are highlighted in orange. Cut site of the nuclease (FokI) is indicated by the red arrow. BsrBI restriction site for activity analysis is indicated in green. (b) TALEN activity test. Exon 2 was amplified from parental DG75 cells or TALEN-nucleofected cells and treated with BsrBI. Treated PCR product was analyzed by agarose gel electrophoresis. (c) Statistics of single-cell clone analysis. Single-cell clones were analyzed by Western blot. Clones lacking PLCγ2 expression were further analyzed by Sanger sequencing to verify mutation on genomic level. (d) Exemplary Western blot analysis of DG75 PLCG2$^{-/-}$ subclone #33. (e) Genomic DNA sequence and corresponding aa sequence of subclone #33 (* = premature STOP codon). Sequence is representative for seven sequencing analyses.

3.2.2.2 Ca^{2+}mobilization in PLCγ2-deficient cells is impaired but not completely abolished

According textbook knowledge, PLCγ2 is of central importance in mediating the mobilization of the second messenger Ca^{2+} in B cells (Engelke et al, 2007). Hence, I first tested the newly generated PLCγ2-deficient DG75 sub-cell line (*PLCG2*$^{-/-}$) for its ability to mobilize Ca^{2+} (figure 12 a). All clones tested PLCγ2-negative on Western blot exhibited 50 % decrease in Ca^{2+} mobilization compared to parental cells (wt) upon BCR stimulation. Ca^{2+} profiles of subclone #16, #33 and #45 were plotted representatively in figure 12 a. IgM-BCR expression of PLCγ2-deficient clones was similar to IgM expression of parental cells (wt), excluding the possibility of low Ca^{2+} mobilization due to low IgM expression (figure 12 b). To test PLCγ2 independent off-target effects, I reconstituted PLCγ2-deficient DG75 with EGFP-tagged PLCγ2 and repeated the Ca^{2+} mobilization assay. Reconstitution of PLCγ2-deficient DG75 (*PLCG2*$^{-/-}$ EGFP-PLCγ2) could restore the ability to mobilize Ca^{2+} entirely and hence rule out unwanted off-targets (figure 12 c & d). Nevertheless, considering the role of PLCγ2 it is surprising that the capability of Ca^{2+} mobilization is not completely abolished in these cells. This could be due to other PLC isoforms that are expressed in B cells and compensate for the loss of PLCγ2. One candidate is the functional analogue of PLCγ2 in T cells, namely PLCγ1, which is also highly expressed in B cells.

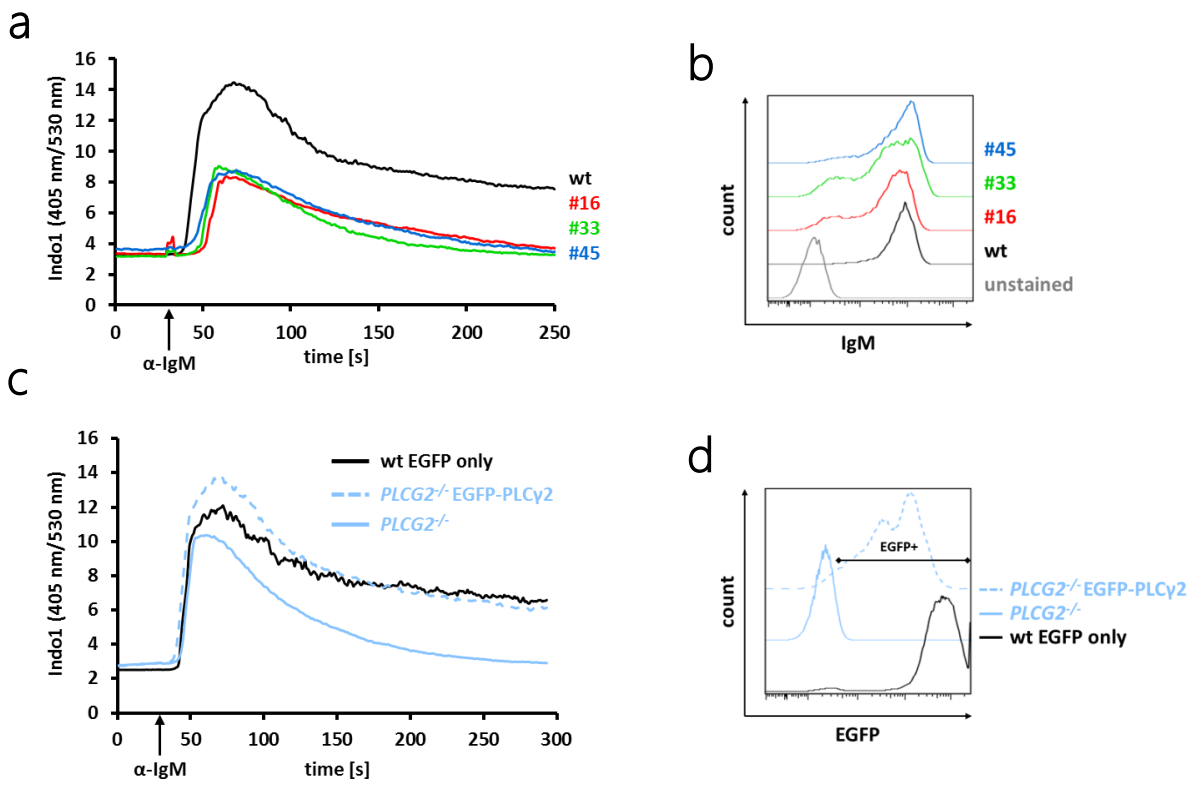

Figure 12. Impaired Ca^{2+} mobilization in PLCγ2-deficient cells. (a) Ca^{2+} mobilization analysis of three representative PLCγ2-deficient subclones (#16, #33, #45). Baseline was recorded for 30 s before cells were stimulated via the IgM-BCR (time point of stimulation is indicated by the arrow). Ca^{2+} mobilization was monitored for 250 s in total by flow cytometry using the ratiometric Ca^{2+} sensitive dye Indo-1. (b) IgM-BCR expression level in PLCγ2-deficient clones. $1x10^6$ cells were stained with a FITC-labelled α-IgM antibody and analyzed by flow cytometry. (d) Ca^{2+} mobilization assay of PLCγ2-deficient cells reconstituted with N-terminally EGFP-tagged PLCγ2 (*PLCG2*$^{-/-}$ EGFP-PLCγ2), compared to DG75 parental cells (wt) transduced with EGFP-only and DG75 *PLCG2*$^{-/-}$. (d) Expression level of EFGP-tagged PLCγ2 in PLCγ2 deficient DG75 and of EGFP only in parental cells (wt). Due to a slight overlap of EGFP and Indo-1 emission wavelength, the control cells DG75 *PLCG2*$^{-/-}$ and parental cells (wt) were transduced with EGFP-only for better comparability of the Ca^{2+} mobilization profiles.

3.2.2.3 Generation of a PLCγ1/2-double deficient B cell line

Since Ca^{2+} mobilization in PLCγ2-deficient DG75 cells was not completely abolished, I supposed that PLCγ2 can be functionally compensated by PLCγ1 which is also highly expressed in human B cells. Moreover, it has analogue functions to PLCγ2 in T cells regarding its role in Ca^{2+} mobilization. Hence, I generated a PLCγ1/2-double-deficient sub-cell line (*PLCG1/2*$^{-/-}$) on the background of PLCγ2-deficient DG75 by TALEN-based genome editing for further investigation of Ca^{2+} independent Erk activation. The TALEN constructs for mutating the *PLCG1* gene (kindly provided by K. Vanshylla) were designed to target exon 2 in transcript variant PLCG1-005 according to the ensembl data base. Furthermore, TALEN cut site was directed to a BsmFI

restriction site that was used for later activity tests of the TALEN constructs (figure 13 a). After introduction of TALEN constructs by nucleofection, cells were sorted for double positive cells as described before, expanded and tested for activity. Therefore, exon 2 of the *PLCG1* gene was amplified by PCR from parental cells or TALEN-nucleofected cells and treated with BsmFI. Exon 2 from the parental cells was completely digested by BsmFI, whereas exon 2 from TALEN-treated cells is almost completely intact, confirming the activity of the TALEN-constructs in the majority of cells from this population (figure 13 b). Following, cells were subcultured to obtain single-cell clones and analyzed by Western blot and Sanger sequencing. 18 subclones from 77 analyzed clones exhibited a loss of PLCγ1 protein expression. Exemplary Western blot analysis (figure 13 d) confirms complete PLCγ1 deficiency in PLCγ1 single-deficient DG75 (*PLCG1*$^{-/-}$; provided by K. Vanshylla) and PLCγ1/2-double deficient DG75 (*PLCG1/2*$^{-/-}$) compared to parental cells (wt). Three out of four subclones analyzed by Sanger sequencing could be confirmed as PLCγ1-deficient on genomic level (figure 13 c). Subclone #2 exhibited a 4 bp deletion on allele 1 and a 5 bp deletion on the second allele (figure 13 e). For further analysis I used subclone #2, in the following referred to as PLCγ1/2-double deficient DG75 (*PLCG1/2*$^{-/-}$).

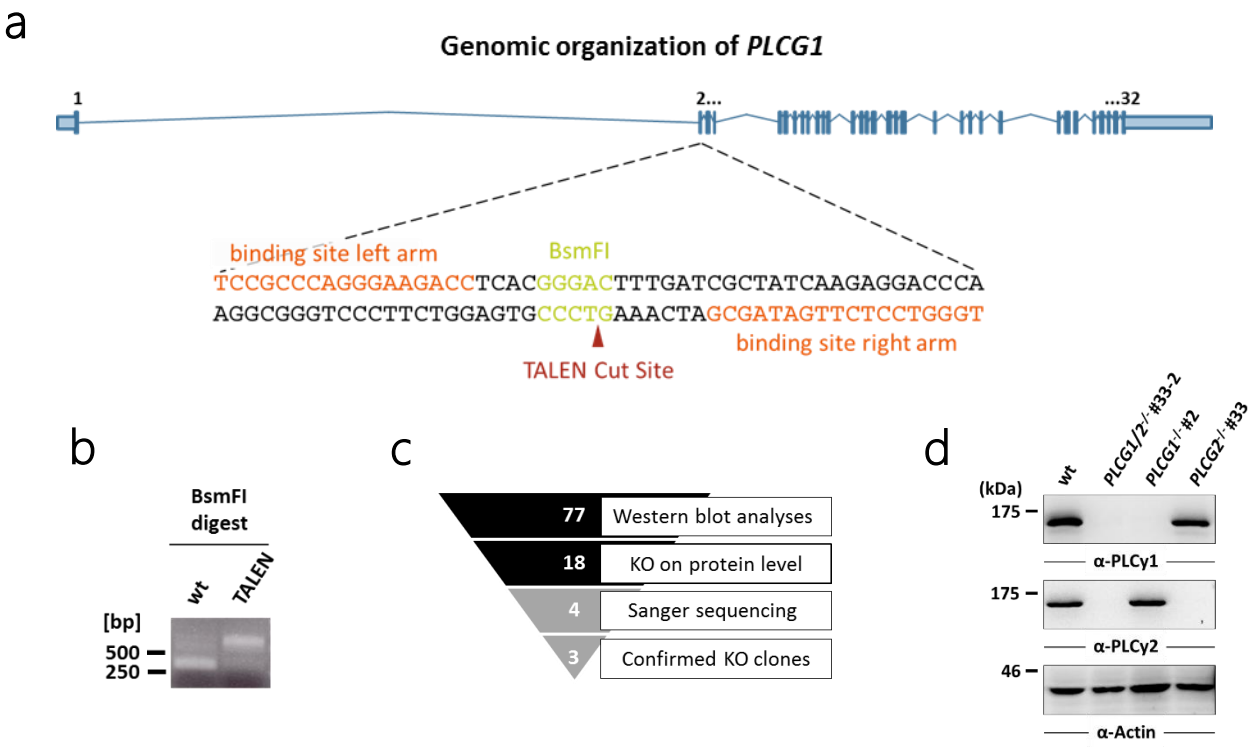

Figure 13. Generation of PLCγ1/2-double deficient B cell line using TALEN. (a) Exon structure of the PLCG1 gene and sequence of the targeted exon 2. TALEN binding sites are highlighted in orange, TALEN cut site is indicated by a red arrow and BsmFI restriction site is highlighted in green. (b) TALEN activity test. Exon 2 was amplified from parental DG75 (wt) cells or TALEN-nucleofected cells and treated with BsmFI. Treated PCR product was analyzed by agarose gel electrophoresis. (c) Statistics of single-cell clone analysis. Single-cell clones were analyzed by Western blot. Clones lacking PLCγ1 expression were further analyzed by Sanger sequencing to verify mutation on genomic level. (d) Exemplary Western blot analysis of PLCγ1/2-double deficient DG75 (*PLCG1/2*$^{-/-}$) subclone #2 compared with parental cells (wt), PLCγ2-deficient DG75 (*PLCG2*$^{-/-}$) and PLCγ1-deficient DG75 (*PLCG1*$^{-/-}$). (e) Genomic DNA sequence and corresponding aa sequence of subclone #2 (* = premature STOP codon). Sequence is representative for at least seven sequencing analyses.

3.2.2.4 PLCγ1 and 2 are required for full Ca^{2+} mobilization in human B cells

Against current textbook knowledge, I could show that the loss of PLCγ2 in human B cells did not lead to a complete abrogation of Ca^{2+} mobilization upon BCR stimulation. In order to test, whether residual Ca^{2+} mobilization can be attributed to functional compensation by PLCγ1, I analyzed the newly established PLCγ1/2-double deficient DG75 sub-cell line (*PLCG1/2*$^{-/-}$) with regard to Ca^{2+} mobilization. In total, I analyzed 13 PLCγ1/2-deficient subclones for Ca^{2+} mobilization. Clone #2, #4 and #10 were plotted exemplarily in figure 14 a. In total, Ca^{2+} mobilization upon stimulation via the IgM-BCR was completely abolished in all 13 sublclones. IgM-BCR surface expression was similar to IgM expression in parental (wt) cells, excluding the possibility of low Ca^{2+} mobilization due to low IgM expression (figure 14 b).

Consequently, I concluded, that PLCγ1 indeed can compensate for PLCγ2 function in human B cells. To exclude that the effect occurs due to off-target effects, I retrovirally transduced PLCγ1/2-double deficient DG75 with N-terminally EGFP-tagged PLCγ1 (*PLCG1/2*$^{-/-}$ EGFP-PLCγ1) and repeated the Ca^{2+} mobilization assay. Thereby, I compared these cells with untransduced PLCγ1/2-double deficient DG75 (*PLCG1/2*$^{-/-}$), PLCγ2-deficient DG75 (*PLCG2*$^{-/-}$) and DG75 parental cells (wt) expressing EGFP only (figure 14 c & d). Expression of citrine-tagged PLCγ1 in PLCγ1/2-deficient cells could restore Ca^{2+} mobilization to the Ca^{2+} mobilization level observed in PLCγ2-deficient DG75 (*PLCG2*$^{-/-}$) (figure 14 c). As Ca^{2+} mobilization is completely abolished, PLCγ1/2-double deficient DG75 are a suitable model for studying Ca^{2+} independent activation of Erk.

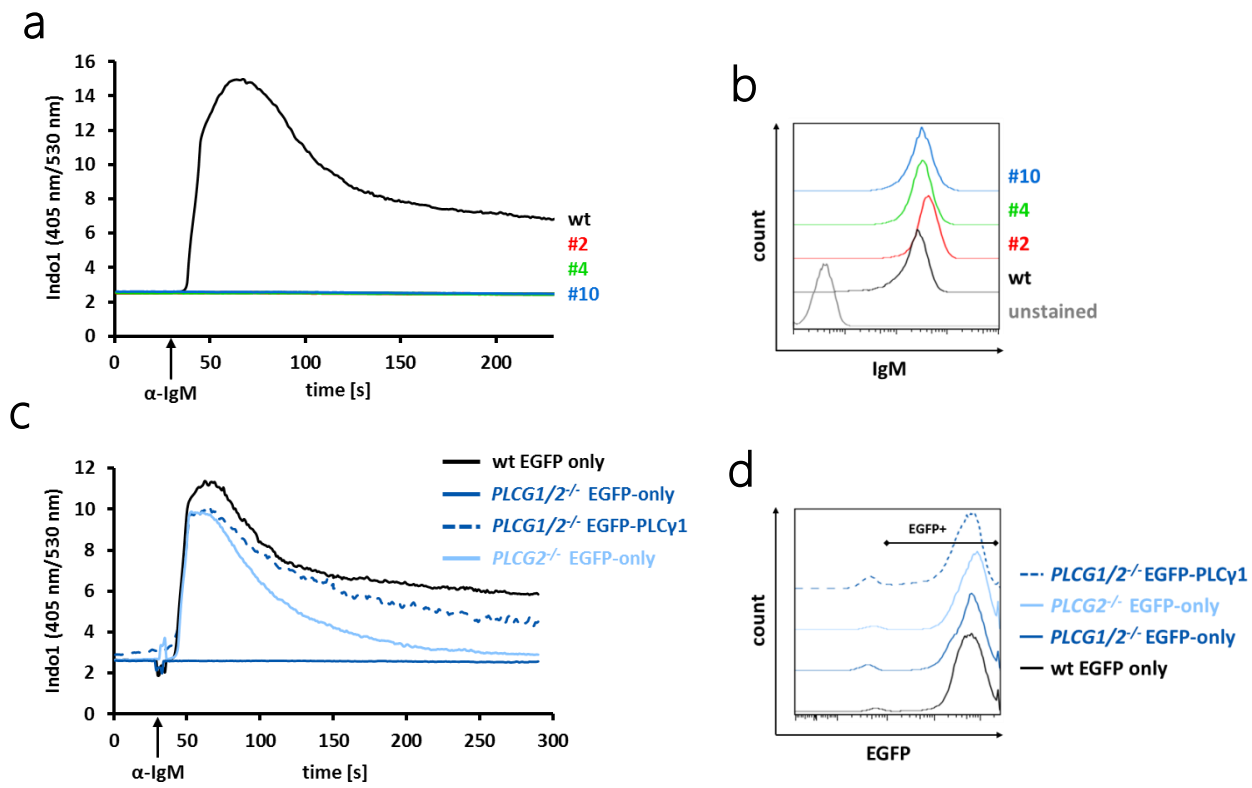

Figure 14. Impaired Ca^{2+} mobilization in the PLCγ1/2-deficient B cells. (a) Ca^{2+} mobilization analysis of three representative PLCγ1/2-double deficient DG75 subclones (#2, #4, #10). Baseline was recorded for 30 s before cells were stimulated via the IgM-BCR with 10 µg/ml F(ab')2 (time point of stimulation is indicated by arrow). Ca^{2+} mobilization was monitored for 300 s in total by flow cytometry using the ratiometric Ca^{2+} sensitive dye Indo-1. (b) IgM-BCR expression level in PLCγ1/2-double deficient DG75 subclones. 1x10^6 cells were stained with a FITC-labelled α-IgM antibody and analyzed by flow cytometry. (c) Ca^{2+} mobilization assay of PLCγ1/2-double deficient DG75 reconstituted with N-terminally EGFP-tagged PLCγ1 (*PLCG1/2*$^{-/-}$ EGFP-PLCγ1), untransduced PLCγ1/2-double deficient DG75 (*PLCG1/2*$^{-/-}$), PLCγ2-deficient DG75 (*PLCG2*$^{-/-}$) and DG75 parental cells (wt) transduced with EGFP-only. (d) Expression level of EFGP-tagged PLCγ1 and EGFP-only. Due to a slight overlap of EGFP and Indo-1 emission wavelength, the control cells DG75 *PLCG2*$^{-/-}$, DG75 *PLCG1/2*$^{-/-}$ and parental cells (wt) were transduced with EGFP-only for better comparability of the Ca^{2+} mobilization profiles.

3.2.2.5 Erk activation in human B cells does not depend on PLCγ activity

Studies in DT40 chicken B cells and murine B cells revealed that PLCγ2 is indispensable for the activation of Erk via RasGRP3 and DAG. Hence, Erk activation in DT40 chicken B cells also correlates with the mobilization of Ca^{2+} (Oh-hora et al, 2003; Coughlin et al, 2005). However, my results showed that in the human B cell line DG75, Erk activation is mediated independently of the Ca^{2+} mobilization complex and presumably also independent of the activity of PLCγ, reflecting species specific differences between chicken, mice and human. In order to test this hypothesis, I compared PLCγ2-deficient DG75 (*PLCG2*$^{-/-}$) and PLCγ1/2-double deficient DG75

(*PLCG1/2*$^{-/-}$) with PLCγ1-deficient DG75 (*PLCG1*$^{-/-}$) and parental cells (wt) with regard to Ca^{2+} mobilization (figure 15 a) and Erk phosphorylation (figure 15 b-d). As already shown in the previous sections, PLCγ2 deficiency alone led to a 50 % decrease in Ca^{2+} mobilization, while Ca^{2+} mobilization in PLCγ1/2-double deficient DG75 was completely abolished. In contrast, Ca^{2+} mobilization in PLCγ1-single deficient cells is similar to Ca^{2+}mobilization in parental (wt) cells. Consequently, PLCγ1 can indeed partially compensate for PLCγ2 function, but does not play a major role in Ca^{2+} mobilization of human B cells (figure 15 a). However, analysis of Erk activation by Western blot probing for phosphorylated Erk, revealed no change of Erk phosphorylation in all PLCγ-deficient cell lines compared to parental (wt) cells (figure 15 b). This I could confirm by intracellular staining for phosphorylated Erk, following stimulation via the BCR for 0, 3, 10 and 20 min (figure 15 c & d). The bar diagraph (figure 15 d) displays the average of the median fluorescence intensity (MFI) of five independent experiments. Taken together, these results confirm that Erk activation in the human B cell line DG75 occurs independently of PLCγ.

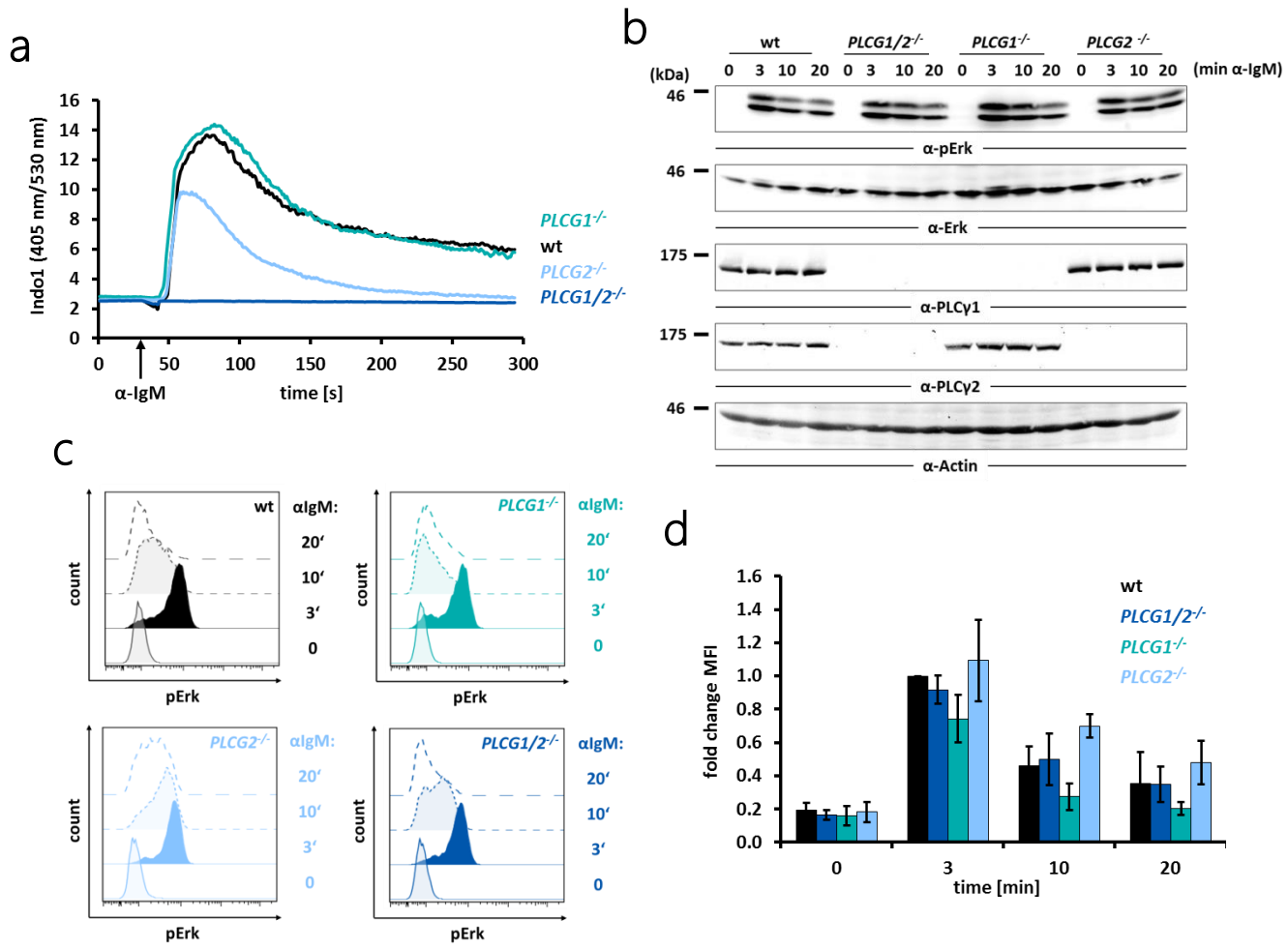

Figure 15. BCR-mediated Erk activation occurs independently of PLCγ1 and 2. (a) Ca^{2+} mobilization assay of PLCγ-deficient DG75. Baseline was recorded for 30 sec. PLCγ1-deficient (*PLCG1*$^{-/-}$), PLCγ2-deficient (*PLCG2*$^{-/-}$), PLCγ1/2-double deficient (*PLCG1/2*$^{-/-}$) and parental DG75 (wt) were stimulated with 10 µg/ml F(ab')2 α-IgM (time point of stimulation indicated by arrow). Mobilization of Ca^{2+} was monitored for 300 s by flow cytometry using the ratiometric dye Indo-1. (b) Western blot analysis for phosphorylated Erk. Cells were stimulated with 10 µg/ml F(ab')2 for 0, 3, 10 and 20 min. Cells were lysed and analyzed by Western blot probing for phosphorylated Erk (α-pErk). Expression of total Erk, PLCγ1 and 2 was verified with respective antibodies. Actin served as loading control. (c & d) Intracellular staining of phosphorylated Erk. Cells were stimulated with 10 µg/ml F(ab')2 for 0, 3, 10 and 20 min, fixed, permeabilized and analyzed by flow cytometry using an ALEXA647 coupled antibody specific for phosphorylated Erk. (c) Representative histograms of Erk phosphorylation in different PLCγ-deficient cells. (d) Fold change of median fluorescence intensity (MFI)/Erk phosphorylation in PLCγ-deficient cells. Mean values and standard deviation of five independent experiments.

3.2.2 Human B cells exhibit low expression levels of RasGRP 1 and 3

Since activation of Erk in human B cells is mediated completely independently of PLCγ, I concluded that also RasGRP3, which is activated via PLCγ2 and DAG, does not play a role in Erk activation in human B cells. However, our model cell line DG75 exhibits low RasGRP3 expression levels, which could already limit activation of Erk by RasGRP3. In order to test whether the B cell line DG75 is a suitable representative physiological model to study Erk activation in human B cells, I compared expression of RasGRPs in DG75 cells with RasGRP expression in human primary B cells. To this end, I isolated human primary B cells from peripheral blood of a voluntary donor by CD19-positive selection. Isolated B cells were analyzed for CD19 and IgM expression (figure 16 a), lysed and analyzed by Western blot analysis for RasGRP expression (figure 16 b). Flow cytometry analysis for CD19 and IgM expression revealed a purification yield of 94.2 % $CD19^+$ B cells. The major population (86.1 %) expressed IgM, thus it is probably constituted of naïve B cells. However, ca. 26 % of the CD19-positive population is IgM-negative. These cells probably resemble a memory B cell population (figure 16 a). RasGRP expression in human primary B cells was analyzed by Western blot and compared to RasGRP expression of the human B cell lines DG75, Raji as well as the human T cell line JURKAT. In contrast to Raji and JURKAT cells, DG75 cells and human primary B cells only express low levels of RasGRP1 and RasGRP3. However, RasGRP2 expression was detected to similar extents in Raji, DG75 and JURKAT cells, whereas human primary B cells expressed higher levels of RasGRP2. Grb2 and GRAP expression was equal in the cell lines, but slightly lower in the primary B cells. Btk was used as B cell- and SLAP130 as T cell-specific loading control. Actin served as additional loading control (figure 16 b). To sum up, the expression of RasGRP1 and 3 in human primary B cells isolated from peripheral blood is similar to RasGRP 1 and 3 expression of DG75 cells. Only RasGRP2 expression appeared to be higher in human primary B cells than in DG75. However, in terms of RasGRP1, RasGRP3, Grb2 and GRAP expression, DG75 cells resemble the situation of human primary B cells. Hence they are a representative model to study Erk activation in human B cells.

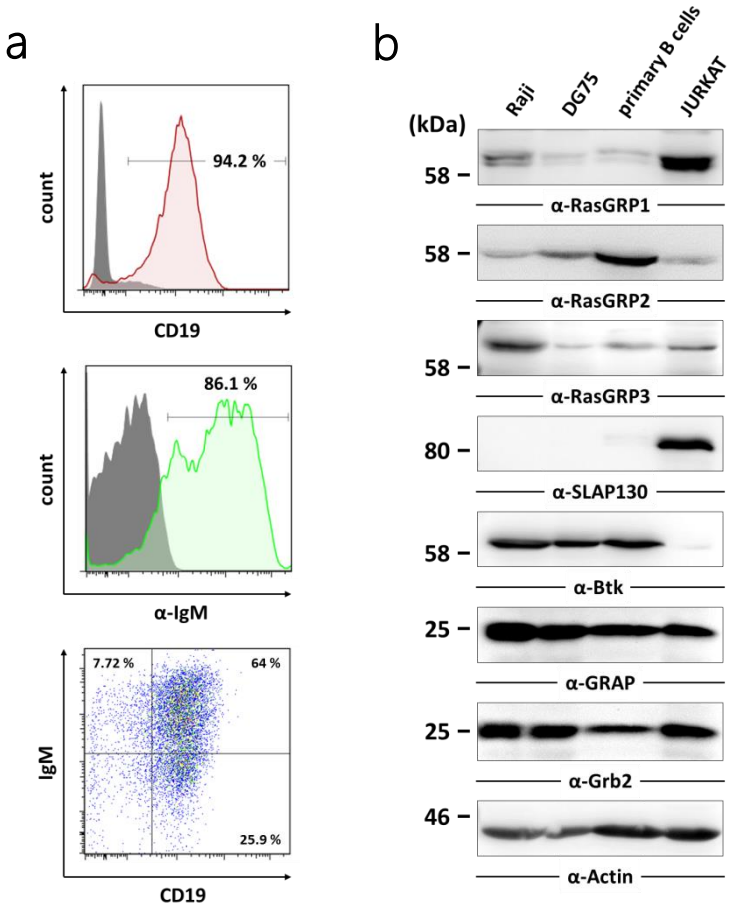

Figure 16. Human B cells exhibit low expression levels of RasGRPs. (a) Purity analysis of human primary B cells isolated from peripheral blood. Cells were isolated by CD19-positive selection, before they were incubated in R10 for 30 min at 37°C in order to recycle CD19 expression. Isolation yield was analyzed by flow cytometry via surface staining of CD19 and IgM. (b) Comparison of RasGRP expression in human primary B cells and the human B cell lines Raji and DG75 as well as the JURKAT T cell line by Western blot analysis. Membrane was probed for RasGRP1, 2 and 3 as well as for Grb2 and GRAP. Btk served as B cell-specific and SLAP130 as T cell-specific loading control. Actin served as general loading control.

3.2.3 Grb2 cooperates with GRAP in activation of Erk

My results revealed that PLCγ1 and 2 are dispensable for the BCR-induced Erk activation in human B cells in contrast to Erk activation in chicken and mouse B cells which depends on PLCγ2. (Oh-hora et al, 2003; Bell et al, 2004). Further, I suppose that human B cells do not require RasGRPs for BCR-mediated activation of Erk but rather rely on another guanine nucleotide exchange factor, namely Sos, as described for EGFR signaling. Sos gets recruited to the EGFR by constitutive interaction with the adapter protein Grb2 (Lowenstein et al, 1992). Indeed, Erk

activation studies in Grb2-deficient DG75 (*GRB2*$^{-/-}$) (figure 10) revealed that Grb2 is important for the activation of Erk, although Erk phosphorylation in Grb2-deficient cells was not completely abolished. This could be due to GRAP, another member of the Grb2-family of adapters, that shares 60 % structural homology with Grb2 and could be compensating for Grb2. In contrast to Grb2, GRAP expression is restricted to lymphocytes (Trüb et al, 1997). However, its role in B lymphocytes is yet unknown. In order to test this hypothesis, I generated a Grb2/GRAP-double deficient cell line and analyzed it for activation of Erk.

3.2.3.1 Generation of a Grb2/GRAP-double deficient B cell line

The Grb2/GRAP-double deficient DG75-sub-cell line (*GRB2/GRAP*$^{-/-}$) was generated by using the TALEN-based genome editing technique on the background of the Grb2-deficient DG75-sub cell line (*GRB2*$^{-/-}$). TALENs were designed to target exon 2 of the *GRAP* gene. TALEN cut site was chosen to be located in a BsRI restriction site, that was used for later TALEN activity test (figure 17 a). The TALEN pair was introduced in Grb2-deficient DG75 by nucleofection via an IRES-GFP, or IRES-RFP cassette containing vector. Double positive cells were sorted and analyzed for TALEN activity. Therefore, exon 2 was amplified from genomic DNA from the sorted population or parental cells, respectively and treated with BsRI. BsRI treatment revealed partial activity of the TALEN constructs of the TALEN-electroporated cell population (figure 17 b). Next, cells were subcultured in order to obtain single cell clones. Resulting clones were analyzed for GRAP-protein expression on Western blot and by Sanger-sequencing analysis. In total, 237 potential Grb2/GRAP-double deficient clones were screened by Western blot. Thereof only 11 subclones were tested negatively for GRAP-protein expression (figure 17 c). An exemplary Western blot analysis is depicted in figure 17 d, comparing GRAP-protein expression in Grb2/GRAP-double deficient (*GRB2/GRAP*$^{-/-}$) clone #81, in GRAP-single deficient (*GRAP*$^{-/-}$) clone #5 and Grb2-deficient (*GRB2*$^{-/-}$) as well as DG75 parental cells (wt). Sequencing analysis of seven of these double-deficient clones revealed that the TALEN-mediated modification within the *GRAP* gene was either heterozygous or encompasses a bp-deletion of a multiple of three, leading to a loss of a few amino acids. This led to the assumption, that a homozygous modification of the *GRAP*-gene, along with a Grb2-deficiency, is lethal. However, I specified clone #81 as Grb2/GRAP-deficient subclone. It carries a 9 bp deletion on allele 1 and an 18 bp deletion

on allele 2, each leading to a loss of 3 and 6 amino acids including the tryptophan at position 36 (W36) that is conserved among Grb2 and GRAP (figure 17 e). Loss of W36 leads to inactivation of the N-terminal SH2 domain, important for adapter-protein functions of Grb2 (Cully et al, 2004) and GRAP.

The GRAP-single deficient DG75 cell line (*GRAP*$^{-/-}$) was generated with the same TALEN-constructs as described for the double deficient cells. As for the Grb2/GRAP-double deficient cells (*GRB2/GRAP*$^{-/-}$), sequencing analysis of the GRAP-deficient clones revealed either a heterozygous modification within the GRAP gene or deletions encompassing a bp-deletion of a multiple of three (not shown). In total, I analyzed 69 clones, whereof 13 were GRAP-negative on protein level. I specified clone #5 as GRAP-deficient which carries a 7 bp deletion on allele 1. The second allele could not be amplified and sequenced.

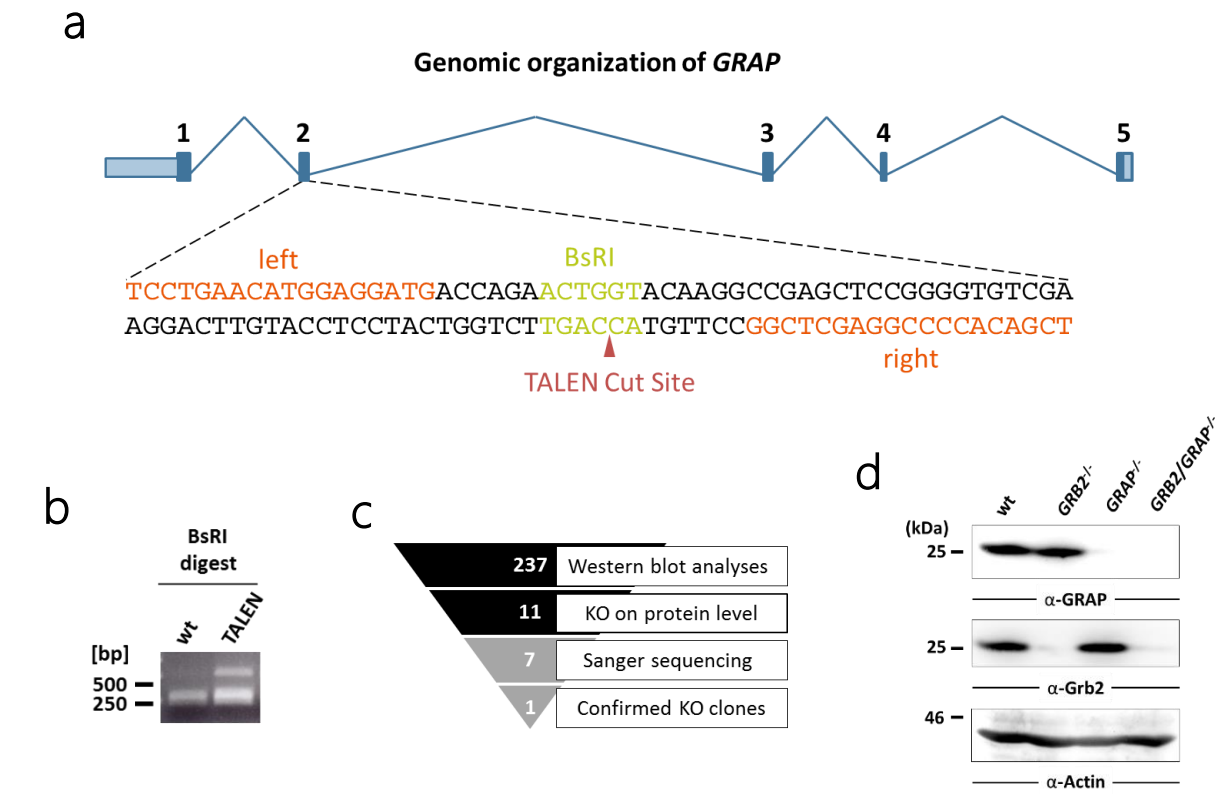

e

DNA sequence Exon 2 *GRAP* from Grb2/GRAP-double deficient cells

```
wt       ...ATCCTGAACATGGAGGATGACCAGAACTGGTACAAGGCCGAGCTCCGG...
#81.7
 allele 1 ...ATCCTGAACATGGAGGATGACCA---------CAAGGCCGAGCTCCGG...   Δ 9 bp
 allele 2 ...ATCCTGAACATGGA------------------CAAGGCCGAGCTCCGG...   Δ 18 bp
```

amino acid sequence

```
wt       ...ilnmeddqnwykaelrgvegfipknyirvkphpw...
#81.7
 allele 1 ...ilnmeddh---kaelrgvegfipknyirvkphp...  Δ 3 aa
 allele 2 ...ilnmd------kaelrgvegfipknyirvkphp...  Δ 6 aa
```

Figure 17. Generation of a Grb2/GRAP-double deficient cell line using TALEN. (a) Exon structure of the *GRAP* gene and sequence of the targeted exon 2. TALEN binding sites for left and right arm are highlighted in orange, TALEN cut site is indicated by a red arrow and BsRI restriction site is highlighted in green. (b) TALEN activity test. Exon 2 was amplified from parental DG75 cells (wt) or TALEN-nucleofected cells and treated with BsRI. Treated PCR product was analyzed by agarose gel electrophoresis. (c) Statistics of single-cell clone analysis. Single cell clones were analyzed by Western blot. Clones lacking GRAP-protein expression were further analyzed by Sanger sequencing to verify mutation on genomic level. (d) Exemplary Western blot analysis of DG75 *GRB2/GRAP*$^{-/-}$ subclone #81 compared with DG75 *GRAP*$^{-/-}$ subclone #5, DG75- and DG75 *GRB2*$^{-/-}$ parental cells. (e) Genomic DNA sequence and corresponding aa sequence of DG75 *Grb2/GRAP*$^{-/-}$ subclone #81. Sequence is representative for at least seven sequencing analyses.

3.2.3.2 GRAP partially can compensate for Grb2 in Erk activation

Erk activation in Grb2-deficient DG75 (*GRB2*$^{-/-}$) was remarkably diminished, but not completely abolished. In order to test, whether this is due to expression of GRAP, I analyzed Erk activation following BCR activation in the newly generated Grb2/GRAP-double deficient DG75-sub cell line (*GRB2/GRAP*$^{-/-}$) by Western blot analysis probing for pErk (figure 18 a) and by intracellular staining for phosphorylated Erk for flow cytometry by using a fluorescence-labelled pErk antibody (figure 18 b & c). The Western blot analysis revealed that compared to DG75 parental cells (wt), Erk activation (pErk) in Grb2-deficient DG75 (*GRB2*$^{-/-}$) upon 3 min of BCR stimulation was clearly diminished, while Grb2/GRAP-double deficient DG75 (*GRB2/GRAP*$^{-/-}$) exhibited almost no Erk-phosphorylation. However, GRAP-single deficient DG75 (*GRAP*$^{-/-}$) show normal, or even stronger Erk activation compared to parental cells (wt) (figure 18 a). These observations are supported by intracellular staining of phosphorylated Erk that allows better quantification of Erk-phosphorylation (figure 18 b & c). Upon 3 min of BCR stimulation, Erk activation in GRAP-deficient cells (*GRAP*$^{-/-}$) was not changed compared to parental cells, while Erk activation in Grb2-deficient cells (*GRB2*$^{-/-}$) was more than 50 % diminished. Additional editing of GRAP (*GRB2/GRAP*$^{-/-}$) almost reduced the p-Erk-signal to the p-Erk level of unstimulated cells (figure 18 b & c). To sum up, to small extents GRAP indeed seems to be able to compensate for Grb2 in Erk activation. However, GRAP alone does not play an important role in Erk activation in human B cells.

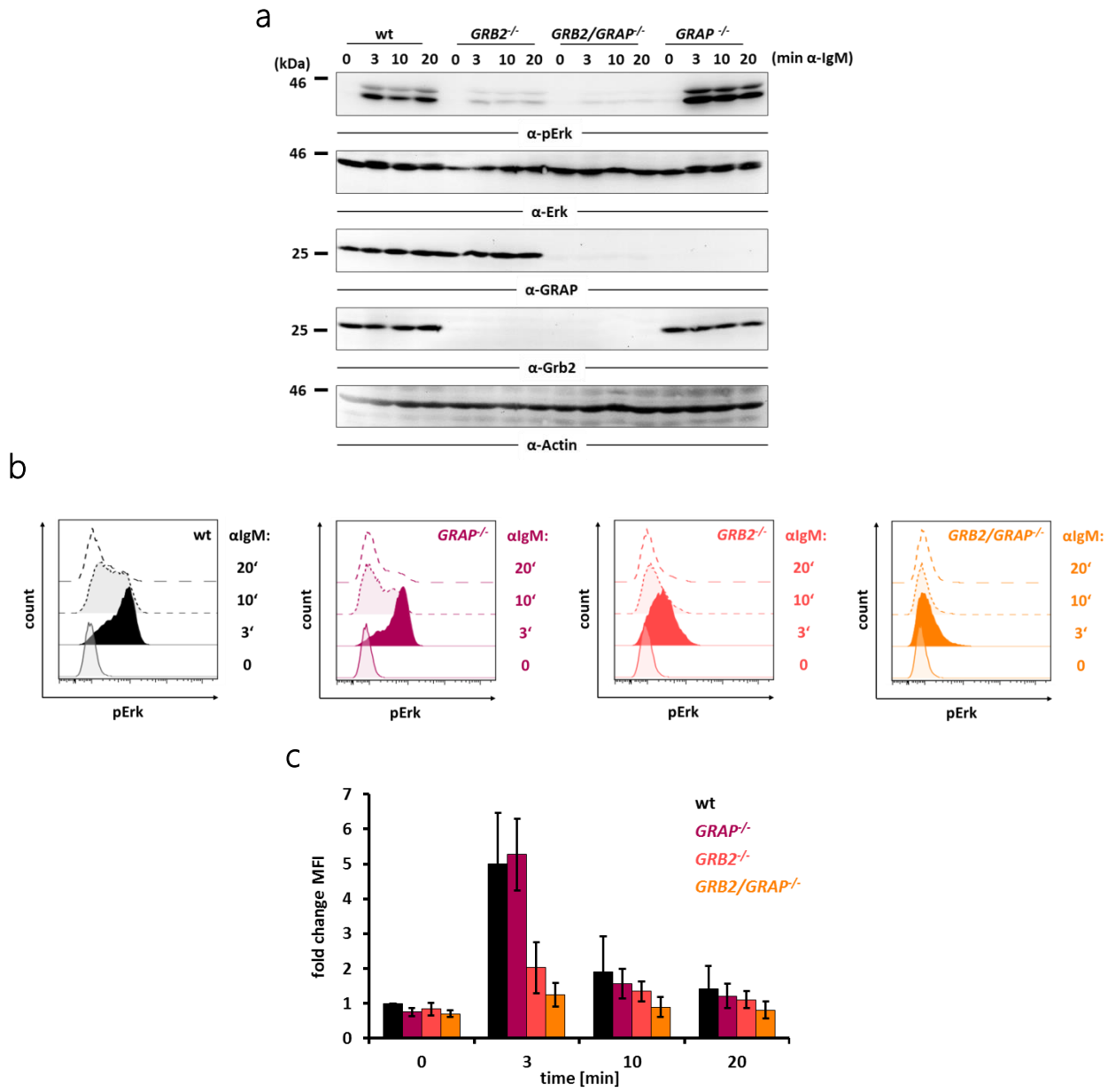

Figure 18. Cooperation of Grb2 and GRAP in Erk activation. (a) Western blot analysis for phosphorylated Erk. DG75 parental cells (wt), DG75 *GRB2*$^{-/-}$, DG75 *GRAP*$^{-/-}$ and DG75 *GRB2/GRAP*$^{-/-}$ B cells were stimulated with 10 µg/ml F(ab')2 for 0, 3, 10 and 20 min. Cells were lysed and analyzed by Western blot probing for phosphorylated Erk (α-pErk). Expression of total Erk, Grb2 and GRAP was verified with respective antibodies. Actin served as loading control. (b & c) Intracellular staining for phosphorylated Erk. DG75 parental cells (wt), DG75 *GRB2*$^{-/-}$, DG75 *GRAP*$^{-/-}$ and DG75 *GRB2/GRAP*$^{-/-}$ B cells were stimulated with 10 µg/ml F(ab')2 for 0, 3, 10 and 20 min, fixed, permeabilized and analyzed by flow cytometry using an ALEXA647 coupled antibody specific for phosphorylated Erk. (b) Representative histograms of Erk phosphorylation in DG75 parental cells (wt), DG75 B cells deficient for Grb2 (*GRB2*$^{-/-}$), GRAP (*GRAP*$^{-/-}$) or both (*GRB2/GRAP*$^{-/-}$). (c) fold change of median fluorescence intensity (MFI)/Erk phosphorylation in DG75 parental cells (wt), DG75 B cells deficient for Grb2 (*GRB2*$^{-/-}$), GRAP (*GRAP*$^{-/-}$) or both (*GRB2/GRAP*$^{-/-}$). Mean values and standard deviation of three independent experiments.

In order to confirm the role of GRAP in Erk activation and exclude off target effects, I reconstituted the Grb2/GRAP-double deficient DG75 with GRAP cDNA by retroviral transduction and analyzed them for their ability to activate Erk upon BCR activation (figure 19). The Western blot analysis showed an increase in BCR-induced Erk activation (pErk) in Grb2/GRAP-double deficient DG75 (*GRB2/GRAP*$^{-/-}$) reconstituted with GRAP compared to untransduced DG75 *GRB2/GRAP*$^{-/-}$(figure 19 a). ICS of phosphorylated Erk revealed a recovery of Erk activation upon GRAP reconstitution to the level of Erk activation in Grb2-deficient DG75 (*GRB2*$^{-/-}$) (figure 19 b & c). Thus, the reconstitution of GRAP in Grb2/GRAP-double deficient DG75 (*GRB2/GRAP*$^{-/-}$) excluded an off-target effect by the GRAP TALEN-construct, confirming a minor compensatory role for GRAP in BCR-induced Erk activation. Taken together, these results reveal a partial involvement of GRAP in the BCR-mediated activation of Erk when Grb2 is absent. Grb2/GRAP-double deficiency in the human B cell line DG75 almost led to a complete loss of their ability for Erk activation following BCR stimulation.

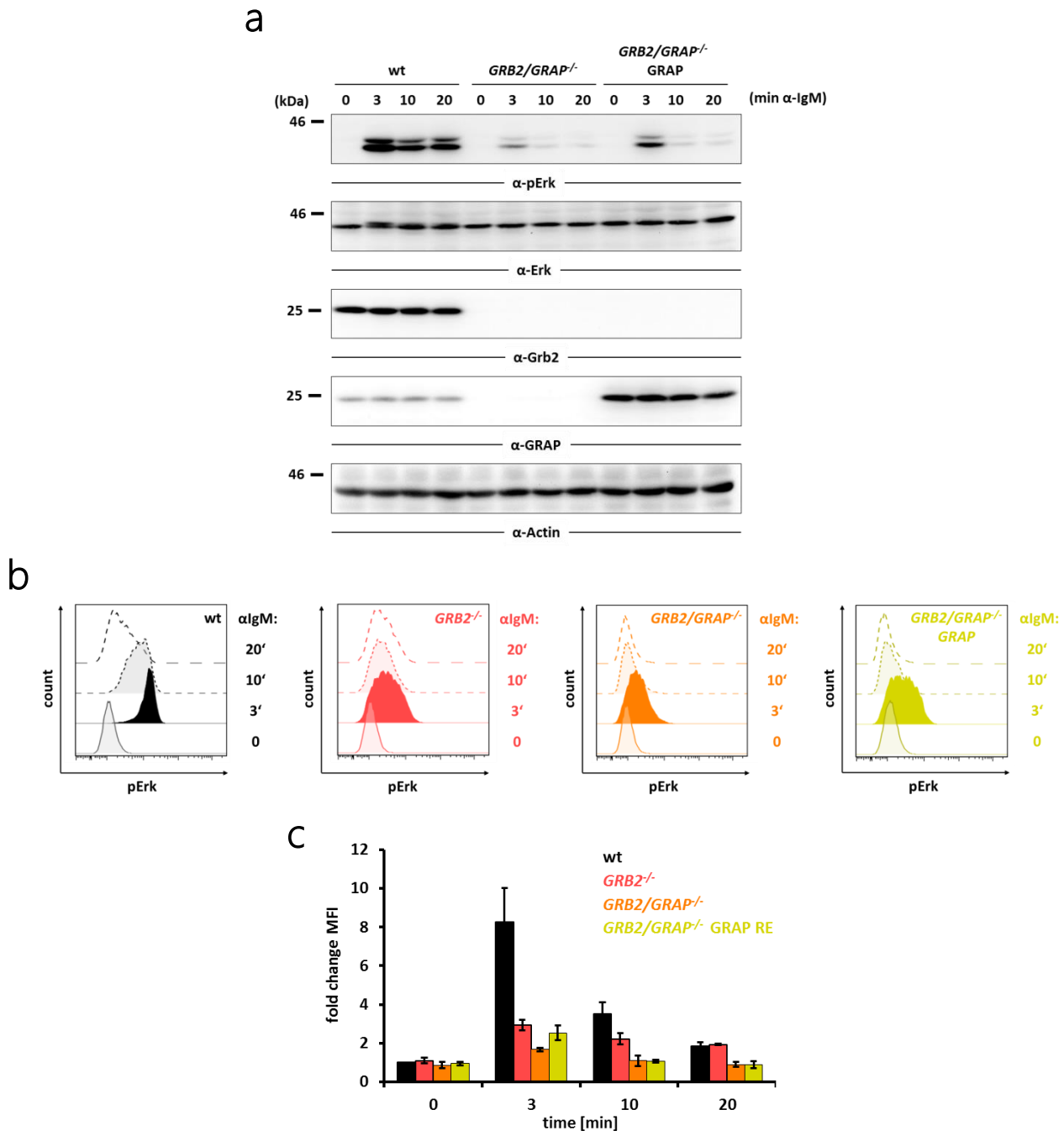

Figure 19. Reconstitution of GRAP in Grb2/GRAP-double deficient B cells. (a) Western blot analysis for phosphorylated Erk. DG75 parental cells (wt), DG75 *GRB2*$^{-/-}$, DG75 *GRB2/GRAP*$^{-/-}$ and DG75 *GRB2/GRAP*$^{-/-}$ GRAP (transduced with GRAP) were stimulated with 10 µg/ml F(ab')2 for 0, 3, 10 and 20 min. Cells were lysed and analyzed by Western blot probing for phosphorylated Erk (α-pErk). Expression of total Erk, Grb2 and GRAP was verified with respective antibodies. Actin served as loading control. (b & c) Intracellular staining for phosphorylated Erk. Cells were stimulated with 10 µg/ml F(ab')2 for 0, 3, 10 and 20 min, fixed, permeabilized and analyzed by flow cytometry using an ALEXA647 coupled antibody specific for phosphorylated Erk. (b) Representative histograms of Erk phosphorylation in DG75 parental cells (wt), DG75 *GRB2*$^{-/-}$, DG75 *GRB2/GRAP*$^{-/-}$ and DG75 *GRB2/GRAP*$^{-/-}$ GRAP. (c) Fold change of median fluorescence intensity (MFI)/Erk phosphorylation in DG75 parental cells (wt), DG75 *GRB2*$^{-/-}$, DG75 *GRB2/GRAP*$^{-/-}$ and DG75 *GRB2/GRAP*$^{-/-}$ GRAP (transduced with GRAP). Mean values and standard deviation of three independent experiments.

3.2.4 Ectopic expression of RasGRP3 in Grb2/GRAP-double deficient B cells can reconstitute BCR-mediated Erk activation

By disrupting Grb2 and GRAP expression, the human B cell line DG75 almost completely lost its ability for BCR-mediated Erk activation. This is probably due to the potential of Grb2, and presumably also of GRAP, to link the guanine nucleotide exchange factor Sos to the activated B cell receptor by constitutive interaction with Sos by virtue of both Grb2-SH3 domains (Lowenstein et al, 1992). Hence, Sos would loose its ability to activate Ras, which in turn would lead to activation of Erk via the Ras/MAPK pathway. The guanine nucleotide exchange factor RasGRP3, that has been shown to arbitrate BCR-mediated Erk activation via DAG and PKC in the chicken B cell line DT40 as well as in murine B cells, is only expressed to small amounts in human B cells and hence is dispensable for Erk activation in human B cells (figure 20). However, I hypothesized that ectopically expressed RasGRP3 can reconstitute BCR-mediated Erk activation in Grb2/GRAP-double deficient DG75. In order to test the hypothesis, I retrovirally transduced RasGRP3 in Grb2/GRAP-double deficient DG75 (*GRB2/GRAP*$^{-/-}$) and analyzed their potential for Erk activation upon BCR stimulation. Western blot analysis following 3, 10 and 20 min of BCR stimulation showed that Erk activation (pErk) can be completely reconstituted in Grb2/GRAP-double deficient DG75 transduced with RasGRP3 (*GRB2/GRAP*$^{-/-}$ RasGRP3) (figure 20).

To sum up, ectopic expression of RasGRP3 in Grb2/GRAP-double deficient DG75 could restore BCR-mediated Erk activation completely, revealing that human B cells potentially are able to use RasGRPs. However, low endogenous expression of RasGRP1 and RasGRP3 in human B cells limits RasGRP dependent Erk activation.

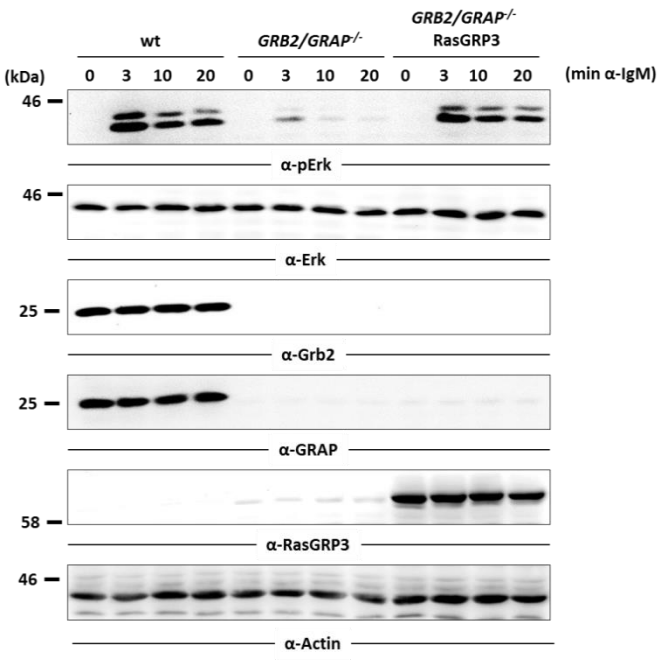

Figure 20. Ectopic expression of RasGRP3 in Grb2/GRAP-double deficient DG75. Western blot analysis for phosphorylated Erk. DG75 parental cells (wt), Grb2/GRAP-double deficient DG75 (*GRB2/GRAP*$^{-/-}$) and Grb2/GRAP-double deficient DG75 transduced with RasGRP3 (*GRB2/GRAP*$^{-/-}$ RasGRP3) were stimulated with 10 µg/ml F(ab')2 for 0, 3, 10 and 20 min. Cells were lysed and analyzed by Western blot probing for phosphorylated Erk (α-pErk). Expression of total Erk, Grb2, GRAP and ectopically expressed RasGRP3 was verified with respective antibodies. Actin served as loading control.

3.2.5 Erk activation requires recruitment of Grb2 to the signalosome of the activated BCR

3.2.5.1 Grb2 domains cooperate in the activation of Erk

I could show that Grb2 is indispensable for the activation of Erk. The requirement of Grb2 in Erk activation in turn implemented that the activation of Erk in human B cells is dependent on Sos, which constitutively interacts with Grb2 via both Grb2-SH3 domains (Lowenstein et al, 1992). To functionally dissect which Grb2 domains in particular are important for Erk activation, I reconstituted Grb2-deficient cells with Grb2 variants harboring amino acid substitutions leading to inactivation of the ligand binding ability of the respective domains. Substitution of W by K (W being tryptophan, K being lysine) at position 36 (W36K) leads to inactivation of the N-terminal SH3 domain (N-SH3 mutant), R86K (R being arginine) inactivates the SH2 domain (SH2 mutant) and W193K the C-terminal SH3 domain (C-SH3 mutant, figure 21 a) (Cully et al, 2004). Erk phosphorylation analysis by ICS revealed that Erk activation capability following 3 min of BCR stimulation can be restored by reconstitution of Grb2-deficient DG75 (*GRB2*$^{-/-}$) with Grb2 wt.

However, neither the N-SH3 mutant, the SH2 mutant nor the C-SH3 mutant can functionally replace the Grb2 wt variant in the activation of Erk. Erk activation in cells reconstituted with the triple mutant is comparable to Erk activation in Grb2-deficient cells (figure 21 c & d). To conclude, all three domains of Grb2 play an important role in the activation of Erk. The importance of both SH3 domains supports the involvement of Grb2 in Erk activation due to its role in facilitating Ras activation via Sos, since both SH3 domains were shown to be important for the interaction of Grb2 with Sos (Neumann et al, 2009). In addition, the requirement for a functional SH2 domain shows that BCR mediated Erk activation requires recruitment of Grb2 to the activated BCR complex, more precisely to a phosphorylated (p)YXN motif via its SH2 domain. However, in contrast to memory B cells, a ligand for the SH2 domain of Grb2 in naïve (IgM-positive) B cells within the BCR complex has not been described, yet.

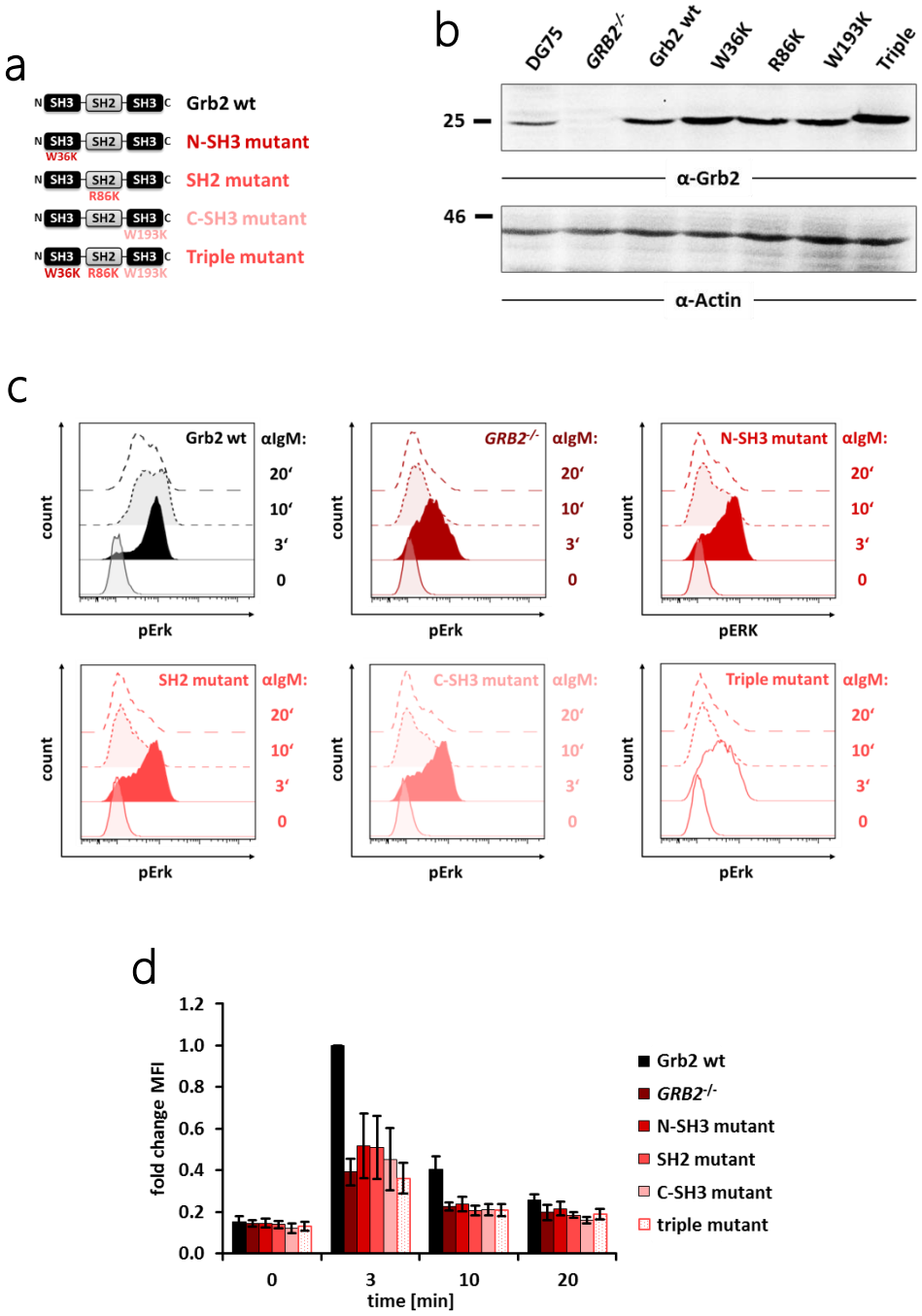

Figure 21. Functional dissection of Grb2 in Erk activation. (a) Schematic depiction of Grb2 variants with respective amino acid substitution introduced by site directed mutagenesis in order to inactivate the domains. W36K = N-SH3 mutant, R86K = SH2 mutant, W193K = C-SH3 mutant. Grb2 variant with all three mutations was termed as triple mutant. (b) Expression level of Grb2 variants in Grb2-deficient DG75 (*GRB2*$^{-/-}$) compared to parental cells (wt). (c & d) Intracellular staining for phosphorylated Erk (pErk). Cells were stimulated with 10 µg/ml F(ab')2 for 0, 3, 10 and 20 min, fixed, permeabilized and analyzed by flow cytometry using an ALEXA647 coupled antibody specific for phosphorylated Erk. (c) Representative histograms of Erk phosphorylation in Grb2-deficient DG75 (*GRB2*$^{-/-}$) transduced with different mutant variants of Grb2. (d) fold change of median fluorescence intensity (MFI)/Erk phosphorylation. Mean values and standard deviation of 7 independent experiments.

3.2.5.2 Grb2 is recruited to the BCR signalosome by virtue of its SH2 domain

Since the Grb2-SH2 domain seems to be important for BCR-mediated Erk activation, I concluded, that Erk activation requires recruitment of Grb2 to the signalosome of the activated BCR via the Grb2-SH2 domain. However, for direct recruitment in a SH2-domain dependent manner, Grb2 requires a pYXN motif, which is neither present within IgM-BCR nor within the Igα/β heterodimer. In order to address SH2-mediated Grb2 recruitment to the activated BCR signalosome, I performed a GST-pulldown assay with cleared cellular lysates (CCL) from DG75 cells stimulated via the BCR, using the recombinant GST-tagged SH2 domain of Grb2. Western blot analysis of the pulldown revealed an enrichment in tyrosine-phosphorylated proteins from lysates of cells stimulated via the BCR (not shown). To analyze the purified protein complexes, I repeated the GST-pulldown assay and sent the samples for Stable isotope labeling with amino acids in cell culture (SILAC)-based mass spectrometry (MS) analysis. SILAC-based MS is a quantitive proteomic approach allowing simultaneous relative quantification of proteins derived from different cellular conditions. Therefore, cells are cultured in different media containing normal (light) or heavy isotope amino acids that are metabolically incorporated into proteins during protein synthesis. Incorporation of heavy isotope amino acids into proteins leads to an increase of the molecular masses of the proteins. Thus, peptides derived from this sample can be easily identified and distinguished from the sample of cells cultured in normal (light) medium in the MS spectra (Zhang & Neubert, 2009). To identify Grb2-SH2 domain interaction partners, I cultured Grb2-deficient DG75 either in light (R0/K0) or heavy (R6/K4) SILAC medium. In heavy SILAC medium R (being arginine) and K (being lysine) are substituted by heavy labeled amino acids. In R6 six carbon atoms (C^{12}) are replaced by C^{13} leading to a mass increase of 6 Dalton (Da), while K4 contains 4 deuterium instead of 4 hydrogens, leading to a 4 Da mass increase. Prior GST-pulldown assay, cells were stimulated via the BCR for 3 min. Lysates from cells cultured in the heavy medium were incubated with GST-Grb2 SH2 fusion protein for 2 h, whilst cells cultured in the light medium were incubated with the GST-Grb2 SH2 R86L (inactive) fusion protein that served as a negative control. GST-pulldown eluates of both samples were mixed in a 1:1 ratio and analyzed by LC-MS/MS by the core facility at University medical center, Göttingen. Relative abundance (H/L ratio) of BCR relevant proteins enriched with the GST-Grb2 SH2 domain is shown in the scatter plot (figure 22) and is listed in table 26 including Uniprot accession

numbers. Proteins with a heavy/light ratio >2 were considered as enriched in the pulldown with the intact Grb2-SH2 domain. Proteins with relevance in BCR signaling were highlighted in blue (BCR complex) or in red (BCR associated proteins). The most abundant proteins I identified, were Igα, as well as several components of membrane IgM (highlighted in blue), confirming that Grb2 via its SH2-domain indeed is directed to the signalosome of the activated BCR. Moreover, I identified several well-described interaction partners of Grb2, as for example the phosphatases SHP1, SHP2 and SHIP1 as well as the adapter proteins Dok3, Gab1 and SHC1, and the inhibitory BCR coreceptor CD22. However, a direct interaction via the Grb2-SH2 domain was only described for SHC1 (Harmer & DeFranco, 1997), SHP2 (Vogel & Ullrich, 1996), Dok3 (Honma et al, 2006; Stork et al, 2007), Gab1 (Bardelli et al, 1997; Holgado-Madruga et al, 1996) and CD22 (Yohannan et al, 1999; Otipoby et al, 2001). The interaction of Grb2 with SHP1 and SHIP1 so far has been attributed to the SH3 domains (Saci et al, 2002; Otipoby et al, 2001). Hence, the enrichment of SHP1 and SHIP1 could be explained by indirect interactions, for example via SHC1 (Poe et al, 2000).

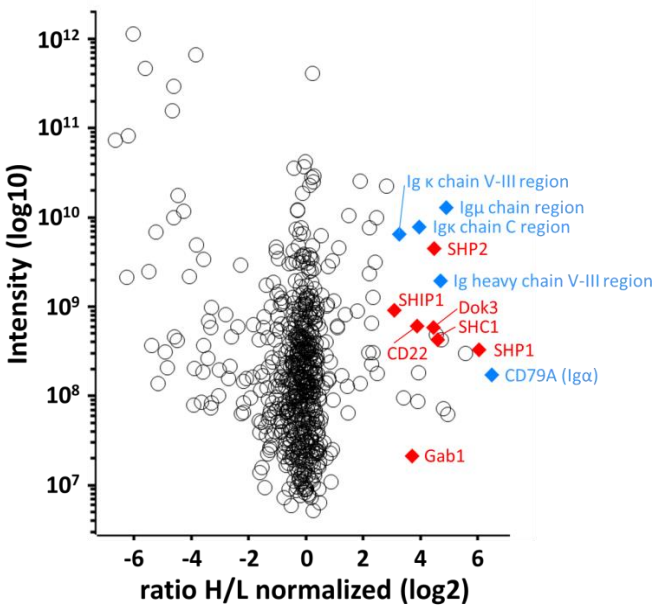

Figure 22. Scatter plot of SILAC-based mass spectrometry analysis. DG75 cells were either incubated in light (arginine +0/lysine +0) or in heavy SILAC medium (arginine +6/lysine +4). For GST-pulldown assay cells were stimulated via the BCR for 3 min, lysed and incubated either with GST-GRB2 SH2 (heavy medium cultured cells) or with GST-GRB2 SH2 R86L (inactive SH2 domain; light medium cultured cells). The eluate was pooled in a 1:1 ratio, processed and analyzed by LC-MS/MS. In the scatter plot the log(2) transformed heavy/light (h/l) ratio was plotted against the log(10) transformed peptide intensity. Proteins with a H/L ratio >2 were considered as enriched by the Grb2-SH2 domain. Proteins with relevance to BCR signaling were highlighted in blue (BCR complex) or red (BCR associated proteins).

Table 26. Interactome of the Grb2-SH2 domain in the human B cell line DG75, activated via the B cell antigen receptor. DG75 cells were either incubated in light (arginine +0/lysine +0) or in heavy SILAC medium (arginine +6/lysine +4). For GST-pulldown assay cells were stimulated via the BCR for 3 min, lysed and incubated either with GST-GRB2 SH2 (heavy medium cultured cells) or with GST-GRB2 SH2 R86L (inactive SH2 domain; light medium cultured cells). The eluate was pooled in a 1:1 ratio, processed and analyzed by LC-MS/MS. In the scatter plot the log(2) transformed heavy/light (h/l) ratio was plotted against the log(10) transformed peptide intensity. Proteins with a H/L ratio >2 were considered as enriched by the Grb2-SH2 domain. Proteins with relevance to BCR signaling were highlighted in blue (BCR complex) or red (BCR associated proteins).

	Protein	H/L	H/L log2	Accession number	Grb2-SH2
BCR complex	CD79A (Igα)	89.6	6.5	P11912	-
	Igμ chain region	30.12	4.9	A0A075B6N9	-
	Ig heavy chain V-III region	26.06	4.7	P01765	-
	Igκ chain C region	15.44	3.9	P04206	-
	Ig κ chain V-III region	9.63	3.2	A0A087X130	-
BCR associated proteins	SHP1 (Tyrosine-protein phosphatase non-receptor type 6)	65.81	6.0	P29350	-
	SHC1 (SHC-transforming protein 1)	24.52	4.6	P29353-2	Lankester et al, 1994; Harmer et al, 1997
	SHP2 (Tyrosine-protein phosphatase non-receptor type 11)	22.18	4.5	Q06124	Vogel 1996
	Dok3	22.03	4.5	D6RAM3	Stork et al, 2007, Honma et al, 2006
	CD22	14.74	3.9	P20273-4	Otipoby et al, 2001, Yohannan et al, 1999
	Gab1 (Grb2-associated protein)	13.13	3.7	Q13480	Bardelli et al, 1997
	SHIP1 (Phosphatidylinositol 3,4,5-trisphosphate 5 phosphatase 1)	8.53	3.1	Q92835-2	-
cytoskeleton/ intracellular trafficking	Signal transducing adapter molecule 2 (STAM2)	28.20	4.81	O75886	-
	Epidermal growth factor receptor substrate 15-like 1	26.7	4.7	Q9UBC2-4	-
	Intersectin-2	23.65	4.6	Q9NZM3-2	-
	Hepatocyte growth factor-regulated tyrosine kinase substrate	15.14	3.9	O14964-2	-
	Sorting nexin-18	10.62	3.4	Q96RF0-3	-
	Dystonin	5.35	2.4	Q03001-3	-
	Neuralized-like protein 4 (NEURL4)	4.69	2.2	I3L2W2	-
DNA replication and repair	Replication protein a 70kDa subunit (RPA1)	7.05	2.81	P27694	-
	DNA topoisomerase 3-alpha	5.61	2.48	Q13472-2	-
	Bloom syndrome protein	5.08	2.34	P54132	-
	E3 ubiquitin-protein ligase HERC2	5.05	2.33	O95714	-
	RecQ-mediated genome instability protein 1 (RMI1)	4.9	2.3	Q9H9A7	-
	Replication protein a 32kDa subunit (RPA2)	4.9	2.3	P15927	-
	Replication protein a 14kDa subunit (RPA3)	4.6	2.2	P35244	-

The results acquired from the mass spectrometry analysis confirmed that upon stimulation Grb2 gets recruited to the signalosome of the activated BCR via its SH2 domain. The most abundant protein in this analysis was the transmembrane protein Igα (CD79a), which is part of the BCR complex. Biochemical verification of the mass spectrometry data confirmed the recruitment of

the Grb2-SH2 domain to Igα as well as the interaction with SHC1 upon 3 min of BCR stimulation, whereas the inactivated Grb2-SH2 domain (R86L) failed to interact with Igα and SHC1 (figure 23). However, so far a binding motif for Grb2 (pYXN) in the Igα molecule has not been described, yet. Hence, I assumed that this interaction between Grb2 and Igα is mediated indirectly. A possible connection between Grb2 and Igα could be the adapter protein SHC1, which was shown to be recruited to the activated BCR via the phosphorylated ITAM of Igα and Igβ (Baumann et al, 1994; D'Ambrosio et al, 1996). Moreover, SHC1 was shown to form a complex with Grb2 and Sos upon BCR activation, already suggesting SHC1 as a linker for Grb2 to the BCR complex (Smit et al, 1994).

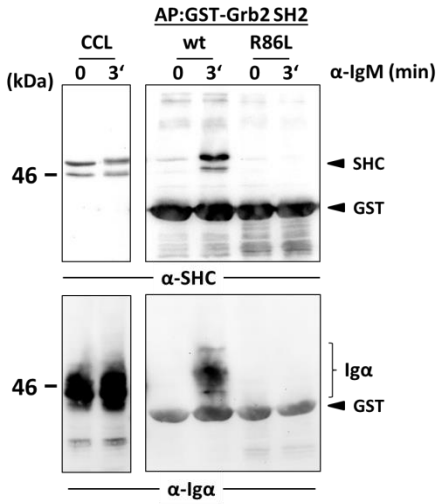

Figure 23. Confirmation of the association of SHC1 and Igα with the Grb2-SH2 domain. $35x10^6$ cells per sample were harvested and stimulated via the BCR for 3 min. For GST-pulldown assay, lysates were incubated either with the GST-Grb2-SH2 fusion protein or with the GST-Grb2-SH2 (R86L; defective SH2 domain) for 2 h. Purified proteins were analyzed by Western blot, probing for SHC or Igα. CCL=Cleared cellular lysates; AP=affinity purification.

3.2.6 Role of SHC1 in Erk activation

The results of the mass spectrometry analysis and the GST-pulldown assay brought the adapter protein SH2 containing transforming protein 1 (SHC1) again into play. SHC1 was shown to be involved in many receptor systems, thereby amongst others contributing to the activation of Erk by linking Grb2:Sos to respective receptors (reviewed in Finetti et al, 2009). In B cells SHC1 was already suggested a long time ago to link Grb2 and Sos to the activated BCR and to be involved in the activation of Erk (Smit et al, 1994; Saxton et al, 1994). However, the discovery of the guanine nucleotide exchange factor RasGRP3 challenged the relevance of Sos in the activation of Erk (Oh-hora et al, 2003). Hence, the involvement of SHC1 in Grb2:Sos recruitment and Erk activation was not followed further. However, I showed that in human B cells rather Grb2 and Sos and not RasGRP3 play an important role in Erk activation. In order to test, whether SHC provides the linkage between the activated BCR and activation of Erk via GRB2:Sos, I generated a SHC1 deficient DG75 sub-cell line by using CRISPR/Cas and analyzed it for Erk activation.

3.2.6.1 Generation of a SHC1-deficient B cell line using CRISPR/Cas

In order to target the major isoforms of SHC1 expressed in B cells, namely p66, p52 and p46 (according to ensembl.org), I chose to target Exon 5 (p66) which all three isoforms have in common (figure 24 a). Western blot analysis of DG75 cell lysates showed high expression of p46 and p52, whereas p66 was only expressed weakly (not shown). Constructs were designed by using the web based software http://crispr.mit.edu/. The guide RNA was chosen to direct the Cas9 nuclease to target an NspI restriction site (highlighted in green), allowing to check for CRISPR activity by NspI restriction digest (figure 24 a). The guide RNA construct was synthesized by MWG eurofins and cloned into the pSpCas9(BB)-2A-GFP vector. DG75 B cells were transfected by nucleofection and were enriched for GFP expression by flow cytometry 72 h later. In order to test the activity of the CRISPR/Cas9 construct, exon 5 was amplified from genomic DNA from parental cells or targeted cells and treated with NspI. After digest the PCR product was analyzed on agarose gel. Activity test of the CRISPR/Cas9 construct targeting SHC1 revealed only a partial digest of exon 5 in targeted cells indicating CRISPR/Cas9 activity, whereas exon 5 from parental cells was digested completely (figure 24 b). Following, cells were subcultured to obtain single cell subclones and analyzed by Western blot and Sanger sequencing. 7 of 88 clones analyzed by

Western blot were shown to be negative for all three SHC1 isoforms (figure 24 c and d). 5 of the 7 clones were subjected to sequencing analysis, revealing a SHC1 deficiency on genomic level for clone #46, #72 and #82. Clone #33 exhibited a deletion of a multiple of three on both alleles and for clone #78 only one allele could be sequenced. Exemplarily, the exon sequences of both SHC1 alleles of #72 are depicted in figure 24 e. Targeting by CRISPR/Cas9 led to a 1 bp insertion on allele 1 and to a 13 bp deletion on allele 2, both leading to a premature STOP codon and termination of the amino acid sequence (figure 24 e).

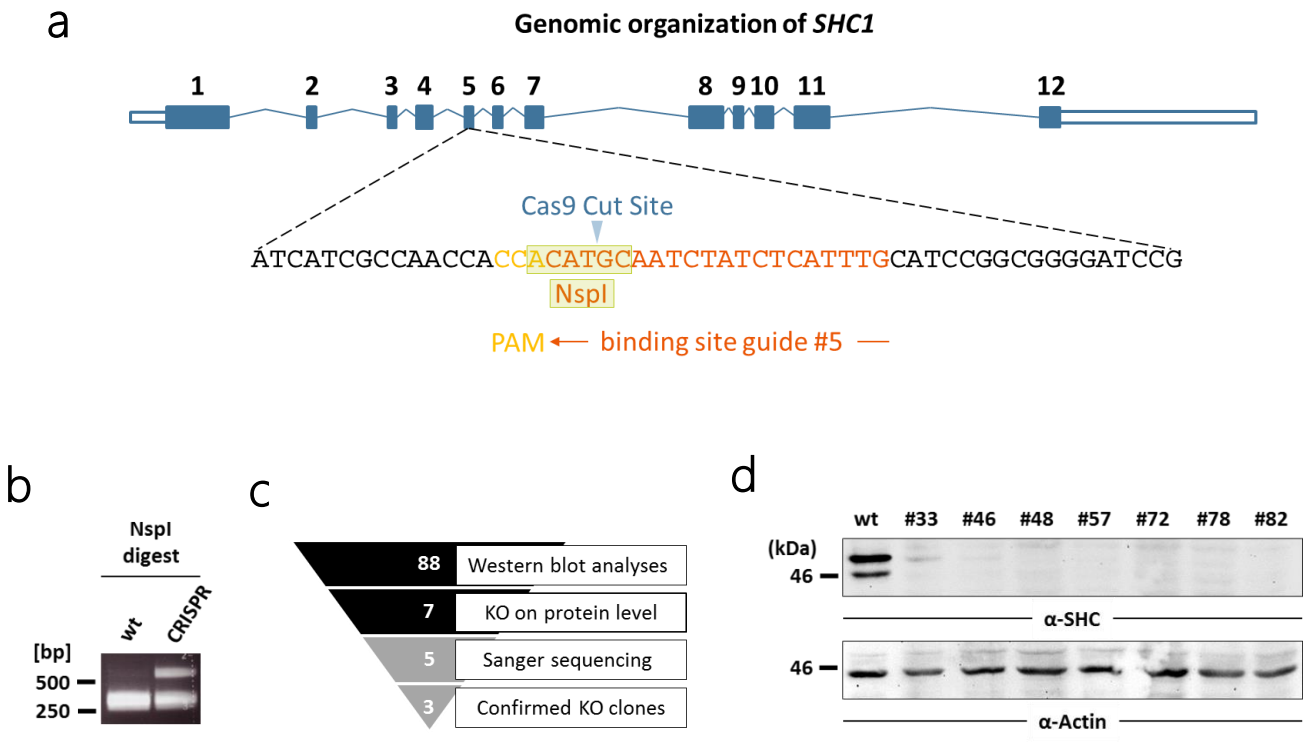

Figure 24. Generation of a SHC1 deficient cell line using CRISPR/Cas. (a) Exon structure of the SHC1 gene (isoform p66) and sequence of the targeted exon 5. Binding site of the guide RNA is highlighted in orange, PAM sequence is indicated in yellow, blue arrow indicates Cas9 cut site 3 nucleotides upstream of the PAM sequence. NspI restriction site is highlighted in green. (b) CRISPR/Cas9 activity test. Exon 5 was amplified from parental DG75 cells or CRISPR-targeted cells and treated with NspI. Treated PCR product was analyzed by agarose gel electrophoresis. (c) Statistics of single-cell clone analysis. Single cell clones were analyzed by Western blot. Clones lacking SHC1-protein expression were further analyzed by Sanger sequencing to verify mutation on genomic level. (d) Western blot analysis of DG75 *SHC1*$^{-/-}$ subclones compared to parental cells. (e) Genomic DNA sequence and corresponding aa sequence of DG75 *SHC1*$^{-/-}$,#72.(* = premature STOP codon). Sequence is representative for at least seven sequencing analyses

3.2.6.2 SHC1 is dispensable for BCR-induced Erk activation

Resulting SHC1-deficient DG75 were analyzed for the mobilization of Ca^{2+} and phosphorylation of Erk (figure 25). Ca^{2+} mobilization was elevated in all SHC1 deficient clones except #82, where Ca^{2+} mobilization profile was similar to Ca^{2+} mobilization in parental cells (wt). In figure 25 a Ca^{2+} mobilization following BCR activation in clone #48, clone #72 and #82 is depicted. However, also clone #33, #46, clone #57 and clone #78 showed an elevated Ca^{2+} mobilization in response to BCR stimulation (not shown). This could be explained by the involvement of SHC1 in signaling of the inhibitory coreceptor CD22 (Poe et al, 2000). Erk activation analysis by Western blot (figure 25 b) and intracellular staining for phosphorylated Erk (figure 25 c & d) revealed normal Erk phosphorylation in clone #46, #57, #78 and #82 upon 3, 10 and 20 min of BCR stimulation. However, Erk activation in clone #33, #48 and #72 was impaired or almost completely abolished. Erk phosphorylation of the clones #72 and #82 is shown representatively for each situation in figure 25 b, c and d. To sum up, disruption of SHC1 expression in DG75 cells led to divergent results in terms of BCR-mediated Erk activation. Three out of seven *SHC1*-deficient clones revealed a defect in Erk activation, while the rest exhibited normal Erk activation following BCR stimulation.

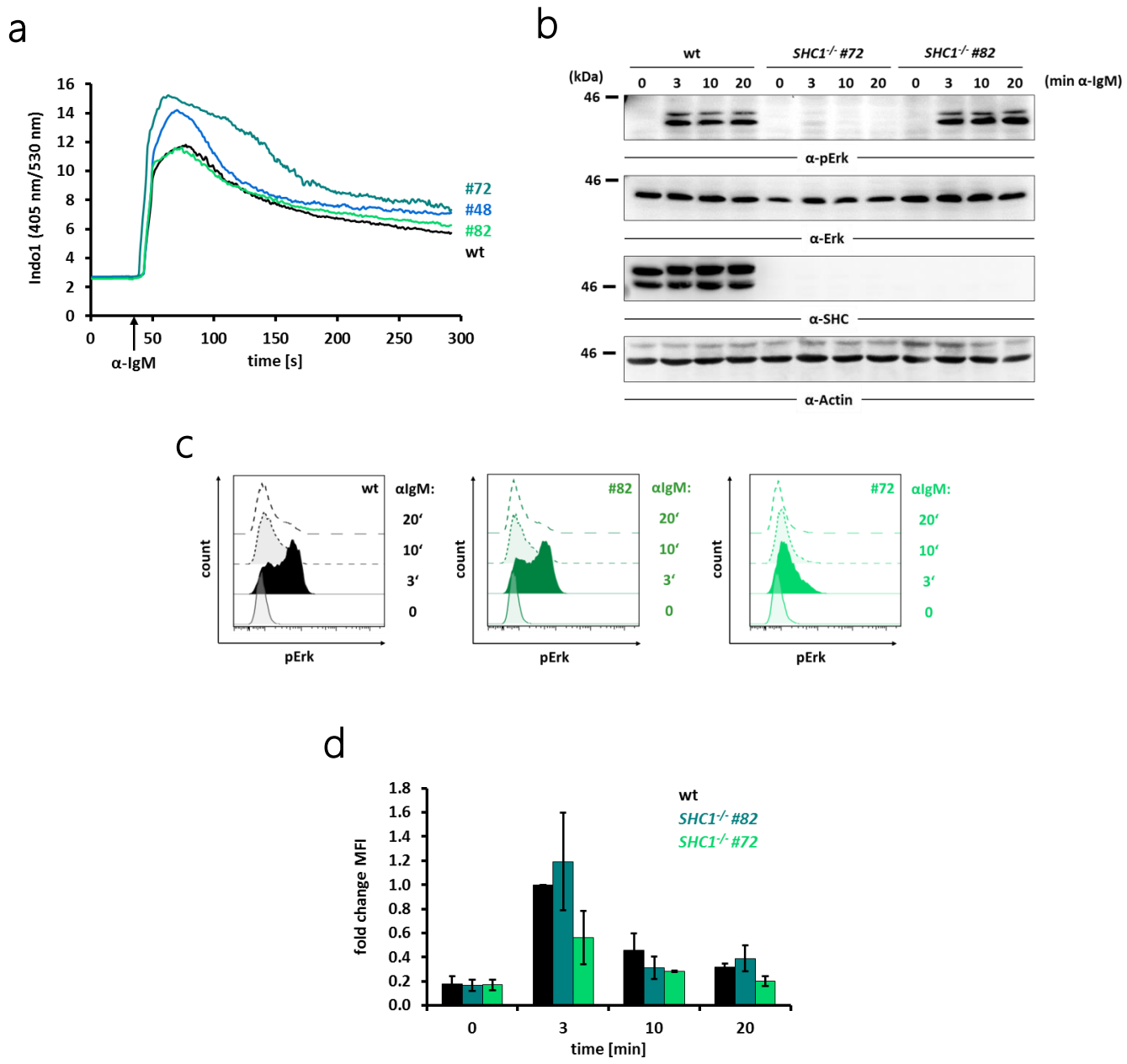

Figure 25. Impact of SHC1 on Erk activation. (a) Ca^{2+} mobilization assay of SHC1-deficient DG75 clones compared to DG75 parental cells (wt). Baseline was recorded for 30 sec. Different subclones were stimulated with 10 µg/ml F(ab')2 α-IgM (time point of stimulation indicated by arrow). Mobilization of Ca^{2+} was monitored for 300 s by flow cytometry using the ratiometric dye Indo-1. (b) Western blot analysis for phosphorylated Erk. SHC1-defcient DG75 clones #72 and #82 or DG75 parental cells (wt) were stimulated with 10 µg/ml F(ab')2 for 0, 3, 10 and 20 min. Cells were lysed and analyzed by Western blot probing for phosphorylated Erk (α-pErk). Expression of total Erk, and SHC1 was verified with respective antibodies. Actin served as loading control. (c & d) Intracellular staining for phosphorylated Erk. Cells were stimulated with 10 µg/ml F(ab')2 for 0, 3, 10 and 20 min, fixed, permeabilized and analyzed by flow cytometry using an ALEXA647 coupled antibody specific for phosphorylated Erk. (c) Representative histograms of Erk phosphorylation in SHC1-deficient DG75 clones #72 and #82. (d) Fold change of median fluorescence intensity (MFI)/Erk phosphorylation in SHC1-deficient cells. Mean values and standard deviation of five independent experiments.

To rule out off target effects induced by the CRISPR construct, I transfected the DG75 SHC1 knock-out clone #72, which exhibited a defect in Erk phosphorylation, with either the SHC1 isoforms p52 or p46 and analyzed the transfectants for BCR induced Erk activation. Since endogenous expression of the isoform p66 in DG75 is only weak, I did not include exogenously expressed p66 into the reconstitution experiment. Since expression of the different SHC1 isoforms is regulated by alternative start codons, transduction of the SHC1 p52 cDNA led to protein expression of both, the larger SHC1 p52 and the shorter p46 isoform (figure 26 a). SHC1 p52 and SHC1 p46 were equipped with an IRES-EGFP cassette or with an IRES-RFP cassette respectively, allowing indirect control of SHC1 p52 and SHC1 p46 expression levels by flow cytometry (figure 26 b). Erk phosphorylation in *SHC1*-deficient DG75 following 0, 3 10 and 20 min of BCR stimulation could neither be reconstituted by ectopically expressed SHC1 p52 nor by p46 (figure 26 c & d). Thus, I concluded that the defect of Erk phosphorylation in *SHC1* deficient cells was due to an off target effect caused by the CRISPR construct. However, the off target analysis of the SHC1 CRISPR construct did not reveal any BCR relevant targets, but sequence comparison revealed sequence similarities between SHC1 and SHC2, especially in the CRISPR target site. Although, SHC2 expression in B cells has not been reported, it should be taken into account. In summary, the adapter protein SHC1 is not involved in Grb2 mediated Erk activation.

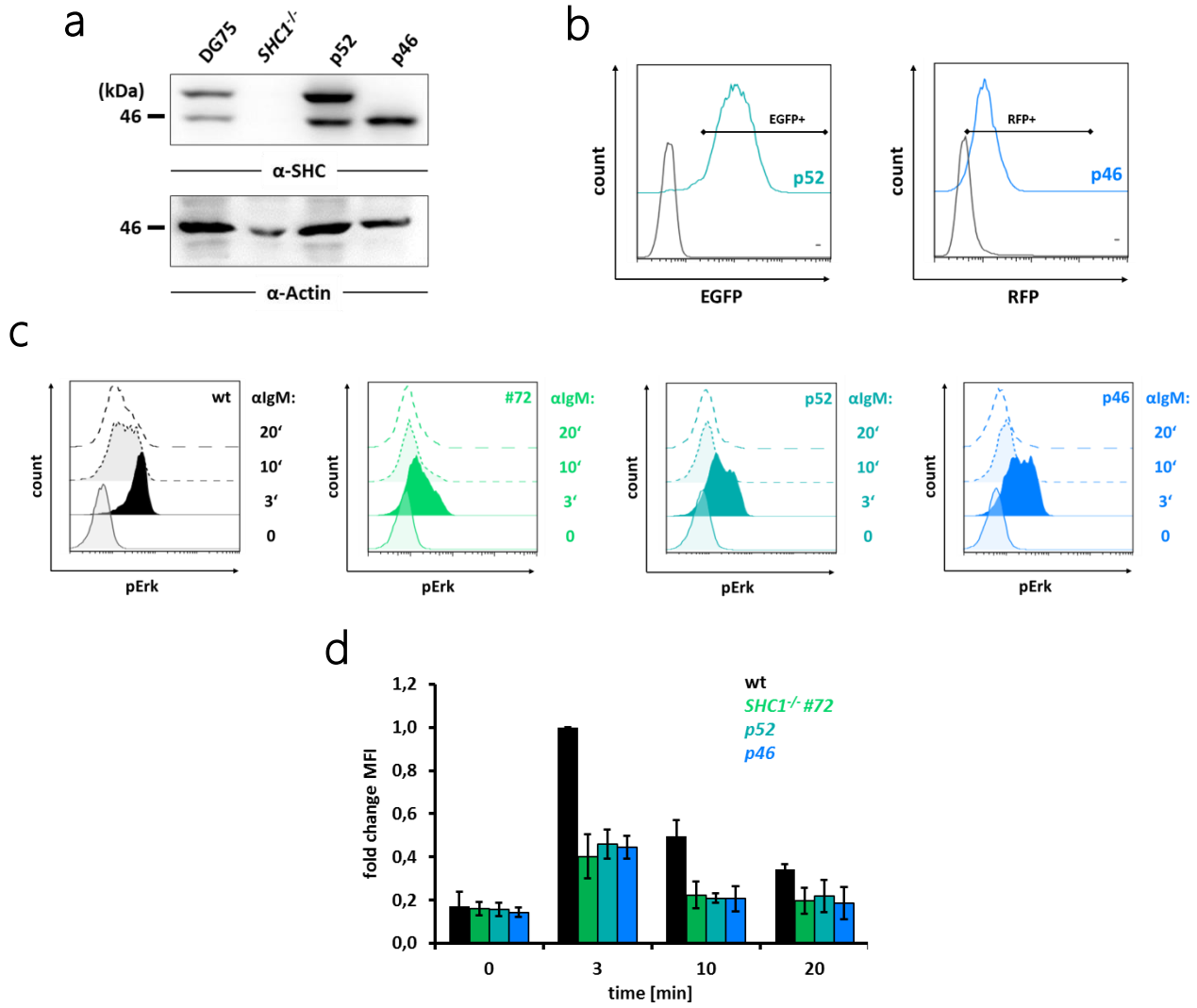

Figure 26. Reconstitution of SHC1 in SHC1-deficient B cells. (a) Western blot for analysis of SHC1 expression in SHC1-deficient DG75 ectopically expressing SHC1 p52 or SHC1 p46. (b) Flow cytometry analysis of IRES-EGFP and IRES-RFP expression for indirect control of SHC1 p52 or SHC1 p46 expression, respectively. (c & d) DG75 parental cells (wt), DG75 *SHC1*$^{-/-}$ #72, DG75 *SHC1*$^{-/-}$ #72 transduced with SHC1 p52 (p52) and DG75 *SHC1*$^{-/-}$ #72 transduced with SHC1 p46 (p46). were stimulated with 10 µg/ml F(ab')2 for 0, 3, 10 and 20 min, fixed, permeabilized and analyzed by flow cytometry using an ALEXA647 coupled antibody specific for phosphorylated Erk. Mean values and standard deviation of three independent experiments.

Since SHC1 turned out to be dispensable for the activation of Erk following BCR-stimulation, the question for the Grb2-membrane anchor that is involved in BCR-mediated Erk activation remains. Direct SH2-dependent interaction of Grb2 requires a phospho-tyrosine motif with the consensus sequence pYXN. Unlike the IgG/E-BCR of memory B cells which harbors a pYXN referred to as ITT, the IgM-BCR of naïve B cells lacks such a motif (Engels et al, 2009). However,

several inhibitory and activating coreceptors that are involved in the modification of BCR signaling, as for example CD19, CD22, CD27 or FcγRIIB, carry pYXN motifs, serving as docking sites for Grb2 and thereby mediating costimulatory functions (Neumann et al, 2009). The recently discovered FcμR was also shown to have an ITT-like motif within its cytoplasmic domain that by sequence homology could also serve as a Grb2 binding site upon phosphorylation (Shima et al, 2010). However, the function of the FcμR is still unknown and is currently challenged by several groups.

3.3 Molecular characterization of the cytoplasmic domain of FcμR

Since the FcμR could serve as another membrane anchor for Grb2 in human B cells, I aimed to investigate the molecular signaling features of its cytoplasmic domain. The FcμR is expressed on B cells as well as on T cells and according to a few studies also on cells of the innate immune system (Kubagawa et al, 2009; Lang et al, 2013). Its role on B cells is still controversially discussed. I investigated the FcμR on the molecular level with regard to its potential Grb2 binding site and costimulatory function.

3.3.1 The cytoplasmic domain of FcμR can functionally replace the cytoplasmic domain of murine IgG2

Endogenous expression of FcμR on our model cell line was relatively low and attempts of ectopic expression only led to low surface expression of FcμR that limited the ability for receptor stimulation. Thus, I generated chimeras consisting of the extracellular domain of murine (m)IgG2a and the intracellular domain of the FcμR, to analyze the signaling properties of the FcμR and expressed them in DG75 B cells (figure 27 a). In order to investigate the relevance of the ITT-like motif, I inactivated the motif by substituting the tyrosine at position 385 by a phenylalanine (Y385F) by using site directed mutagenesis (figure 27 b). Phenylalanine is structural identical to tyrosine except for the hydroxyl group, hence, it cannot be modified by phosphorylation. At first, I analyzed whether the ITT-like motif within the cytoplasmic domain of FcμR can serve as a binding site for Grb2. Therefore, I stimulated the cells expressing either mIgG2a-FcμR wt or mIgG2a-FcμR Y385F with F(ab')2 α-mIgG, performed an immunoprecipitation (IP) and analyzed precipitated proteins by Western blot by probing for tyrosine phosphorylated proteins (α-pY100) and for Grb2 (figure 27 c). Following IgG2a

activation, the precipitation yield of surface IgG was much lower compared to unstimulated receptor. This is probably due to the clustering of activated BCRs in lipid rafts, which depending on the detergent used in the lysis buffer, exacerbated the purification. Nevertheless, tyrosine phosphorylation increased after 3 min of BCR stimulation, but was not abolished in the YF-mutant. This indicated that at least one of the three other tyrosines present in the cytoplasmic domain also gets phosphorylated upon stimulation. However, the IgG2a-FcμR wt chimera recruited Grb2 upon stimulation, whereas the YF mutant lost its ability to interact with Grb2 (figure 27 c).

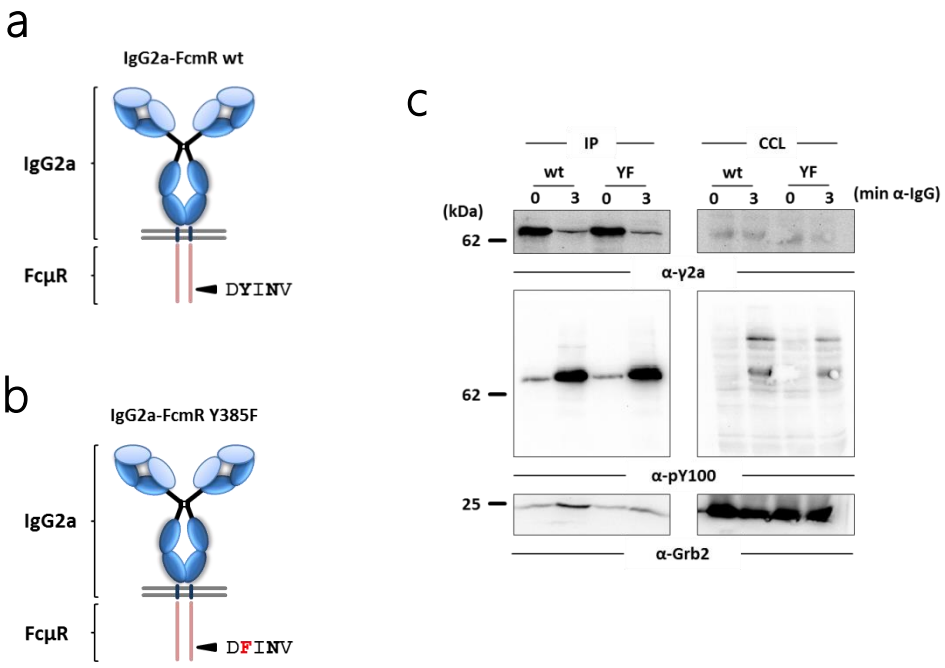

Figure 27. Grb2 interacts with the cytoplasmic domain of the FcμR. (a) Schematic depiction of the chimera assembly. The cytoplasmic domain of murine IgG2a was replaced with the cytoplasmic domain of FcμR by molecular cloning. The resulting chimera was expressed in DG75 B cells. (b) For analysis of the potential ITT-like motif the motif was inactivated by substituting the tyrosine residue at position 385 by phenylalanine (Y385F). (c) Immunoprecipitation of IgG2a-FcμR chimeras. 30-40 x106 IgG2a-FcμR wt or IgG2a-FcμR Y385F expressing cells were stimulated with 10 µg/ml biotinylated α-mIgG for 0 and 3 min. Precipitation was performed by using streptavidin-beads for 1 h at 4°C. Precipitated proteins were eluted from the beads by boiling and analyzed by Western blot.

To further analyze the properties of the cytoplasmic domain and the ITT-like motif of the FcμR, I compared both chimeras with regard to Ca^{2+} mobilization (figure 28 a). Therefore, I stimulated the cells with F(ab')2 α-mIgG and monitored the Ca^{2+} mobilization by flow cytometry. Compared to the IgG2a-FcμR wt chimera, Ca^{2+} mobilization in cells expressing the chimera with the

inactivated ITT-like motif (Y385F) was remarkably decreased (figure 28 a), while surface expression of both IgG-chimeric receptors was equal (figure 28 b). To check the general ability for Ca^{2+} mobilization in the transduced cells, I analyzed Ca^{2+} mobilization induced by the endogenous IgM-BCR by stimulating the cells with F(ab')2 α-IgM. Interestingly, Ca^{2+} mobilization in cells expressing the IgG2a chimera with the inactivated ITT-like motif (Y385) is stronger than Ca^{2+} mobilization in IgG2a-FcμR wt cells (figure 28 c), although IgM surface expression was similar (figure 28 d). In summary, the ITT-like motif in the cytoplasmic tail of the FcμR can serve as Grb2 docking site, at least in the IgG2a chimera setting and has costimulatory properties as it was described for the ITT (Engels et al, 2009). Thus, the cytoplasmic domain of the FcμR can functionally replace the cytoplasmic domain of mIgG2a.

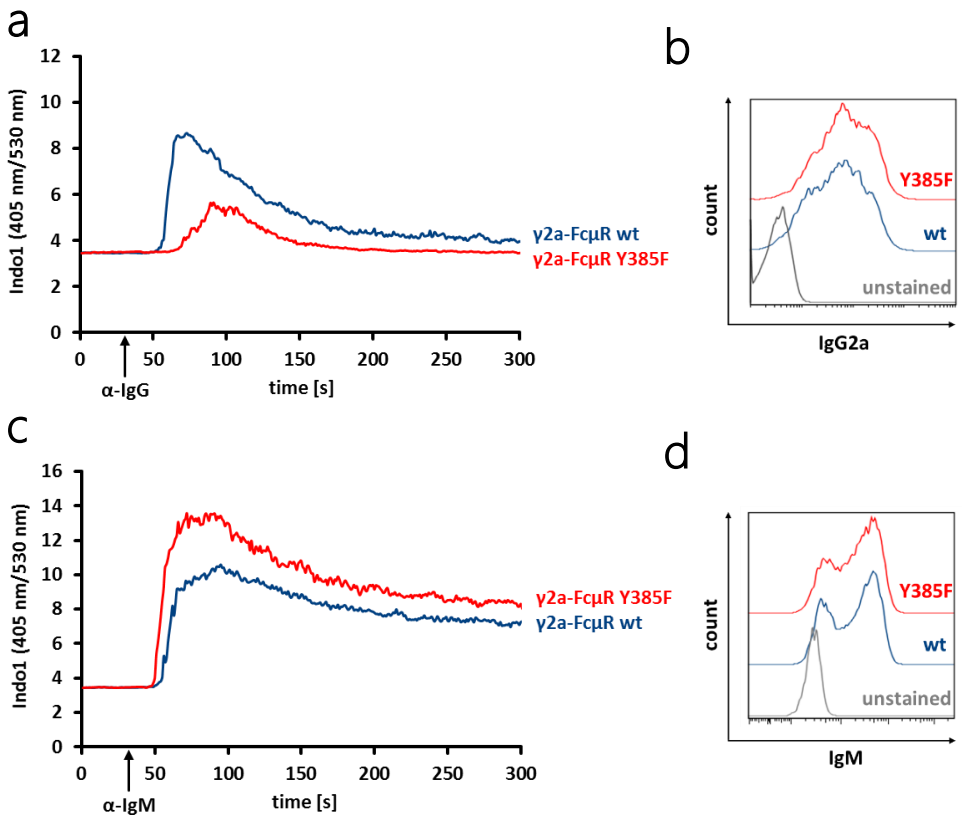

Figure 28. Functional replacement of the cytoplasmic domain of mIgG2a with the cytoplasmic domain of FcμR. (a & c) Ca^{2+} mobilization analysis of cells expressing chimeric receptors. Baseline was recorded for 30 sec. DG75 FcμR wt or DG75 FcμR Y385F were stimulated with 10 µg/ml F(ab')2 α-mIgG (a) or 10 µg/ml F(ab')2 α-IgM (c) (time point of stimulation indicated by arrow). Mobilization of Ca2+ was monitored for 300 s by flow cytometry using the ratiometric dye Indo-1. (b & d) Surface expression analysis of IgG2a-chimeras and endogenous IgM-BCR by flow cytometry using fluorescence labeled antibodies against murine IgG or human IgM.

3.3.2 The FcμR-ITT like motif can functionally replace the ITT of murine IgG2a

In order to test, whether the FcμR-ITT like motif functionally resembles the ITT, I mutated the ITT motif of the mIgG2a to an FcμR-ITT like motif (figure 29 a). Therefore, I exchanged four amino acids (depicted in red) by site directed mutagenesis and expressed the modified mIgG2a in DG75 B cells (figure 29 b). For functional analysis of the ITT-like motif, I inactivated the ITT-like motif by replacement of tyrosine for phenylalanine (YF). Following, I compared tyrosine phosphorylation and Grb2 recruitment in the IgG2a and IgG2a-FcμR-ITT transduced cells by performing an IP as described in the previous section. The IP revealed that the FcμR-ITT like motif as well as the wt ITT gets phosphorylated upon 3 min of BCR stimulation, although phosphorylation of the FcμR-ITT like motif is much stronger compared to phosphorylation of the wt ITT. Inactivation (YF) of the ITT in both cases led to ablation of tyrosine phosphorylation of the IgG2a. Corresponding to the strength of tyrosine phosphorylation, Grb2 coprecipitation is much stronger for the FcμR-ITT like motif than for the IgG2a-ITT. Substitution of Y to F led to ablation of Grb2 recruitment to IgG2a, as well as to IgG2a-ITT FcμR (figure 29 c). In accordance to the IP data, Ca^{2+} mobilization analysis exhibited a likewise lower Ca^{2+} mobilization for IgG2a YF (figure 29 d) and IgG2-FcμR-ITT YF (figure 29 e) as compared to the respective wildtype situation, where Ca^{2+} mobilization was much more sustained. These data confirm that the FcμR-ITT like motif indeed has the potential to serve as a costimulatory motif through the recruitment of Grb2. However, whether this resembles the situation for the full length molecule yet has to be elucidated. Still it is conceivable, that the FcμR interferes with BCR signaling via the ITT-like motif in an inhibitory or activating manner.

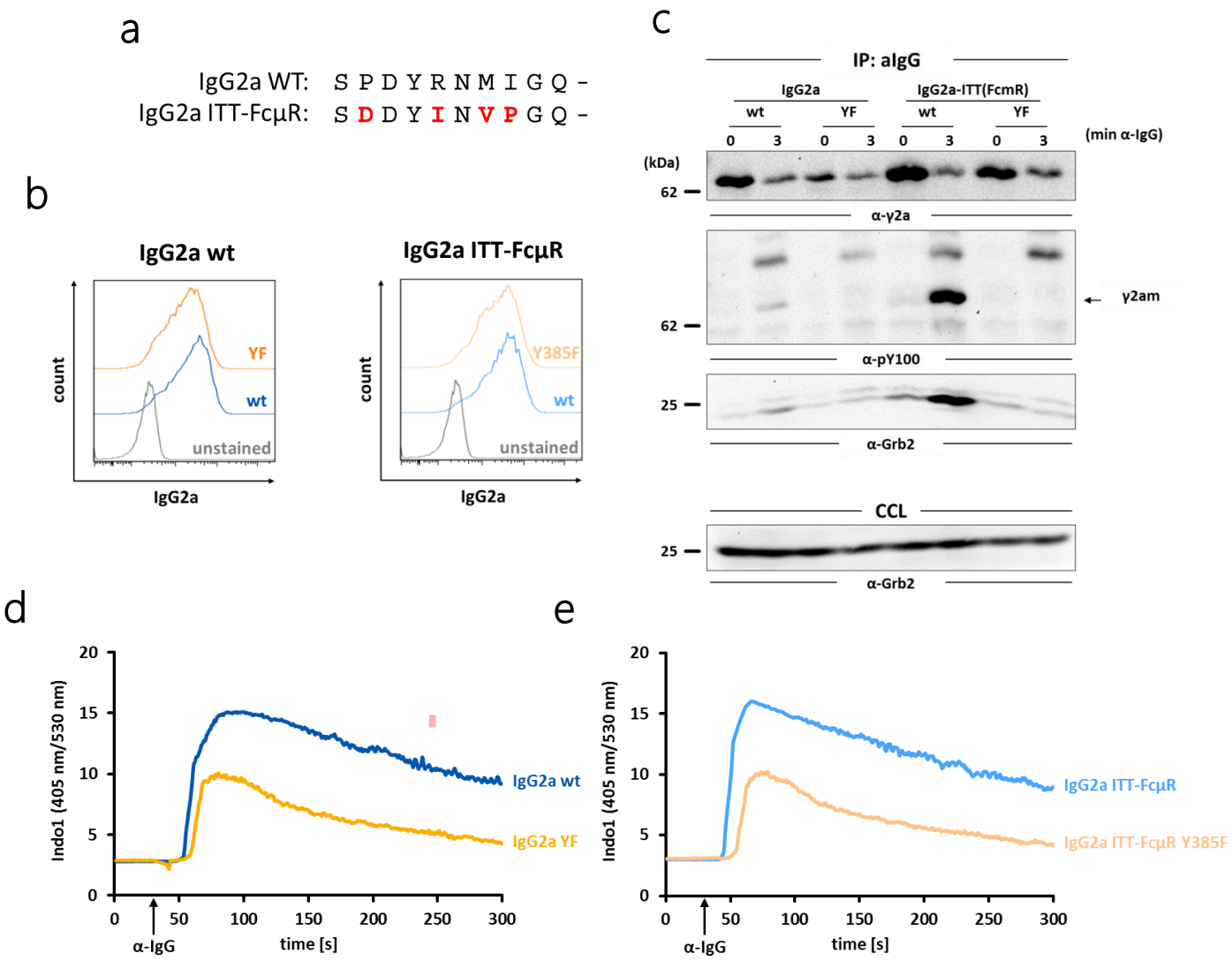

Figure 29. Replacement of the ITT of mIgG by the FcμR ITT-like motif. (a) Amino acid sequence of the ITT of murine (m)IgG2a and the ITT-like motif of the FcμR. Amino acids depicted in red were substituted in order to replace the ITT by the FcμR-ITT like motif. For analysis of the potential ITT-like motif the motif was inactivated by substituting the tyrosine residue at position 385 by phenylalanine (Y385F). (b) For immunoprecipitation of IgG2a 30-40 x10^6 DG75 B cells expressing either mIgG2a wt, mIgG2a YF, mIgG ITT FcμR or mIgG ITT FcμR Y385F were stimulated with 10 µg/ml biotinylated α-IgG for 0 and 3 min. Precipitation was performed by using streptavidin-beads for 1 h at 4°C. Precipitated proteins were eluted from the beads by boiling and analyzed by Western blot. (c & e) Ca^{2+} mobilization analysis of cells expressing IgG2a wt and IgG2a YF, or IgG2a-FcμR ITT and IgG2a-FcμR ITT YF. Baseline was recorded for 30 sec. Cells were stimulated with 10 µg/ml F(ab')2 α-IgG (time point of stimulation indicated by arrow). Mobilization of Ca2+ was monitored for 300 s by flow cytometry using the ratiometric dye Indo-1. (d & f) Surface expression analysis of IgG2a by flow cytometry using fluorescence labeled antibodies against murine IgG.

4 Discussion

BCR ligation leads to activation of multiple signaling pathways determining the B cells fate. Depending on developmental stage, type of antigen, strength of activation or costimulatory signals, BCR activation results in survival, proliferation, differentiation or apoptosis. The activation of different pathways following BCR activation is facilitated by a complex interplay of a plethora of different adapter and effector proteins and requires tight regulation by positive and negative regulatory elements. Regulation is mediated by several coreceptors as for example CD19 and CD22 as well as by costimulatory elements as the ITT within IgG/E containing BCRs and by Fc receptors that play a crucial role in regulating the humoral immune response. The simple but versatile adapter protein Grb2 has been shown to be a common element in the positive and negative regulation of the BCR via many coreceptors and effectors. Imbalance of this tight regulation can lead to autoimmune disorders as for example ITP or SLE.

In the first part of this study, I analyzed the ability of human recombinant sFcγRIIB, a new treatment option for Ig-mediated autoimmune diseases, to bind to membrane IgG *in vitro*. Analysis of signal transduction upon BCR stimulation with multimeric variants of sFcγRIIB revealed induction of downstream BCR signaling, giving a first hint that the sFcγRIIB as such could bind to membrane IgG *in vivo*. Interestingly, stimulation with the multimeric variants of sFcγRIIB induced Erk activation without the phosphorylation of SLP65, which is crucial for the formation of the Ca^{2+} initiation complex and the activation of PLCγ2. This suggests an alternative pathway for the BCR-induced Erk activation in human B cells, different from chicken and murine B cells, where Erk activation crucially depends on PLCγ2 activity and thus on the formation of the Ca^{2+} initiation complex.

Subsequently, I revisited BCR signaling with regard to the activation of the Ras/Raf/MEK/Erk pathway in human B cells in the second part of this study. This brought the adapter protein Grb2 into play again, which was originally suggested to mediate BCR-induced Erk activation via its constitutive interaction with Sos. The findings revealing that Grb2 is indispensable for the activation of Erk following BCR liagtion in human B cells, gave rise to the question for the membrane anchor for Grb2 leading me to the third part of this study. Here, I investigated the

molecular signaling properties of the recently discovered FcμR as a potential membrane anchor for Grb2.

4.1 Multimerized sFcγRIIB induces IgG-specific BCR signaling

The recombinant soluble human FcγRIIB is being tested as a new treatment option for Ig mediated autoimmune diseases in phase II clinical studies. Due to the long lasting effects that have been observed in ITP patients, we hypothesized a dual mode of function for the human recombinant sFcγRIIB. Besides competing with membrane bound FcγRIIB in binding of IgG-immune complexes, sFcγRIIB could also interfere with the formation of plasma cells and hence with the formation of new autoantibodies by binding to membrane IgG on memory B cells.

To test, whether the sFcγRIIB binds to membrane IgG, I used functional read-out systems as Ca^{2+} mobilization and western blot analysis monitoring the activation of the BCR. Due to the low binding affinity of the sFcγRIIB (Maenaka et al, 2001) it was not possible to directly test sFcγRIIB-binding by fluorescently labelled sFcγRIIB-specific antibodies or fluorescently labelled sFcγRIIB itself. Treatment of IgG-expressing B cells with the dimeric and tetrameric sFcγRIIB led to mobilization of the second messenger Ca^{2+} as well as to activation of Akt and Erk, although phosphorylation of SLP65 was not detectable. However, Ca^{2+} mobilization appeared to be weaker but more sustained compared to IgG-expressing B cells stimulated with IgG-specific F(ab')2 fragment. SLP65 is important for the formation of the Ca^{2+} initiation complex and hence for the activation of PLCγ2, which mediates the mobilization of Ca^{2+} and the activation of Erk via DAG and RasGRP. The fact that Erk activation in IgG-expressing cells stimulated with multimeric sFcγRIIB variants was as high as in cells stimulated with IgG-specific F(ab')2 can be explained in different ways. First, low undetectable levels of phosphorylated SLP65 could be sufficient for the activation of Erk. Second, other adapter proteins could compensate for SLP65 in Ca^{2+} mobilization. This would explain why IgG-expressing B cells upon stimulation with multimeric sFcγRIIB still mobilize Ca^{2+}, although SLP65 phosphorylation is diminished. Furthermore, gene targeting studies in mice revealed that SLP65 is not exclusively essential for Ca^{2+} mobilization in B cells (Gerlach et al, 2003). The third option is that Erk in human B cells is activated by an alternative pathway different from the RasGRP3 axis described for mice and chicken B cells.

The monomeric sFcγRIIB representing the molecule that is being tested in clinical studies did not induce any signaling in IgG expressing B cells *in vitro*. Nevertheless, results obtained from the functional analysis with the dimeric and tetrameric variant of sFcγRIIB suggest that the molecule *per se* can bind to membrane IgG. However, since I could not detect any signaling events induced by the monomeric sFcγRIIB, it is unlikely that it induces BCR activation *in vivo,* unless it dimerizes by interaction with serum proteins. Indeed, the sFcγRIIB comprises a large uncharged patch forming a hydrophobic ridge which could serve as binding site for other proteins than the IgG (Sondermann et al, 1999). Another conceivable model is that the monomeric sFcγRIIB does not activate the BCR itself but rather modulates (auto) antigen mediated BCR activation in vivo.

To sum up, functional assays revealed BCR activation upon stimulation of IgG-B cells with dimeric and tetrameric but not with monomeric sFcγRIIB. Even though I could not show it biochemically, I can conclude that B cell activation via the sFcγRIIB occurs in a BCR-dependent manner, most probably via direct interaction of the sFcγRIIB with the IgG-BCR. Furthermore, it is conceivable that also the monomeric sFcγRIIB is able to bind to the IgG-BCR, although it did not induce BCR signaling in our read-out systems. However, it is not possible to predict how the monomeric sFcγRIIB behaves in vivo. Whether it interferes with plasma cell formation in vivo still remains to be investigated. Therefore, a suitable in vitro model including an IgG-B cell line that is able to differentiate into plasma cells is required to test the influence of sFcγRIIB on plasma cell formation.

4.2 Revisiting the role of Grb2 in Erk activation in human B cells

Activation of Erk requires PLCγ2 activity and thus is accompanied by the mobilization of Ca^{2+}. However, experiments that contributed to this conclusion were performed in the DT40 chicken B cell line and in mice. Stimulation of human IgG-B cells with multimeric sFcγRIIB led to induction of signaling events downstream of the BCR including Ca^{2+} mobilization as well as activation of Erk despite the absence of SLP65 phosphorylation. These observations revealed species specific differences between chicken, mice and human regarding the BCR-induced activation of Erk. This led us to the hypothesis that Erk activation upon BCR stimulation in human B cells occurs independently of the Ca^{2+} initiation complex via an alternative pathway.

4.2.1 Erk activation following BCR stimulation occurs independently of PLCγ but requires Grb2

Consistent with the role of SLP65 and Btk in formation of the Ca^{2+} initiation complex (Engelke et al, 2007), DG75 B cells deficient for SLP65 or Btk exhibited a remarkable decrease in mobilization of Ca^{2+} upon BCR activation, while Grb2-deficiency had no effect on Ca^{2+}mobilization. In contrast, Erk activation was not affected in SLP65- and Btk- deficient DG75 and thus occurred independently of the mobilization of Ca^{2+}. Grb2-deficient DG75 B cells on the other hand revealed a defect in Erk activation following BCR activation, leading to the hypothesis that Erk activation in human B cells occurs independently of PLCγ2 activity but requires Grb2.

To directly test the involvement of PLCγ2, I generated a PLCγ2-deficient DG75 sub-cell line. Unexpectedly, PLCγ2-deficient DG75 B cells only revealed a reduction of about 50 % in Ca^{2+} mobilization following BCR stimulation. The functional homologue of PLCγ2 in T cells, namely PLCγ1 (Kane et al, 2000), appeared to be redundant in B cells in the presence of PLCγ2. Yet, in the absence of PLCγ2 it can partially compensate for the loss of PLCγ2 as became evident by comparing Ca^{2+} mobilization in PLCγ2 single-deficient and Ca^{2+} mobilization in PLC1/2 double-deficient B cells. The ability to mobilize Ca^{2+} was completely abrogated in PLCγ1/2-double deficient DG75 B cells, while Erk phosphorylation was not affected. Thus, Erk activation following BCR stimulation in human B cells is completely independent of PLCγ activity.

4.2.2 Human B cells exhibit low RasGRP1 and 3 expression levels

Since I showed that PLCγ is dispensable for the activation of Erk following BCR activation, I thus proposed that human B cells in contrast to chicken and mouse B cells do not require the RasGEF RasGRP3, which is activated via DAG and PLCγ2. RasGRP3 protein expression in the model B cell line DG75 was shown to be rather low. To test whether this is representative for the human system, I compared expression of RasGRP isoforms in different B- and T cell lines and human primary B cells isolated from peripheral blood. RasGRP1, which is the functional analogue of RasGRP3 in T cells (Stone, 2011), as well as RasGRP3 expression was low in both, DG75 B cells and human primary B cells. Compared to the Raji B cell line and the Jurkat T cell line, DG75 B cells and human primary B cells revealed a higher RasGRP2 expression. According to several studies, RasGRP2 expression within the hematopoietic system is restricted to platelets,

megakaryocytes and neutrophils (Crittenden et al, 2004; Carbo et al, 2010). Detailed studies regarding RasGRP2 expression and function in T and B cells have not been published. In platelets and neutrophils RasGRP2 has been shown to mediate the activation of integrins via Rap, a small GTPase that is similar to Ras (Yamashita et al, 2000). Integrins mediate extracellular adhesion, facilitating platelet aggregation as well as neutrophil adhesion and chemotaxis (Crittenden et al, 2004; Stolla et al, 2011). Despite structural homology to RasGRP3, the C1 domain of RasGRP2 does not bind DAG and is not recruited to the plasma membrane by DAG analogs (Irie et al, 2004; Johnson et al, 2007; Czikora et al, 2016). Hence, plasma membrane recruitment of RasGRP2 is facilitated via an alternative membrane anchor, probably independent of PLCγ activity. Although there is no hint for RasGRP2 involvement in Erk activation in general, this should be addressed in future experiments. To sum up, RasGRP1 and RasGRP3 expression levels in the DG75 B cell line as well as in human primary B cells are similarly low. Also expression levels of Grb2 and GRAP are similar between DG75 and primary B cells, confirming the DG75 B cell line as a suitable representative model to investigate Erk signaling.

Compared to DG75 B cells, Raji B cells that also represent a Burkitt lymphoma cell line, expressed higher levels of RasGRP1 and RasGRP3. Beside Raji B cells, upregulated RasGRP3 expression was also observed in the Burkitt lymphoma cell lines Daudi and Ramos as well as in the pre-B cell leukemia cell line Hoon (Teixeira et al, 2003). My results show that the DG75 B cell line constitutes an exception among Burkitt lymphoma cell lines and rather resembles the physiological situation in terms of RasGRP3 expression in human B cells.

4.2.3 The Grb2 family member GRAP partially compensates for Grb2 function

Lack of Grb2 in the human B cell line DG75 led to a decreased Erk phosphorylation following BCR activation. Nevertheless, Erk activation was not abrogated completely. Thus, I hypothesized that the adapter protein GRAP, which belongs to the Grb2 family of adapter proteins and shares 60 % homology with Grb2 (Feng et al, 1996), could account for residual activation of Erk. Indeed, analysis of Grb2/GRAP double-deficient DG75 B cells revealed further reduction of Erk activation following BCR activation. Like Grb2, GRAP has been shown to interact with Sos via both SH3 domains and is suggested to be involved in Ras/Raf/MEK/Erk cascade following T cell receptor activation (Feng et al, 1996; Trüb et al, 1997). Thus, I concluded that GRAP can partially

compensate for Grb2 function. When Grb2 is present, GRAP seems to be redundant for BCR-mediated Erk activation. GRAP single-deficient DG75 B cells exhibited no change in Erk activation following BCR stimulation. Expression of GRAP in Grb2/GRAP double-deficient B cells reconstituted Erk phosphorylation to the level of Erk phosphorylation in Grb2 single-deficient B cells, but could not completely compensate for the lack of Grb2. Nevertheless, I can conclude that residual Erk activation following BCR stimulation is due to partial compensation of Grb2 function by GRAP and not due to other effectors.

4.2.4 The PLCγ/RasGRP axis is dispensable for the activation of Erk in human B cells

In the nineties the DT40 chicken B cell line has become an elegant model to analyze BCR signaling by gene disruption experiments. Compared to other eukaryotic systems, where gene targeting efficiency is low, DT40 B cells exhibit a high potential for efficient gene targeting due to its exceptional high level of homologues recombination. Most of what we know about the complex network of BCR signaling has been elucidated in this cell line (reviewed in Winding & Berchtold, 2001).

Data from DT40 chicken cells and mice implied that Erk activation following BCR stimulation is exclusively mediated via PLCγ/RasGRP, while Sos was thought to be redundant (Oh-hora et al, 2003; Coughlin et al, 2005). However, more recent data from different T and B cell lines have shown that RasGRP and Sos cooperate to establish a sensitive and robust activation of Erk by virtue of a Sos-mediated positive feedback loop (Roose et al, 2007). This is mediated by binding of RasGTP as a product of RasGRP and Sos to an allosteric pocket within the Sos molecule, thereby greatly accelerating Sos activity (Margarit et al, 2003). RasGRP was shown to be dominant over Sos leading to an impaired Ras/Erk activation in the absence of RasGRP, although the absence of Sos also led to a reduction of BCR-induced Erk activation, but only upon suboptimal BCR stimulation. Hence, the interplay of both ensures maximal Ras/Erk activation even in response to physiological low levels of antigen (Roose et al, 2007).

New gene targeting techniques as Zinc finger nucelases (ZFN)-, TALEN- and CRISPR/Cas-genome editing techniques that are based on the introduction of DSBs by site-specific nucleases, enable efficient gene disruption also in mammalian cells (Gaj et al, 2013). I could show by gene targeting experiments using the TALEN-based genome editing technique that in the human DG75 B cell line the PLCγ/RasGRP pathway plays a neglectable role in BCR-induced Erk activation. On the other hand, the adapter protein Grb2 appeared to be indispensable for BCR-mediated Erk activation, suggesting that Erk activation in human B cells is mediated via Grb2:Sos. These experiments are in contrast to the findings in chicken DT40 B cells and mice, revealing species specific differences in Erk activation following BCR stimulation. However, this raised the question of whether these observations apply on human B cells in general or whether the preference of either the Grb2/Sos or the PLCγ/RasGRP3 pathway depends on developmental stages of the B cell.

A simple explanation was delivered by analysis of RasGRP expression levels, revealing low RasGRP1 and RasGRP3 expression levels in the B cell line DG75 as well as in human primary B cells. Furthermore, exogenous expression of RasGRP3 in Grb2/GRAP-double deficient B cells could completely reconstitute their ability to activate Erk upon BCR stimulation. Consequently, I concluded that human B cells potentially can use the Ras/Raf/MEK/Erk pathway, but due to a lack of RasGRP3 expression, human B cells predominantly use another RasGEF to mediate Erk activation following BCR stimulation, most presumably Sos.

Since the B cell line DG75 represents a naïve B cell expressing surface IgM, it would be interesting to test RasGRP3 expression in human B cells from other developmental stages. The memory-like B cell lines HF1 (follicular lymphoma) and SUDHL-4 (Non-hodgkin lymphoma) exhibited high RasGRP3 expression levels compared to DG75 (data not shown). RasGRP3 expression in memory-like primary B cells should be addressed in further experiments.

4.2.5 Grb2 is recruited to the signalosome of the activated IgM-BCR by virtue of its SH2 domain

To further dissect Grb2 function in BCR-mediated Erk activation, I investigated Erk activation following BCR stimulation in Grb2 single-deficient DG75 B cells reconstituted with different Grb2

variants either defective for one of the SH3 domains, the SH2 domain or for all of the three domains. Interestingly, all domains appeared to be important for sufficient activation of Erk. The importance of both Grb2-SH3 domains for Erk activation can be explained by the fact that Sos-interaction requires both Grb2-SH3 domains (Neumann et al, 2009). This also confirms the suggested involvement of Sos in BCR-mediated Erk activation, although definite confirmation by Sos gene targeting for example would be necessary. The need of the Grb2-SH2 domain for sufficient Erk activation upon BCR activation reflects the requirement for the recruitment of Grb2 to the activated BCR via a phosphorylation motif. Unlike the IgG/IgE-BCR of memory B cells, the IgM-BCR complex of naïve B cells lacks a suitable Grb2 docking site.

Indeed, mass spectrometry based interactome analysis of Grb2-SH2 interaction partners following BCR stimulation revealed interaction of the Grb2-SH2 domain with the BCR complex including Igα as well as heavy and light chain regions of IgM. Furthermore, I identified several BCR associated proteins whose interaction with Grb2 has been reported in several studies (Neumann et al, 2009).

Due to the lack of a putative Grb2 binding site, I assumed that interaction of Grb2-SH2 domain with the BCR complex occurs indirectly. A potential Grb2 interaction partner that could link Grb2 to the activated BCR complex is the adapter protein SHC1. SHC1 belongs to the SHC adapter family that encompasses four members with multiple isoforms being involved in signaling of various surface receptors (Finetti et al, 2009). Early studies already reported SHC1 association with Grb2 and Sos by virtue of the Grb2-SH2 domain upon BCR activation, suggesting its involvement in the activation of Ras and MAPKs (Smit et al, 1994; Saxton et al, 1994). Transfection of transformed murine pre-B cells with variants of SHC1 defective for Grb2-binding sites led to a decrease in Ras and Erk activation, supporting the hypothesis of SHC1 involvement in the Ras/Raf/MEK/Erk pathway (Baughn & Rosenberg, 2005). SHC1 constitutively interacts with a DCSM (Asp-Cys-Ser-Met) motif within Igα and additionally gets recruited to the phosphorylated ITAMs of Igα/β via its SH2 domain upon BCR stimulation (Baumann et al, 1994; D'Ambrosio et al, 1996). However, when RasGRP1 and 3 were identified to mediate Erk activation downstream of the T and B cell antigen receptor in a PLCγ dependent manner, SHC1 faded from the spotlight. However, later studies revealed a tight interplay between RasGRP and Grb2:Sos in

the activation of Erk (Roose et al, 2007). Since Erk activation in the B cell line DG75 seems to be mediated via Grb2:Sos, this cell line provides a good model to study SHC1 involvement in the Grb2:Sos pathway. To this end, I generated a SHC1-deficient DG75 sub cell-line and analyzed it with regard to Erk activation following BCR activation. Interestingly, three out of seven SHC1 deficient clones exhibited a remarkable decrease in Erk phosphorylation. This effect could not be reconstituted by expression of the SHC1 isoforms p52 and p46, revealing the effect on Erk phosphorylation as an off-target effect of the CRISPR construct. Yet, it is striking that three out of seven clones designated as SHC1 deficient are defective in Erk activation following BCR stimulation. Off-target analysis of the CRISPR/Cas construct did not reveal BCR relevant off-targets. However, sequence alignment of SHC family members revealed similarities between SHC1 and SHC2 (also termed ShcB), especially in the CRISPR target site. SHC2 is predominantly expressed in the CNS (Central nervous system) (O'Bryan et al, 1996). Currently, there are no reports about expression and function of SHC2 in immune cells, but SHC2 should be taken into account in future experiments.

4.2.6 The search for the membrane anchor of Grb2

Grb2 has been shown to be recruited to the plasma membrane following BCR activation in multiple ways by virtue of its SH3 domains or its SH2 domain. My results showed that BCR-induced Erk activation does not solely depend on the Grb2-SH3 domains but also on the Grb2-SH2 domain, suggesting the requirement for plasma membrane recruitment of Grb2 to a phosphorylation-motif within the BCR signalosome for sufficient Erk activation.

Via its SH2 domain, Grb2 was shown to associate with SHC1, CD19 and SLP65 as well as with SHP2 and several inhibitory coreceptors (Neumann et al, 2009). However, none of these interactions appeared to be important for the activation of Erk, as shown in this study for SHC1 and SLP65. Moreover, Erk activation following BCR activation in CD19-deficient cells was also not affected (data not shown). Grb2 was shown to interact with Btk which is translocated to the plasma membrane by virtue of its PH domain (Engels et al, 2014; Takata & Kurosaki, 1996). Since the Btk:Grb2 interaction depends on the Grb2-SH3 domain and not on the Grb2-SH2 domain, Btk might not be the missing link recruiting Grb2 to the signalosome of the activated BCR.

Furthermore, Erk activation following BCR stimulation in Btk-deficient B cells was not or only to small extents impaired.

A study in the Burkitt lymphoma cell line BL41 suggested Grb2-asscociated binding protein 1 (Gab1) as a major regulator of Erk. siRNA knockdown of Gab1 almost completely blocked the activation of Erk. Gab1 is constitutively associated with Grb2 via proline rich sequences of Grb2 and associates with phosphorylated signaling molecules as for example SHC1 by virtue of its SH2 domains. Via its PH domain it is able to bind to PIP3 and thus is recruited to the plasma membrane (Angyal et al, 2006). Therefore, Gab1 which was also identified in the Grb2-SH2 interactome in this study, provides a further potential membrane anchor for Grb2.

Igα was the most abundant protein identified in the mass spectrometry interactome of the Grb2-SH2 domain. This implies a direct interaction with Grb2, although it does not encompass a Grb2-docking site matching the consensus phosphorylation motif. To examine, whether Grb2 is capable to be recruited to phosphorylated ITAMs directly, synthetic phosphorylated and unphosphorylated peptides containing the ITAMs or the non-ITAM could be used for pulldown analysis in DG75 B cell lysates in future experiments.

Taken together, I assume that the recruitment of the adapter protein Grb2 to the signalosome of the activated BCR complex does not rely on single protein interactions but rather is mediated by many factors involved in Grb2 recruitment via interaction with either the Grb2-SH3 domains or the Grb2-SH2 domain. Yet another protein that could serve as potential membrane anchor for the Grb2-SH2 domain is the newly identified FcμR, which harbors a putative Grb2 docking site (ITT-like motif) within its cytoplasmic domain.

4.3 The FcμR constitutes another membrane anchor for Grb2

For quite a long time the FcμR defied identification, although its existence has been suggested for more than 30 years (Sanders et al, 1987; Ohno et al, 1990; Nakamura et al, 1993). Different from other Fc receptors, the Fc receptor for IgM does not carry a conventional ITAM or ITIM signaling motif in its cytoplasmic domain. Instead it harbors a phosphorylation motif similar to the ITT in the cytoplasmic domain of the IgG/E BCR that could serve as a potential Grb2 binding site (Kubagawa et al, 2009). Considering the multifaceted properties of Grb2, the potential

ITT-like motif within the FcμR could either have costimulatory or inhibitory functions. Since exogenous expression of the full length FcμR only led to low surface expression levels, I investigated the molecular signaling properties of the cytoplasmic domain of the FcμR in the context of the murine IgG2a-BCR. The results obtained with DG75 B cells expressing the IgG2a-FcμR chimera indeed confirmed the FcμR-ITT motif as a Grb2 binding site. Moreover, the FcμR-ITT was able to functionally replace the original ITT in terms of costimulatory functions. Whether this also resembles the properties of the full-length FcμR has to be elucidated in future. Nevertheless, co-crosslinking of the FcμR and the BCR on human primary B cells using BCR specific IgM suggested a costimulatory role for the FcμR, although the costimulatory effect was rather low. Furthermore, the same study revealed a costimulatory role for the FcμR also when co-crosslinked with CD2 or the T cell antigen receptor of the Jurkat T cell line (Honjo et al, 2015). The FcμR ITT-like motif (Y385) as well as the tyrosine at position 366 was shown to be involved in receptor internalization following IgM binding (Honjo et al, 2015). This could also be mediated via Grb2 which was shown to be involved in receptor internalization by interacting with dynamin (Malhotra et al, 2009). To conclude, the FcμR-ITT-like motif once phosphorylated indeed constitutes a Grb2 docking site, which in context of the IgG2a-chimera fulfills costimulatory functions. Thus, the FcμR can be added to the list of Grb2 membrane anchor.

5 Summary and Conclusion

In my PhD project I investigated different modes of BCR activation and the outcome in intracellular signaling. Antigens and BCR specific antibodies are well established reagents to activate the BCR. However, multimeric soluble FcγRIIB is able to interact with the IgG-BCR on memory-like B cells leading to BCR specific induction of signaling events. Thus, multimeric soluble FcγRIIB represents a new tool to induce BCR signaling in different strength and quality compared to stimulation with BCR specific antibodies. BCR stimulation with soluble FcγRIIB suggested a signaling pathway leading to the activation of Erk independent of SLP65 and hence independent of the Ca^{2+} initiation complex. In contrast to chicken DT40 B cells, my results show that Erk activation following BCR ligation in human B cells is independent of the PLCγ/RasGRP axis revealing species specific differences between chicken and human with regard to BCR-induced Erk activation. Erk activation in human B cells depends on the adapter protein Grb2, which most likely mediates Erk activation by linking the RasGEF Sos to the signalosome of the activated BCR. However, the Grb2 membrane anchor within the signalosome of the activated BCR which is important for the activation of Erk is still unknown. Indirect recruitment of Grb2 to the BCR complex via SHC1 turned out to be dispensable for Erk activation following BCR activation. With the newly identified FcμR, I found a new membrane anchor for Grb2. However, its role with regard to BCR signaling remains to be elucidated.

6 Bibliography

Ackermann JA, Radtke D, Maurberger A, Winkler TH & Nitschke L (2011) Grb2 regulates B-cell maturation, B-cell memory responses and inhibits B-cell Ca2+ signalling. *The EMBO journal* **30:** 1621–1633

Ahmed R & Gray D (1996) Immunological memory and protective immunity: understanding their relation. *Science (New York, N.Y.)* **272:** 54–60

Andrian UH von & Mempel TR (2003) Homing and cellular traffic in lymph nodes. *Nature reviews. Immunology* **3:** 867–878

Angyal A, Medgyesi D & Sarmay G (2006) Grb2-associated binder 1 (Gab1) adaptor/scaffolding protein regulates Erk signal in human B cells. *Annals of the New York Academy of Sciences* **1090:** 326–331

Astier A, La Salle H de, La Salle C de, Bieber T, Esposito-Farese ME, Freund M, Cazenave JP, Fridman WH, Teillaud JL & Hanau D (1994) Human epidermal Langerhans cells secrete a soluble receptor for IgG (Fc gamma RII/CD32) that inhibits the binding of immune complexes to Fc gamma R+ cells. *J Immunol* **152:** 201–212

Baerenwaldt A & Nimmerjahn F (2008) Immune regulation: FcgammaRIIB--regulating the balance between protective and autoreactive immune responses. *Immunology and cell biology* **86:** 482–484

Bardelli A, Longati P, Gramaglia D, Stella MC & Comoglio PM (1997) Gab1 coupling to the HGF/Met receptor multifunctional docking site requires binding of Grb2 and correlates with the transforming potential. *Oncogene* **15:** 3103–3111

Bar-Sagi D (1994) The Sos (Son of sevenless) protein. *Trends in endocrinology and metabolism: TEM* **5:** 165–169

Baughn LB & Rosenberg N (2005) Disruption of the Shc/Grb2 complex during abelson virus transformation affects proliferation, but not apoptosis. *Journal of virology* **79:** 2325–2334

Baumann G, Maier D, Freuler F, Tschopp C, Baudisch K & Wienands J (1994) In vitro characterization of major ligands for Src homology 2 domains derived from protein tyrosine kinases, from the adaptor protein SHC and from GTPase-activating protein in Ramos B cells. *European journal of immunology* **24:** 1799–1807

Beck G & Habicht GS (1996) Immunity and the invertebrates. *Scientific American* **275:** 60-3, 66

Bell SE, Vigorito E, McAdam S, Reynolds HM, Caraux A, Colucci F & Turner M (2004) PLCgamma2 regulates Bcl-2 levels and is required for survival rather than differentiation of marginal zone and follicular B cells. *European journal of immunology* **34:** 2237–2247

Bengtsson AA & Ronnblom L (2016) Systemic lupus erythematosus: still a challenge for physicians. *Journal of internal medicine*

Boes M (2000) Role of natural and immune IgM antibodies in immune responses. *Molecular Immunology* **37:** 1141–1149

Bolland S & Ravetch JV (1999) Inhibitory pathways triggered by ITIM-containing receptors. *Advances in immunology* **72:** 149–177

Buday L & Downward J (1993) Epidermal growth factor regulates p21ras through the formation of a complex of receptor, Grb2 adapter protein, and Sos nucleotide exchange factor. *Cell* **73:** 611–620

Campbell SL, Khosravi-Far R, Rossman KL, Clark GJ & Der CJ (1998) Increasing complexity of Ras signaling. *Oncogene* **17:** 1395–1413

Carbo C, Duerschmied D, Goerge T, Hattori H, Sakai J, Cifuni SM, White GC2, Chrzanowska-Wodnicka M, Luo HR & Wagner DD (2010) Integrin-independent role of CalDAG-GEFI in neutrophil chemotaxis. *Journal of leukocyte biology* **88:** 313–319

Chen K & Cerutti A (2010) New insights into the enigma of immunoglobulin D. *Immunological reviews* **237:** 160–179

Cheng AM, Saxton TM, Sakai R, Kulkarni S, Mbamalu G, Vogel W, Tortorice CG, Cardiff RD, Cross JC, Muller WJ & Pawson T (1998) Mammalian Grb2 regulates multiple steps in embryonic development and malignant transformation. *Cell* **95:** 793–803

Chiu CW (2002) BLNK: Molecular scaffolding through 'cis'-mediated organization of signaling proteins. *The EMBO journal* **21:** 6461–6472

Choi S, Wang H, Tian L, Murakami Y, Shin D, Borrego F, Morse HC3 & Coligan JE (2013) Mouse IgM Fc receptor, FCMR, promotes B cell development and modulates antigen-driven immune responses. *Journal of immunology (Baltimore, Md. : 1950)* **190:** 987–996

Cines DB & Blanchette VS (2002) Immune thrombocytopenic purpura. *The New England journal of medicine* **346:** 995–1008

Cines DB & Bussel JB (2005) How I treat idiopathic thrombocytopenic purpura (ITP). *Blood* **106:** 2244–2251

Clark, Johnson SA & Cambier JC (1994) Analysis of Ig-alpha-tyrosine kinase interaction reveals two levels of binding specificity and tyrosine phosphorylated Ig-alpha stimulation of Fyn activity. *The EMBO journal* **13:** 1911–1919

Coopamah MD, Garvey MB, Freedman J & Semple JW (2003) Cellular immune mechanisms in autoimmune thrombocytopenic purpura: An update. *Transfusion medicine reviews* **17:** 69–80

Cooper MD (2015) The early history of B cells. *Nature reviews. Immunology* **15:** 191–197

Coughlin JJ, Stang SL, Dower NA & Stone JC (2005) RasGRP1 and RasGRP3 regulate B cell proliferation by facilitating B cell receptor-Ras signaling. *Journal of immunology (Baltimore, Md. : 1950)* **175:** 7179–7184

Crittenden JR, Bergmeier W, Zhang Y, Piffath CL, Liang Y, Wagner DD, Housman DE & Graybiel AM (2004) CalDAG-GEFI integrates signaling for platelet aggregation and thrombus formation. *Nature medicine* **10:** 982–986

Cully M, Elia A, Ong S, Stambolic V, Pawson T, Tsao M & Mak TW (2004) grb2 heterozygosity rescues embryonic lethality but not tumorigenesis in pten+/- mice. *Proceedings of the National Academy of Sciences of the United States of America* **101:** 15358–15363

Czikora A, Lundberg DJ, Abramovitz A, Lewin NE, Kedei N, Peach ML, Zhou X, Merritt RC, JR, Craft EA, Braun DC & Blumberg PM (2016) Structural Basis for the Failure of the C1 Domain of Ras Guanine Nucleotide Releasing Protein 2 (RasGRP2) to Bind Phorbol Ester with High Affinity. *The Journal of biological chemistry* **291:** 11133–11147

D'Ambrosio D, Hippen KL & Cambier JC (1996) Distinct mechanisms mediate SHC association with the activated and resting B cell antigen receptor. *Eur. J. Immunol.* **26:** 1960–1965

Das J, Ho M, Zikherman J, Govern C, Yang M, Weiss A, Chakraborty AK & Roose JP (2009) Digital signaling and hysteresis characterize ras activation in lymphoid cells. *Cell* **136:** 337–351

Dempsey PW, Vaidya SA & Cheng G (2003) The art of war: Innate and adaptive immune responses. *Cellular and molecular life sciences : CMLS* **60:** 2604–2621

Egan SE, Giddings BW, Brooks MW, Buday L, Sizeland AM & Weinberg RA (1993) Association of Sos Ras exchange protein with Grb2 is implicated in tyrosine kinase signal transduction and transformation. *Nature* **363:** 45–51

Engelke M, Engels N, Dittmann K, Stork B & Wienands J (2007) Ca(2+) signaling in antigen receptor-activated B lymphocytes. *Immunological reviews* **218:** 235–246

Engels N, Wollscheid B & Wienands J (2001) Association of SLP-65/BLNK with the B cell antigen receptor through a non-ITAM tyrosine of Ig-alpha. *European journal of immunology* **31:** 2126–2134

Engels N, Konig LM, Schulze W, Radtke D, Vanshylla K, Lutz J, Winkler TH, Nitschke L & Wienands J (2014) The immunoglobulin tail tyrosine motif upgrades memory-type BCRs by incorporating a Grb2-Btk signalling module. *Nature communications* **5:** 5456

Engels N, König LM, Heemann C, Lutz J, Tsubata T, Griep S, Schrader V & Wienands J (2009) Recruitment of the cytoplasmic adaptor Grb2 to surface IgG and IgE provides antigen receptor-intrinsic costimulation to class-switched B cells. *Nature immunology* **10:** 1018–1025

Epstein AL & Kaplan HS (1979) Feeder layer and nutritional requirements for the establishment and cloning of human malignant lymphoma cell lines. *Cancer research* **39:** 1748–1759

Epstein MA, Achong BG, Barr YM, Zajac B, Henle G & Henle W (1966) Morphological and virological investigations on cultured Burkitt tumor lymphoblasts (strain Raji). *Journal of the National Cancer Institute* **37:** 547–559

Eray M, Tuomikoski T, Wu H, Nordstrom T, Andersson LC, Knuutila S & Kaartinen M (1994) Cross-linking of surface IgG induces apoptosis in a bcl-2 expressing human follicular lymphoma line of mature B cell phenotype. *International immunology* **6:** 1817–1827

Feng G, Ouyang Y, Hu D, Shi Z, Gentz R & Ni J (1996) Grap Is a Novel SH3-SH2-SH3 Adaptor Protein That Couples Tyrosine Kinases to the Ras Pathway. *Journal of Biological Chemistry* **271:** 12129–12132

Finetti F, Savino MT & Baldari CT (2009) Positive and negative regulation of antigen receptor signaling by the Shc family of protein adapters. *Immunological reviews* **232:** 115–134

Floto RA, Clatworthy MR, Heilbronn KR, Rosner DR, MacAry PA, Rankin A, Lehner PJ, Ouwehand WH, Allen JM, Watkins NA & Smith KGC (2005) Loss of function of a lupus-associated FcgammaRIIb polymorphism through exclusion from lipid rafts. *Nature medicine* **11:** 1056–1058

Fu C, Turck CW, Kurosaki T & Chan AC (1998) BLNK: a central linker protein in B cell activation. *Immunity* **9:** 93–103

Futterer K, Wong J, Grucza RA, Chan AC & Waksman G (1998) Structural basis for Syk tyrosine kinase ubiquity in signal transduction pathways revealed by the crystal structure of its regulatory SH2 domains bound to a dually phosphorylated ITAM peptide. *Journal of molecular biology* **281:** 523–537

Gabay C, Ben-Bassat H, Schlesinger M & Laskov R (1999) Somatic mutations and intraclonal variations in the rearranged Vkappa genes of B-non-Hodgkin's lymphoma cell lines. *European journal of haematology* **63:** 180–191

Gaj T, Gersbach CA & Barbas CF3 (2013) ZFN, TALEN, and CRISPR/Cas-based methods for genome engineering. *Trends in biotechnology* **31:** 397–405

Galon J, Bouchard C, Fridman WH & Sautes C (1995) Ligands and biological activities of soluble Fc gamma receptors. *Immunology letters* **44:** 175–181

Gavin AL, Wines BD, Powell MS & Hogarth PM (1995) Recombinant soluble Fc gamma RII inhibits immune complex precipitation. *Clin Exp Immunol* **102:** 620–625

Gerlach J, Ghosh S, Jumaa H, Reth M, Wienands J, Chan AC & Nitschke L (2003) B cell defects in SLP65/BLNK-deficient mice can be partially corrected by the absence of CD22, an inhibitory coreceptor for BCR signaling. *European journal of immunology* **33:** 3418–3426

Goitsuka R, Fujimura Y, Mamada H, Umeda A, Morimura T, Uetsuka K, Doi K, Tsuji S & Kitamura D (1998) BASH, a novel signaling molecule preferentially expressed in B cells of the bursa of Fabricius. *Journal of immunology (Baltimore, Md. : 1950)* **161:** 5804–5808

Gold, Matsuuchi L, Kelly RB & DeFranco AL (1991) Tyrosine phosphorylation of components of the B-cell antigen receptors following receptor crosslinking. *Proceedings of the National Academy of Sciences of the United States of America* **88:** 3436–3440

Harmer SL & DeFranco AL (1997) Shc contains two Grb2 binding sites needed for efficient formation of complexes with SOS in B lymphocytes. *Molecular and cellular biology* **17:** 4087–4095

Hashimoto A, Okada H, Jiang A, Kurosaki M, Greenberg S, Clark EA & Kurosaki T (1998) Involvement of guanosine triphosphatases and phospholipase C-gamma2 in extracellular signal-regulated kinase, c-Jun NH2-terminal kinase, and p38 mitogen-activated protein kinase activation by the B cell antigen receptor. *The Journal of experimental medicine* **188:** 1287–1295

Hayashi K, Nittono R, Okamoto N, Tsuji S, Hara Y, Goitsuka R & Kitamura D (2000) The B cell-restricted adaptor BASH is required for normal development and antigen receptor-mediated activation of B cells. *Proceedings of the National Academy of Sciences of the United States of America* **97:** 2755–2760

Heesters BA, Myers RC & Carroll MC (2014) Follicular dendritic cells: dynamic antigen libraries. *Nature reviews. Immunology* **14:** 495–504

Hitoshi Y, Lorens J, Kitada S, Fisher J, LaBarge M, Ring HZ, Francke U, Reed JC, Kinoshita S & Nolan GP (1998) Toso, a Cell Surface, Specific Regulator of Fas-Induced Apoptosis in T Cells. *Immunity* **8:** 461–471

Hock M, Vaeth M, Rudolf R, Patra AK, Pham DAT, Muhammad K, Pusch T, Bopp T, Schmitt E, Rost R, Berberich-Siebelt F, Tyrsin D, Chuvpilo S, Avots A, Serfling E & Klein-Hessling S (2013) NFATc1 induction in peripheral T and B lymphocytes. *Journal of immunology (Baltimore, Md. : 1950)* **190:** 2345–2353

Holgado-Madruga M, Emlet DR, Moscatello DK, Godwin AK & Wong AJ (1996) A Grb2-associated docking protein in EGF- and insulin-receptor signalling. *Nature* **379:** 560–564

Honjo K, Kubagawa Y, Jones DM, Dizon B, Zhu Z, Ohno H, Izui S, Kearney JF & Kubagawa H (2012) Altered Ig levels and antibody responses in mice deficient for the Fc receptor for IgM (FcmuR). *Proceedings of the National Academy of Sciences of the United States of America* **109:** 15882–15887

Honjo K, Kubagawa Y, Kearney JF & Kubagawa H (2015) Unique ligand-binding property of the human IgM Fc receptor. *Journal of immunology (Baltimore, Md. : 1950)* **194:** 1975–1982

Honma M, Higuchi O, Shirakata M, Yasuda T, Shibuya H, Iemura S, Natsume T & Yamanashi Y (2006) Dok-3 sequesters Grb2 and inhibits the Ras-Erk pathway downstream of protein-tyrosine kinases. *Genes to cells : devoted to molecular & cellular mechanisms* **11:** 143–151

Ierino FL, Powell MS, McKenzie IF & Hogarth PM (1993) Recombinant soluble human Fc gamma RII: production, characterization, and inhibition of the Arthus reaction. *J Exp Med* **178:** 1617–1628

Irie K, Masuda A, Shindo M, Nakagawa Y & Ohigashi H (2004) Tumor promoter binding of the protein kinase C C1 homology domain peptides of RasGRPs, chimaerins, and Unc13s. *Bioorganic & medicinal chemistry* **12:** 4575–4583

Ishiai M, Sugawara H, Kurosaki M & Kurosaki T (1999) Cutting edge: association of phospholipase C-gamma 2 Src homology 2 domains with BLNK is critical for B cell antigen receptor signaling. *Journal of immunology (Baltimore, Md. : 1950)* **163:** 1746–1749

Isnardi I, Lesourne R, Bruhns P, Fridman WH, Cambier JC & Daeron M (2004) Two distinct tyrosine-based motifs enable the inhibitory receptor FcgammaRIIB to cooperatively recruit the inositol phosphatases SHIP1/2 and the adapters Grb2/Grap. *The Journal of biological chemistry* **279:** 51931–51938

Iwata H, Pipi E, Mockel N, Sondermann P, Vorobyev A, van Beek N, Zillikens D & Ludwig RJ (2015) Recombinant soluble CD32 suppresses disease progression in experimental epidermolysis bullosa acquisita. *The Journal of investigative dermatology* **135:** 916–919

Jang IK, Zhang J & Gu H (2009) Grb2, a simple adapter with complex roles in lymphocyte development, function, and signaling. *Immunological reviews* **232:** 150–159

Johnson JE, Goulding RE, Ding Z, Partovi A, Anthony KV, Beaulieu N, Tazmini G, Cornell RB & Kay RJ (2007) Differential membrane binding and diacylglycerol recognition by C1 domains of RasGRPs. *The Biochemical journal* **406:** 223–236

Jung D, Giallourakis C, Mostoslavsky R & Alt FW (2006) Mechanism and control of V(D)J recombination at the immunoglobulin heavy chain locus. *Annual review of immunology* **24:** 541–570

Kane LP, Lin J & Weiss A (2000) Signal transduction by the TCR for antigen. *Current Opinion in Immunology* **12:** 242–249

Kessels, Helmut W H G, Ward AC & Schumacher TNM (2002) Specificity and affinity motifs for Grb2 SH2-ligand interactions. *Proceedings of the National Academy of Sciences of the United States of America* **99:** 8524–8529

Klasener K, Maity PC, Hobeika E, Yang J & Reth M (2014) B cell activation involves nanoscale receptor reorganizations and inside-out signaling by Syk. *eLife* **3:** e02069

Klein G, Giovanella B, Westman A, Stehlin JS & Mumford D (1975) An EBV-genome-negative cell line established from an American Burkitt lymphoma; receptor characteristics. EBV infectibility and permanent conversion into EBV-positive sublines by in vitro infection. *Intervirology* **5:** 319–334

Kluin-Nelemans HC, Limpens J, Meerabux J, Beverstock GC, Jansen JH, Jong D de & Kluin PM (1991) A new non-Hodgkin's B-cell line (DoHH2) with a chromosomal translocation t(14;18)(q32;q21). *Leukemia* **5:** 221–224

Kometani K, Yamada T, Sasaki Y, Yokosuka T, Saito T, Rajewsky K, Ishiai M, Hikida M & Kurosaki T (2011) CIN85 drives B cell responses by linking BCR signals to the canonical NF-kappaB pathway. *The Journal of experimental medicine* **208:** 1447–1457

Konstaninova TS, Leonidovna IV, Hellmann A, Kyrcz-Krzemien S, Tillmanns S, Sondermann P, et al. Interim results froma phase Ib/ IIa clinical trial with the soluble Fc-gamma IIb receptor SM101 for the treatment of primary immune thrombocytopenia. Blood. 2012;120:3388.

Kubagawa H, Carroll MC, Jacob CO, Lang KS, Lee K, Mak T, McAndrews M, Morse HC3, Nolan GP, Ohno H, Richter GH, Seal R, Wang J, Wiestner A & Coligan JE (2015) Nomenclature of Toso, Fas apoptosis inhibitory molecule 3, and IgM FcR. *Journal of immunology (Baltimore, Md. : 1950)* **194:** 4055–4057

Kubagawa H, Oka S, Kubagawa Y, Torii I, Takayama E, Kang D, Gartland GL, Bertoli LF, Mori H, Takatsu H, Kitamura T, Ohno H & Wang J (2009) Identity of the elusive IgM Fc receptor (FcmuR) in humans. *The Journal of experimental medicine* **206:** 2779–2793

Kulathu Y, Hobeika E, Turchinovich G & Reth M (2008) The kinase Syk as an adaptor controlling sustained calcium signalling and B-cell development. *The EMBO journal* **27:** 1333–1344

Kumar H, Kawai T & Akira S (2009) Pathogen recognition in the innate immune response. *The Biochemical journal* **420:** 1–16

Kurosaki T (1999) Genetic analysis of B cell antigen receptor signaling. *Annual review of immunology* **17:** 555–592

Kurosaki T, Kometani K & Ise W (2015) Memory B cells. *Nature reviews. Immunology* **15:** 149–159

Kurosaki T, Maeda A, Ishiai M, Hashimoto A, Inabe K & Takata M (2000) Regulation of the phospholipase C-gamma2 pathway in B cells. *Immunological reviews* **176:** 19–29

Laemmli UK (1970) Cleavage of structural proteins during the assembly of the head of bacteriophage T4. *Nature* **227:** 680–685

Lang KS, Lang PA, Meryk A, Pandyra AA, Boucher L, Pozdeev VI, Tusche MW, Gothert JR, Haight J, Wakeham A, You-Ten AJ, McIlwain DR, Merches K, Khairnar V, Recher M, Nolan GP, Hitoshi Y, Funkner P, Navarini AA & Verschoor A et al (2013) Involvement of Toso in activation of monocytes, macrophages, and granulocytes. *Proceedings of the National Academy of Sciences of the United States of America* **110:** 2593–2598

Lang PA, Meryk A, Pandyra AA, Brenner D, Brustle A, Xu HC, Merches K, Lang F, Khairnar V, Sharma P, Funkner P, Recher M, Shaabani N, Duncan GS, Duhan V, Homey B, Ohashi PS, Haussinger D, Knolle PA & Honke N et al (2015) Toso regulates differentiation and activation of inflammatory dendritic cells during persistence-prone virus infection. *Cell death and differentiation* **22:** 164–173

Lankester AC, Van Schijndel, Gijs M. W., Rood PML, Verhoeven AJ & Van Lier, René A. W. (1994) B cell antigen receptor cross-linking induces tyrosine phosphorylation and membrane translocation of a multimeric Shc complex that is augmented by CD19 co-ligation. *Eur. J. Immunol.* **24:** 2818–2825

Lemmon MA & Schlessinger J (2010) Cell signaling by receptor tyrosine kinases. *Cell* **141:** 1117–1134

Li Q & Verma IM (2002) NF-kappaB regulation in the immune system. *Nature reviews. Immunology* **2:** 725–734

Li Z, Woo CJ, Iglesias-Ussel MD, Ronai D & Scharff MD (2004) The generation of antibody diversity through somatic hypermutation and class switch recombination. *Genes & development* **18:** 1–11

Liu SK, Berry DM & McGlade CJ (2001) The role of Gads in hematopoietic cell signalling. *Oncogene* **20:** 6284–6290

Lowenstein EJ, Daly RJ, Batzer AG, Li W, Margolis B, Lammers R, Ullrich A, Skolnik EY, Bar-Sagi D & Schlessinger J (1992) The SH2 and SH3 domain-containing protein GRB2 links receptor tyrosine kinases to ras signaling. *Cell* **70:** 431–442

Lutz J, Dittmann K, Bosl MR, Winkler TH, Wienands J & Engels N (2016) Reactivation of IgG-switched memory B cells by BCR-intrinsic signal amplification promotes IgG antibody production. *Nature communications* **6:** 8575

Macian F (2005) NFAT proteins: key regulators of T-cell development and function. *Nature reviews. Immunology* **5:** 472–484

Maenaka K, van der Merwe, P A, Stuart DI, Jones EY & Sondermann P (2001) The human low affinity Fcgamma receptors IIa, IIb, and III bind IgG with fast kinetics and distinct thermodynamic properties. *The Journal of biological chemistry* **276:** 44898–44904

Magnusson SE, Andrén M, Nilsson KE, Sondermann P, Jacob U & Kleinau S (2008) Amelioration of collagen-induced arthritis by human recombinant soluble FcγRIIb. *Clinical Immunology* **127:** 225–233

Malhotra S, Kovats S, Zhang W & Coggeshall KM (2009) Vav and Rac activation in B cell antigen receptor endocytosis involves Vav recruitment to the adapter protein LAB. *The Journal of biological chemistry* **284:** 36202–36212

Margarit S, Sondermann H, Hall BE, Nagar B, Hoelz A, Pirruccello M, Bar-Sagi D & Kuriyan J (2003) Structural Evidence for Feedback Activation by Ras·GTP of the Ras-Specific Nucleotide Exchange Factor SOS. *Cell* **112:** 685–695

Marshall AJ, Niiro H, Yun TJ & Clark EA (2000) Regulation of B-cell activation and differentiation by the phosphatidylinositol 3-kinase and phospholipase Cgamma pathway. *Immunological reviews* **176:** 30–46

Matsuda F, Ishii K, Bourvagnet P, Kuma Ki, Hayashida H, Miyata T & Honjo T (1998) The complete nucleotide sequence of the human immunoglobulin heavy chain variable region locus. *The Journal of experimental medicine* **188:** 2151–2162

Mattila PK, Feest C, Depoil D, Treanor B, Montaner B, Otipoby KL, Carter R, Justement LB, Bruckbauer A & Batista FD (2013) The actin and tetraspanin networks organize receptor nanoclusters to regulate B cell receptor-mediated signaling. *Immunity* **38:** 461–474

McCubrey JA, Steelman LS, Chappell WH, Abrams SL, Wong EWT, Chang F, Lehmann B, Terrian DM, Milella M, Tafuri A, Stivala F, Libra M, Basecke J, Evangelisti C, Martelli AM & Franklin RA (2007) Roles of the Raf/MEK/Erk pathway in cell growth, malignant transformation and drug resistance. *Biochimica et biophysica acta* **1773:** 1263–1284

Medzhitov R & Janeway CA (2002) Decoding the patterns of self and nonself by the innate immune system. *Science (New York, N.Y.)* **296:** 298–300

Metzger H (1992) Transmembrane signaling: the joy of aggregation. *Journal of immunology (Baltimore, Md. : 1950)* **149:** 1477–1487

Morita S, Kojima T & Kitamura T (2000) Plat-E: an efficient and stable system for transient packaging of retroviruses. *Gene therapy* **7:** 1063–1066

Murakami Y, Narayanan S, Su S, Childs R, Krzewski K, Borrego F, Weck J & Coligan JE (2012) Toso, a functional IgM receptor, is regulated by IL-2 in T and NK cells. *Journal of immunology (Baltimore, Md. : 1950)* **189:** 587–597

Nakamura T, Kubagawa H, Ohno T & Cooper MD (1993) Characterization of an IgM Fc-binding receptor on human T cells. *Journal of immunology (Baltimore, Md. : 1950)* **151:** 6933–6941

Nemazee D (2000) Receptor selection in B and T lymphocytes. *Annual review of immunology* **18:** 19–51

Neumann K, Oellerich T, Heine I, Urlaub H & Engelke M (2011) Fc gamma receptor IIb modulates the molecular Grb2 interaction network in activated B cells. *Cellular signalling* **23:** 893–900

Neumann K, Oellerich T, Urlaub H & Wienands J (2009) The B-lymphoid Grb2 interaction code. *Immunological reviews* **232:** 135–149

Nimmerjahn F & Ravetch JV (2007) Fc-receptors as regulators of immunity. *Advances in immunology* **96:** 179–204

Nimmerjahn F & Ravetch JV (2008) Fcgamma receptors as regulators of immune responses. *Nature reviews. Immunology* **8:** 34–47

Nimmerjahn F & Ravetch JV (2010) Antibody-mediated modulation of immune responses. *Immunological reviews* **236:** 265–275

Nitschke L & Tsubata T (2004) Molecular interactions regulate BCR signal inhibition by CD22 and CD72. *Trends in immunology* **25:** 543–550

O'Bryan JP, Songyang Z, Cantley L, Der CJ & Pawson T (1996) A mammalian adaptor protein with conserved Src homology 2 and phosphotyrosine-binding domains is related to Shc and is specifically expressed in the brain. *Proceedings of the National Academy of Sciences of the United States of America* **93:** 2729–2734

Odegard VH & Schatz DG (2006) Targeting of somatic hypermutation. *Nature reviews. Immunology* **6:** 573–583

Oellerich T, Bremes V, Neumann K, Bohnenberger H, Dittmann K, Hsiao H, Engelke M, Schnyder T, Batista FD, Urlaub H & Wienands J (2011) The B-cell antigen receptor signals through a preformed transducer module of SLP65 and CIN85. *The EMBO journal* **30:** 3620–3634

Oh-hora M, Johmura S, Hashimoto A, Hikida M & Kurosaki T (2003) Requirement for Ras guanine nucleotide releasing protein 3 in coupling phospholipase C-gamma2 to Ras in B cell receptor signaling. *The Journal of experimental medicine* **198:** 1841–1851

Ohno T, Kubagawa H, Sanders SK & Cooper MD (1990) Biochemical nature of an Fc mu receptor on human B-lineage cells. *The Journal of experimental medicine* **172:** 1165–1175

Ono M, Bolland S, Tempst P & Ravetch JV (1996) Role of the inositol phosphatase SHIP in negative regulation of the immune system by the receptor Fc(gamma)RIIB. *Nature* **383:** 263–266

Osaki M, Oshimura M & Ito H (2004) PI3K-Akt pathway: its functions and alterations in human cancer. *Apoptosis : an international journal on programmed cell death* **9:** 667–676

Osmond DG (1986) Population Dynamics of Bone Marrow B Lymphocytes. *Immunol Rev* **93:** 103–124

Otipoby KL, Draves KE & Clark EA (2001) CD22 regulates B cell receptor-mediated signals via two domains that independently recruit Grb2 and SHP-1. *The Journal of biological chemistry* **276:** 44315–44322

Ouchida R, Mori H, Hase K, Takatsu H, Kurosaki T, Tokuhisa T, Ohno H & Wang J (2012) Critical role of the IgM Fc receptor in IgM homeostasis, B-cell survival, and humoral immune responses. *Proceedings of the National Academy of Sciences of the United States of America* **109:** E2699-706

Pappu R, Cheng AM, Li B, Gong Q, Chiu C, Griffin N, White M, Sleckman BP & Chan AC (1999) Requirement for B cell linker protein (BLNK) in B cell development. *Science (New York, N.Y.)* **286:** 1949–1954

Pieper K, Grimbacher B & Eibel H (2013) B-cell biology and development. *The Journal of allergy and clinical immunology* **131:** 959–971

Pierce SK & Liu W (2010) The tipping points in the initiation of B cell signalling: how small changes make big differences. *Nature reviews. Immunology* **10:** 767–777

Pleass RJ & Woof JM (2001) Fc receptors and immunity to parasites. *Trends in parasitology* **17:** 545–551

Poe JC, Fujimoto M, Jansen PJ, Miller AS & Tedder TF (2000) CD22 forms a quaternary complex with SHIP, Grb2, and Shc. A pathway for regulation of B lymphocyte antigen receptor-induced calcium flux. *The Journal of biological chemistry* **275:** 17420–17427

Porter RR (1959) The hydrolysis of rabbit y-globulin and antibodies with crystalline papain. *The Biochemical journal* **73:** 119–126

Pu J, Frescas D, Zhang B & Feng J (2015) Utilization of TALEN and CRISPR/Cas9 technologies for gene targeting and modification. *Experimental biology and medicine (Maywood, N.J.)* **240:** 1065–1070

Raghavan M & Bjorkman PJ (1996) Fc receptors and their interactions with immunoglobulins. *Annual review of cell and developmental biology* **12:** 181–220

Ran FA, Hsu PD, Wright J, Agarwala V, Scott DA & Zhang F (2013) Genome engineering using the CRISPR-Cas9 system. *Nature protocols* **8:** 2281–2308

Ravetch JV & Kinet JP (1991) Fc receptors. *Annual review of immunology* **9:** 457–492

Reth M (1992) Antigen receptors on B lymphocytes. *Annual review of immunology* **10:** 97–121

Reth M & Wienands J (1997) Initiation and processing of signals from the B cell antigen receptor. *Annual review of immunology* **15:** 453–479

Reth M, Hombach J, Wienands J, Campbell KS, Chien N, Justement LB & Cambier JC (1991) The B-cell antigen receptor complex. *Immunology Today* **12:** 196–201

Rickert RC (2005) Regulation of B lymphocyte activation by complement C3 and the B cell coreceptor complex. *Current Opinion in Immunology* **17:** 237–243

Rickert RC (2013) New insights into pre-BCR and BCR signalling with relevance to B cell malignancies. *Nature reviews. Immunology* **13:** 578–591

Rodeghiero F, Stasi R, Gernsheimer T, Michel M, Provan D, Arnold DM, Bussel JB, Cines DB, Chong BH, Cooper N, Godeau B, Lechner K, Mazzucconi MG, McMillan R, Sanz MA, Imbach P, Blanchette V, Kuhne T, Ruggeri M & George JN (2009) Standardization of terminology, definitions and outcome criteria in immune thrombocytopenic purpura of adults and children: report from an international working group. *Blood* **113:** 2386–2393

Rolli V, Gallwitz M, Wossning T, Flemming A, Schamel WW, Zurn C & Reth M (2002) Amplification of B cell antigen receptor signaling by a Syk/ITAM positive feedback loop. *Molecular cell* **10:** 1057–1069

Roose JP, Mollenauer M, Ho M, Kurosaki T & Weiss A (2007) Unusual interplay of two types of Ras activators, RasGRP and SOS, establishes sensitive and robust Ras activation in lymphocytes. *Molecular and cellular biology* **27:** 2732–2745

Rowley RB, Burkhardt AL, Chao HG, Matsueda GR & Bolen JB (1995) Syk protein-tyrosine kinase is regulated by tyrosine-phosphorylated Ig alpha/Ig beta immunoreceptor tyrosine activation motif binding and autophosphorylation. *The Journal of biological chemistry* **270:** 11590–11594

Rozakis-Adcock M, Fernley R, Wade J, Pawson T & Bowtell D (1993) The SH2 and SH3 domains of mammalian Grb2 couple the EGF receptor to the Ras activator mSos1. *Nature* **363:** 83–85

Saci A, Liu W, Vidal M, Garbay C, Rendu F & Bachelot-Loza C (2002) Differential effect of the inhibition of Grb2-SH3 interactions in platelet activation induced by thrombin and by Fc receptor engagement. *The Biochemical journal* **363:** 717–725

Sanders SK, Kubagawa H, Suzuki T, Butler JL & Cooper MD (1987) IgM binding protein expressed by activated B cells. *Journal of immunology (Baltimore, Md. : 1950)* **139:** 188–193

Saxton TM, van Oostveen I, Bowtell D, Aebersold R & Gold MR (1994) B cell antigen receptor cross-linking induces phosphorylation of the p21ras oncoprotein activators SHC and mSOS1 as well as assembly of complexes containing SHC, GRB-2, mSOS1, and a 145-kDa tyrosine-phosphorylated protein. *Journal of immunology (Baltimore, Md. : 1950)* **153:** 623–636

Scharenberg AM, Humphries LA & Rawlings DJ (2007) Calcium signalling and cell-fate choice in B cells. *Nature reviews. Immunology* **7:** 778–789

Schatz DG & Ji Y (2011) Recombination centres and the orchestration of V(D)J recombination. *Nature reviews. Immunology* **11:** 251–263

Schneider U, Schwenk H & Bornkamm G (1977) Characterization of EBV-genome negative "null" and "T" cell lines derived from children with acute lymphoblastic leukemia and leukemic transformed non-Hodgkin lymphoma. *Int. J. Cancer* **19:** 621–626

Schroeder HW, JR & Cavacini L (2010) Structure and function of immunoglobulins. *The Journal of allergy and clinical immunology* **125:** S41-52

Shima H, Takatsu H, Fukuda S, Ohmae M, Hase K, Kubagawa H, Wang J & Ohno H (2010) Identification of TOSO/FAIM3 as an Fc receptor for IgM. *International immunology* **22:** 149–156

Shlomchik MJ (2008) Sites and stages of autoreactive B cell activation and regulation. *Immunity* **28:** 18–28

Silva NS de & Klein U (2015) Dynamics of germinal centres. *Nature reviews. Immunology* **15:** 137–148

Smit L, Vries-Smits AM de, Bos JL & Borst J (1994) B cell antigen receptor stimulation induces formation of a Shc-Grb2 complex containing multiple tyrosine-phosphorylated proteins. *The Journal of biological chemistry* **269:** 20209–20212

Sondermann P, Huber R & Jacob U (1999) Crystal structure of the soluble form of the human fcgamma-receptor IIb: a new member of the immunoglobulin superfamily at 1.7 A resolution. *The EMBO journal* **18:** 1095–1103

Sondermann P & Jacob U (1999) Human Fcgamma receptor IIb expressed in Escherichia coli reveals IgG binding capability. *Biological chemistry* **380:** 717–721

Sondermann P, Jacob U, Kutscher C & Frey J (1999) Characterization and crystallization of soluble human Fc gamma receptor II (CD32) isoforms produced in insect cells. *Biochemistry* **38:** 8469–8477

Sondermann P (2016) The FcgammaR/IgG Interaction as Target for the Treatment of Autoimmune Diseases. *Journal of clinical immunology*

Spitaler M & Cantrell DA (2004) Protein kinase C and beyond. *Nature immunology* **5:** 785–790

Stavnezer J, Guikema JE & Schrader CE (2008) Mechanism and regulation of class switch recombination. *Annual review of immunology* **26:** 261–292

Stavnezer J & Schrader CE (2014) IgH chain class switch recombination: mechanism and regulation. *Journal of immunology (Baltimore, Md. : 1950)* **193:** 5370–5378

Stolla M, Stefanini L, Andre P, Ouellette TD, Reilly MP, McKenzie SE & Bergmeier W (2011) CalDAG-GEFI deficiency protects mice in a novel model of Fcgamma RIIA-mediated thrombosis and thrombocytopenia. *Blood* **118:** 1113–1120

Stone JC (2011) Regulation and Function of the RasGRP Family of Ras Activators in Blood Cells. *Genes & cancer* **2:** 320–334

Stork B, Engelke M, Frey J, Horejsi V, Hamm-Baarke A, Schraven B, Kurosaki T & Wienands J (2004) Grb2 and the non-T cell activation linker NTAL constitute a Ca(2+)-regulating signal circuit in B lymphocytes. *Immunity* **21:** 681–691

Stork B, Neumann K, Goldbeck I, Alers S, Kahne T, Naumann M, Engelke M & Wienands J (2007) Subcellular localization of Grb2 by the adaptor protein Dok-3 restricts the intensity of Ca2+ signaling in B cells. *The EMBO journal* **26:** 1140–1149

Takata M & Kurosaki T (1996) A role for Bruton's tyrosine kinase in B cell antigen receptor-mediated activation of phospholipase C-gamma 2. *The Journal of experimental medicine* **184:** 31–40

Teixeira C, Stang SL, Zheng Y, Beswick NS & Stone JC (2003) Integration of DAG signaling systems mediated by PKC-dependent phosphorylation of RasGRP3. *Blood* **102:** 1414–1420

Tillmanns S, Sondermann P, Schrödter A, Schubert C, Nilius S, Buckel P. Soluble Fc-gamma IIb receptor SM101 as potential therapy in autoimmune diseases – results from a Phase 0/Ia clinical trial in healthy volunteers. Ann Rheum Dis. 2011;70:618.

Tillmanns S, Kolligs C, DP D'C, Doria A, Hachulla E, Voll RE, et al. SM101, a novel recombinant, soluble, human Fc gamma IIb receptor, in the treatment of systemic lupus erythematosus: results of a double-blind, placebo-controlled multicenter study. Arthritis Rheum. 2014;66:S1238.

Tonegawa S (1983) Somatic generation of antibody diversity. *Nature* **302:** 575–581

Towbin H, Staehelin T & Gordon J (1992) Electrophoretic transfer of proteins from polyacrylamide gels to nitrocellulose sheets: procedure and some applications. 1979. *Biotechnology (Reading, Mass.)* **24:** 145–149

Trüb T, Frantz JD, Miyazaki M, Band H & Shoelson SE (1997) The role of a lymphoid-restricted, Grb2-like SH3-SH2-SH3 protein in T cell receptor signaling. *The Journal of biological chemistry* **272:** 894–902

Tuosto L, Capuano C, Muscolini M, Santoni A & Galandrini R (2015) The multifaceted role of PIP2 in leukocyte biology. *Cellular and molecular life sciences : CMLS* **72:** 4461–4474

Tuveson DA, Carter RH, Soltoff SP & Fearon DT (1993) CD19 of B cells as a surrogate kinase insert region to bind phosphatidylinositol 3-kinase. *Science (New York, N.Y.)* **260:** 986–989

Ubelhart R & Jumaa H (2015) Autoreactivity and the positive selection of B cells. *European journal of immunology* **45:** 2971–2977

Vogel W & Ullrich A (1996) Multiple in vivo phosphorylated tyrosine phosphatase SHP-2 engages binding to Grb2 via tyrosine 584. *Cell growth & differentiation : the molecular biology journal of the American Association for Cancer Research* **7:** 1589–1597

Wang H, Coligan JE & Morse HC3 (2016) Emerging Functions of Natural IgM and Its Fc Receptor FCMR in Immune Homeostasis. *Frontiers in immunology* **7:** 99

Watanabe H, Sherris D & Gilkeson GS (1998) Soluble CD16 in the treatment of murine lupus nephritis. *Clinical immunology and immunopathology* **88:** 91–95

Werwitzke S, Trick D, Sondermann P, Kamino K, Schlegelberger B, Kniesch K, Tiede A, Jacob U, Schmidt RE & Witte T (2008) Treatment of lupus-prone NZB/NZW F1 mice with recombinant soluble Fc gamma receptor II (CD32). *Ann Rheum Dis* **67:** 154–161

Wienands J, Schweikert J, Wollscheid B, Jumaa H, Nielsen PJ & Reth M (1998) SLP-65: a new signaling component in B lymphocytes which requires expression of the antigen receptor for phosphorylation. *The Journal of experimental medicine* **188:** 791–795

Winding P & Berchtold MW (2001) The chicken B cell line DT40: A novel tool for gene disruption experiments. *Journal of Immunological Methods* **249:** 1–16

Wines BD, Gavin A, Powell MS, Steinitz M, Buchanan RRC & Mark Hogarth P (2003) Soluble FcgammaRIIa inhibits rheumatoid factor binding to immune complexes. *Immunology* **109:** 246–254

Woodruff MF, Reid B & James K (1967) Effect of antilymphocytic antibody and antibody fragments on human lymphocytes in vitro. *Nature* **215:** 591–594

Woof JM & Burton DR (2004) Human antibody-Fc receptor interactions illuminated by crystal structures. *Nature reviews. Immunology* **4:** 89–99

Yamashita S, Mochizuki N, Ohba Y, Tobiume M, Okada Y, Sawa H, Nagashima K & Matsuda M (2000) CalDAG-GEFIII activation of Ras, R-ras, and Rap1. *The Journal of biological chemistry* **275:** 25488–25493

Yang J & Reth M (2010) Oligomeric organization of the B-cell antigen receptor on resting cells. *Nature* **467:** 465–469

Yang J & Reth M (2010) The dissociation activation model of B cell antigen receptor triggering. *FEBS letters* **584:** 4872–4877

Yasuda T, Kometani K, Takahashi N, Imai Y, Aiba Y & Kurosaki T (2011) Erks induce expression of the transcriptional repressor Blimp-1 and subsequent plasma cell differentiation. *Science signaling* **4:** ra25

Yasuda T & Kurosaki T (2008) Regulation of lymphocyte fate by Ras/Erk signals. *Cell cycle (Georgetown, Tex.)* **7:** 3634–3640

Yohannan J, Wienands J, Coggeshall KM & Justement LB (1999) Analysis of tyrosine phosphorylation-dependent interactions between stimulatory effector proteins and the B cell co-receptor CD22. *The Journal of biological chemistry* **274:** 18769–18776

Yuseff MI, Pierobon P, Reversat A & Am Lennon-Dumenil (2013) How B cells capture, process and present antigens: a crucial role for cell polarity. *Nature reviews. Immunology* **13:** 475–486

Zhang G & Neubert TA (2009) Use of stable isotope labeling by amino acids in cell culture (SILAC) for phosphotyrosine protein identification and quantitation. *Methods in molecular biology (Clifton, N.J.)* **527:** 79-92, xi